Abstracts 6000-6315

SOLID STATE ABSTRACTS

an abstract journal devoted to the theory, production and use of solid state materials and devices

VOLUME 1 NUMBER 1

PHYSICS

METALLURGY

ELECTRONICS

METALS

SEMICONDUCTORS

SUPERCONDUCTORS

PHOSPHORS

MAGNETICS

DIELECTRICS

SOLID STATE ABSTRACTS

VOLUME 1, NUMBER 1

October, 1960

Abstracts 6000–6315

TABLE OF CONTENTS

Abstracts of the Solid State Literature

Solid State Metallurgy and Chemistry
- Alloys . . . 1
- Crystal Structure . . . 1
- Crystal Growth . . . 4
- Crystal Surfaces . . . 7
- Environmental Effects . . . 7

Solid State Physics
- Crystal Physics . . . 9
- Electrical Properties
  - General . . . 10
  - Dielectric Properties . . . 11
  - Carrier Properties . . . 14
  - Conductivity . . . 17
  - Superconductivity . . . 17
  - Breakdown . . . 18
  - Galvanomagnetic Properties . . . 18
  - Other . . . 19
  - Specific Materials . . . 20
- Magnetic Properties
  - Ferromagnetism and Ferrites . . . 20
  - Paramagnetism . . . 24
- Optical Properties . . . 26
- Thermal Properties . . . 30
- Mechanical Properties . . . 31

Solid State Devices
- Diodes
  - Point Contact . . . 32
  - Junction . . . 32
- Transistors
  - Junction . . . 34
- Photodevices . . . 35
- Thermal Devices . . . 36
- Magnetic Devices . . . 36
- Other . . . 38

Solid State Device Measurements . . . 38

Solid State Device Circuits
- General . . . 38
- Amplifiers . . . 39
- Oscillators . . . 40
- Other . . . 40

Solid State Device Applications
- Communications, etc. . . . 41
- Computers, etc. . . . 41
- Power . . . 43
- Control . . . 44
- Instrumentation . . . 44

New Products . . . 45

Subject Index . . . 47

Author Index . . . 55

List of Journals Abstracted . . . 56

Editor: GEOFFREY KNIGHT, JR.

Assistant Editor: MYRON A. COHEN

PUBLISHED MONTHLY BY

Cambridge Communications Corporation, 238 Main Street, Cambridge 42, Massachusetts, Tel. Klrkland 7-1997

Subscription Rate: $25.00 per year. Single Copies and Back Issues: $2.50. Advertising Rates on Request.

Cambridge Communications Corp. is not prepared to furnish copies of the articles abstracted. However, there are many libraries throughout the country which maintain photocopying services.

SYMBOLS USED IN THE ABSTRACTS

L: Letter to the Editor. A: Only an abstract is given in the reference. R: Only a review is given in the reference. E: Erratum.

The reference numbers in the indices are the abstract numbers, not the page numbers.

Copyright 1960 by Cambridge Communications Corp. Printed in the U.S.A. by the University Press, Inc.

Second-class mail privileges applied for at Boston, Massachusetts.

TK
7800
S6
Vol 1
1960/61
n/e

Solid state abstracts journal

NOTICE

THIS VOLUME IS INCOMPLETE

THE FOLLOWING ISSUES ARE NOT AVAILABLE:

VOL. 1 NO. 2 NOVEMBER 1960

BINDING UNIT

24 Jun 69

Digitized by the Internet Archive
in 2024

https://archive.org/details/solid-state-and-superconductivity-abstracts_1960-10_1_1

FOREWORD

With this issue of SOLID STATE ABSTRACTS we introduce an expanded version of our three-year old abstract journal SEMICONDUCTOR ELECTRONICS. In addition to the theory, fabrication, and use of semiconductor materials and devices, this new journal will cover ferrites and other magnetic materials, ferroelectrics and other dielectric materials, superconductors, many topics related to metals and crystalline salts, etc.; in short, everything that has recently come to be known as "the solid state". A glance at the Table of Contents will show that we intend to follow these materials from the time they are removed from the ground for purification and crystallization to the time they are launched from the earth as electronic components in a missile or a sattelite. Along the way we will keep you informed on the latest developments in metallurgy, solid state physics, device theory and fabrication, measurements, basic circuits, and applications.

The publication of a new abstract journal in a field already covered by several excellent abstract journals requires a word of explanation. In this case that word is specialization. In addition to abstracting papers published in technical journals throughout the world, we will bring you in contact with that remarkable mine of detailed information, the U. S. Patent; we will inform you of the content of conference reports so that you can know who is working on what problems months before the information is published; we will present the latest contributions from the academic world in the form of thesis abstracts; and we will help you to keep track of new commercial products in the solid state field as they become available. All this information will be made immediately available by a detailed system of cross references and subject and author indexes in every issue. The result is a depth of coverage and unity of content which are not provided by any other abstract journal in this field.

For those who are actively working in the solid state field, we have carried the idea of an abstract journal a giant step further by printing the same abstracts on 3"x5" file cards. Each abstract is provided with one or more classification numbers (one card is provided for each classification number) which enables a subscriber to file the abstracts in a logical (rather than a chronological) sequence. We are currently preparing abstract references on more than 4000 topics and the number of topics is increasing by more than 100 a month. Eventually we hope to provide in this way a reference system which is unique in completeness and detail, and is never outdated.

FOR SURFACE STUDIES

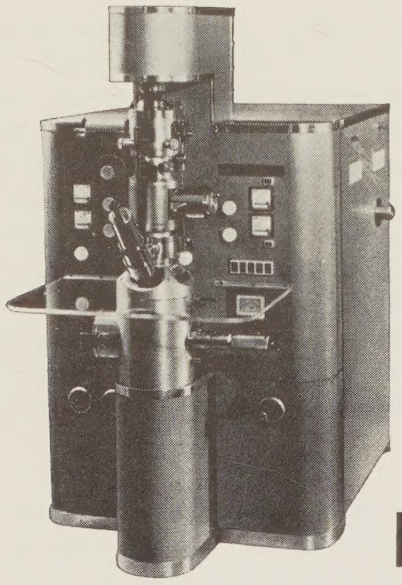

KE1

Trüb, Täuber Secondary Electron Emission Microscope

for direct viewing of metallic and semiconducting specimens by means of secondary electrons released from ion bombardment of the surface — featuring . . .

- Images free of distortion and deformation
- Enlargement up to 1500 X electronoptically
- Resolution 500–600Å
- Object temperature 150°–800° C
- Observable surface of the object 25 mm square
- Differentiation of the material

The Instrument Includes . . .

Electrostatic immersion objective
Ion beam system
Revolving contrast diaphragms
2 electromagnetic projectors
Observation chamber with fluorescent image screen
Recording chamber with plate cassette
High-intensity optical microscope
All-metal housing with vacuum equipment including diffusion pump
High-voltage equipment for 45 kV
Measuring instruments and control equipment

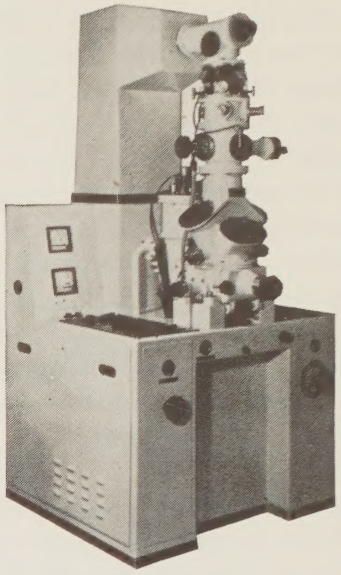

KD3

Trüb, Täuber Electron Diffractograph

for determining the crystalline structure of surfaces, thin layers, and extremely small quantities of material, including dynamic processes — featuring . . .

- Cold-cathode electron gun with practically unlimited life
- Simple design — dependable operation, extreme flexibility
- Balanced optical system
- High resolving power
- Large variety of specimen holders for various methods of investigation
- Devices for heating and cooling the test specimens (from liquid nitrogen to 1000°C)
- Devices for discharging, etching, surface evaporating
- Various cameras for photographic recording on plates and films
- Unique kinematic recorder

Specifications

Acceleration Voltage —	
continuously adjustable:	10 to 50 kV
ripple (fractional):	$\approx 10^{-4}$
stability:	$\pm 0.1\%$
Final vacuum:	approx. 2×10^{-5} mm Hg
Magnification with electronic lens:	75X
Minimum line width:	0.001 mm
Minimum diameter of beam for focussing on specimen, without additional diaphragms:	4μ

Distributed by:

NEW ENGLAND SCIENTIFIC INSTRUMENTS CO.

238 MAIN STREET • CAMBRIDGE 42, MASSACHUSETTS • Kirkland 7-1997

Electron Microscopes • Nuclear Induction Spectrographs • High Voltage Oscillographs • Precision Laboratory Instruments • Nuclear Track Microscopes

ABSTRACTS OF THE SOLID STATE LITERATURE

SOLID STATE METALLURGY AND CHEMISTRY

ALLOYS

6001 GERMANIUM AND SILICON LIQUIDUS CURVES by C. D. Thurmond and M. Kowalchik (Bell Labs.); Bell Sys. Tech. J., Vol. 39, pp. 169-204, Jan. 1960

Measurements of the solubility of germanium in liquid gallium, thallium, tin, arsenic, bismuth, cadmium and zinc, and the solubility of silicon in liquid indium, tin, lead, antimony, bismuth and zinc are reported. The measurements of other workers are reviewed, including those of the solubility of germanium and silicon in liquid copper, silver, gold and aluminum; of germanium in liquid indium, lead and antimony; and of silicon in liquid arsenic and nickel. All but two of the liquidus curves can be described within experimental error by a two-constant equation. The form of this equation suggests that the liquid solutions exhibit certain simple thermodynamic properties, and some evidence which indicates that the constants of this equation can be used to estimate the excess free energy of the solutions is cited.

6002 SOLID SOLUBILITIES OF IMPURITY ELEMENTS IN GERMANIUM AND SILICON by F. A. Trumbore (Bell Labs.); Bell Sys. Tech. J., Vol. 39, pp. 205-232, Jan. 1960

The available data on solid solubilities of impurity elements in germanium and silicon are summarized in the form of solidus or solvus curves. New solubility data are presented for the lead-germanium, zinc-germanium, indium-germanium, antimony-silicon, gallium-silicon and aluminum-silicon systems. The correlation of the solid solubilities with the heats of sublimation and the atom sizes of the impurity elements is considered.

6003 SUBSTITUTION OF GROUP III FOR V ATOMS IN Bi_2Te_3 and Sb_2Te_3 by A. J. Rosenberg and A. J. Strauss (Lincoln Lab.); Bull. Am. Phys. Soc., Ser. II, Vol. 5, p. 78 (A), Jan. 27, 1960

The solid solubilities of In_3Te_3 and "Tl_2Te_3" in Bi_2Te_3 and Sb_2Te_3 have been found to approach 50 mole percent. The lattice parameters of the solid solutions are slightly less than those of the host compounds. Single crystal or coarse-grained polycrystalline samples of the alloys have been prepared by the Bridgman method, and their resistivities, Hall coefficients, and thermoelectric powers have been measured at room temperature. The substitutions of the Group III elements are essentially nondoping. The major effect is a strong reduction in the hole mobility. The significance of these results was discussed with reference to chemical bonding in the C_{33} structure type.

Solid Solution in the System CIS-YIG - See 6159.

Distribution Coefficients of Impurities in InSb - See 6036.

CRYSTAL STRUCTURE

(Including Imperfections and Impurities)

6004 THREE-DIMENSIONAL EXTENSION OF HOUSTON'S METHOD FOR FACE-CENTERED CUBIC CRYSTALS by D.D. Betts (U. Alberta); Bull. Am. Phys. Soc., Ser. II, Vol. 5 p. 49 (A), Jan. 27, 1960

Houston's method of integration of functions of rotational symmetry O_h over the surface of a sphere utilizes the fact that the integrand can be expanded in an orthogonal set of Bethe's Kubic Harmonics having the same symmetry. Of more interest is the problem of integrating functions having both the rotational and translational symmetry of a crystalline space group over a three-dimensional Brillouin zone or cellular polyhedron. In order to develop a Houston-type formula utilizing both types of symmetry, face-centered cubic harmonics, $F_l(x, y, z)$, are defined as polynomials in x, y, and z belonging to the identity representation of the cubic rotation group whose normal derivative vanishes over the faces of the rhombohedral dodecahedron, which is the cellular polyhedron in face-centered cubic crystals. It is not necessary to orthogonalize the F_l to one another completely, but only to $F_0 = 1$. The conditions on the F_1 are so stringent that F_1 is of degree twelve in x, y and z. An integration formula which uses the first fourteen face-centered cubic harmonics to derive the weights for the integrand at fourteen symmetrically arranged points in one forty-eighth of the cellular polyhedron was presented.

Crystal Symmetry of the Low Temperature Phase of Barium Titanate - See 6084.

6005 EFFECTS OF PLASTIC DEFORMATION AT 300°K ON THE X-RAY PRODUCTION OF COLOR CENTERS IN KCl AT 5 and 78°K by H. N. Hersh and J. J. Markham (Zenith); J. Phys. Chem. Solids, Vol. 12, pp. 207-208 (L), Jan. 1960

Observations made on KCl single crystals plastically deformed at 300°K and irradiated with x-rays at 5 and 78°K are reported. The net production of "true" F centers at the low temperatures is not appreciably greater (within about 10 per cent) than in an undeformed crystal. The plastic deformation at 300°K, however, enhances the formation of color centers not found in appreciable numbers in pure, annealed KCl crystals. One of these centers has been identified as the Cl_2 molecule and the other as an electron center or centers to which it is intimately related. Hole traps have not been detected. These observations indicate that the theories of F-center formation by irradiation must be reviewed.

6006 F-CENTER GROWTH CURVES by P. V. Mitchell, D.A. Wiegand, and R. Smoluchowski (Carnegie Inst. Tech.); Phys. Rev., Vol. 117, pp. 442-443, Jan. 15, 1960

It is shown that the increase in the density of F centers in KCl due to x-ray irradiation can be described kinetically by considering two independent groups of negative ion vacancies. One group is composed of vacancies in the lattice before irradiation, while the other is composed of vacancies generated during the irradiation. It is concluded from the differ-

ence in the electron capture cross sections for the two groups of vacancies and the intensity dependence of the rate of generation of new vacancies that the vacancies are generated at dislocations by a multiple ionization process.

Influence of F-Centers on Lattice Thermal Conductivity in LiF - See 6201.

6007 LOCALIZATION OF DISLOCATIONS IN SILICON AND GERMANIUM BY INFRARED MICROSCOPY [in French] by O. Deutschbein and M. Bernard (Ctr. Natl. d'Etudes Telecommun.); Solid State Phys. Electronics and Telecommun., Vol. 1, Part 1, pp. 117-125, 1960

Studies of the crystalline imperfections of silicon and germanium crystals by means of infrared microscopy techniques are reported. Silicon was studied through use of luminescent substances previously activated by ultraviolet light, which emit visible light under the action of infrared rays up to about 1.35μ. A screen supplied with these substances was placed in the image plane of a microscope, thus permitting the dislocations in the Si crystals to be observed in transparency and to be photographed with ordinary photographic plates. This technique cannot be used with Ge since it is opaque for $\lambda > 1.7\mu$. A commercial television apparatus equipped with an analyzing tube of the Resistron type was therefore utilized. The tube, which is sensitive in the infrared to about 1.85μ, permits observation on a television screen of double refraction as well as precipitation of metals in the interior of the Ge wafers. The dislocations caused by both growth faults and by mechanical deformation have been studied with this apparatus.

6008 DETERMINATION OF DISLOCATION DENSITIES IN SILICON CRYSTALS BY AN OPTICAL METHOD by G. Eckhart and S. Lederhandler (RCA); Bull. Am. Phys. Soc., Ser. II, Vol. 5, p. 25 (A), Jan. 27, 1960

A method of determining the average dislocation densities in silicon crystals containing between 10^2 and 10^6 dislocations/cm^2 by a single measurement of the average light intensity transmitted through a sample placed between crossed polarizers in a convergent beam was described. Faster and more accurate routine measurements can be made by this techniaue than by the chemical method.

6009 DISLOCATION STRUCTURE AND THE FORMATION AND STRENGTH OF SODIUM CHLORIDE WHISKERS by W. W. Webb (Union Carbide Metals); J. Appl. Phys., Vol. 31, pp. 194-206, Jan. 1960

Details of dislocation structure which have been determined for a variety of NaCl whiskers and microcrystals grown from porous substrates moistened with supersaturated aqueous solution are discussed. Some of the smaller needle-like crystals have the single dislocation with an axial screw component usually assumed for whiskers. Larger whiskers and platelets often have much more complicated dislocation structures and may have higher dislocation densities than normal bulk crystals. Strengths were compared with dislocation structures and it was found that the nearly theoretical strengths observed in some of these whiskers are not due to merely a size effect but are directly related to the dislocation structure. Even crystals with high dislocation densities exhibited high strength in bending provided that all of the dislocations were so arrayed that they were not influenced by the applied stress. Regular dislocation arrays often occur naturally with this growth mechanism. However, irregular dislocation structures often associated with growth irregularities invariably resulted in low strength. Techniques for application of x-ray diffraction microscopy to determination of the dislocation structure of microcrystals are described.

6010 DISLOCATIONS IN Si SINGLE CRYSTALS by T. Furuoy and Y. Sasaki (Nippon Electric); J. Phys. Soc. Japan, Vol. 15, pp. 205-206 (L), Jan. 1960

Some observations made on dislocations in silicon single crystals grown along the <111> axis by the Teal-Little method are reported. The density of dislocations in the seed was found to increase to about 10^3 to $10^4/cm^2$ when it was dipped into the melt. When the seed was pulled at a low rate (0.2 mm/min.) for about 5 minutes, the dislocation density did not decrease appreciably. At a pulling rate of about 1 mm/min all the dislocations disappeared in 15 to 20 minutes. It is suggested that the dislocations disappear when two screw dislocations having opposite signs combine with each other. Dislocation loops developed when the temperature of the melt was suddenly raised but not when the temperature was lowered. Several photographs are presented.

6011 DISLOCATIONS IN TWO TYPES OF CdS CRYSTALS by D. C. Reynolds (Wright Patterson Air Base) and S. J. Czyzak (U. Detroit); J. Appl. Phys., Vol. 31, pp. 94-98, Jan. 1960

An investigation of dislocation densities in CdS crystals (types I and II) by chemical etching techniques is discussed. There is very little difference in the dislocation densities in the two types of CdS crystals. The dislocation density in both types of growth varies over a range from $10^7/cm^2$ to $10^1/cm^2$. However, type I crystals have a greater tendency to twin and low angle boundaries are generally present in the twinned crystal.

Control of Dislocation Density in Silicon Crystals - See 6025.

6012 OBSERVATION OF LAYER STRUCTURE IN DISLOCATION FREE SILICON CRYSTALS WITH THE USE OF X-RAY ANOMALOUS TRANSMISSION by Z. Ishii (Electrotech. Lab.), T. Furuoya and Y. Sasaki (Nippon Electric), and K. Kohra (U. Tokyo); J. Phys. Soc. Japan, Vol. 15, pp. 206-207 (L), Jan. 1960

Observations of the layer structure of dislocation free silicon crystals by the anomalous transmission of x-rays is reported. One sample from a crystal grown along the <111> axis by the Teal-Little method was studied by the Dash copper decoration technique and an adjacent sample was studied by the anomalous transmission of x-rays. Good agreement was found in the structures measured by both techniques.

Oxygen Dissolved in Silicon - See 6050, 6051.

6013 THE ASSESSMENT OF HIGH PURITY SILICON by N.R. Howard (Brit. Thomson-Houston); Solid State Phys. Electronics and Telecommun., Vol. 1, Part 1, pp. 132-138, 1960

The use of electrical measurements to assess the quality of silicon with respect to impurities such as boron, for which chemical or radiochemical measurements are not applicable or are not sufficiently sensitive, is described. Since these measurements can only be made on single crystals, the pulling techniques employed to convert the aggregate of finely divided particles customary in manufactured silicon into a single crystal are presented. The changes in impurity content caused by this conversion are taken into account. The boron content of the raw material can then be determined from resistivity measurements of the crystal, provided the phosphorous content of the silicon is sufficiently low and the crucible contamination rate is known. Accuracy is greatest when contamination is least.

6014 THE DETERMINATION OF COPPER AND LEAD IN INDIUM ARSENIDE by V. J. Jennings (SERL); Analyst, Vol. 85, pp. 62-68, Jan. 1960

A method for the determination of trace amounts of copper and lead in zone-refined indium arsenide by square wave polarography is described. Concentrations as low as 0.1 p.p.m. copper and 0.2 p.p.m. lead in a 0.5 gm sample of indium arsenide may be determined by this method.

6015 ZONE REFINING AND CRYSTAL GROWTH OF PERITECTIC COMPOUNDS by D. R. Mason and J. S. Cook (U. Mich.); Bull. Am. Phys. Soc., Ser. II, Vol. 5, p. 78 (A), Jan. 27, 1960

The purification and selective contamination of congruently melting materials was described quantitatively using mass balance relationships. By superimposing a proper temperature distribution, dictated in part by the phase diagram of the system, and considering the rate processes accompanying solidification and crystal growth, ingots containing large crystal grains can be produced in zone refining equipment. These concepts have been extended and applied to the peritectic compound cadmium indium telluride, $CdIn_2Te_4$. Homogeneous samples have been prepared for optical and electrical characterization.

6016 CONTINUOUS MULTISTAGE PURIFICATION OF SILICON TETRAIODIDE BY ZONE-MELTING by G. H. Moates (U.S. Air Force Cambridge Res. Ctr.); Solid State Phys. Electronics and Telecommun., Vol. 1, Part 1, pp. 1-8, 1960

A continuous multistage system for purifying silicon tetraiodide by means of the zone-melting technique (zone-void method) described by Pfann is presented. The step-wise processes of sublimation, transfer, zone purification, and cracking are united in three distinct but uninterrupted sets of apparatus which are described in detail. As in all cases of fractional crystallization the effective segregation coefficient varies from the equilibrium value in accordance with the linear velocity of crystallization, the effective boundary layer, and the diffusion coefficients. However, certain inherent limitations of zone purification and batch processing are eliminated or reduced by use of the zone-melting technique.

Preparation of Transistor-Grade Silicon by Zone Purification of SiI_4 - See 6035.

Electron Beam Zone Refiner - See 6305 (New Product Section).

6017 PURIFICATION OF $SiCl_4$ BY ADSORPTION TECHNIQUES by H. C. Theuerer (Bell Labs.); J. Electrochem. Soc., Vol. 107, pp. 29-32, Jan. 1960

The purification of silicon tetrachloride by using adsorption columns filled with hydrous oxides or silicates is discussed. Hydrogen reduction of this purified halide leads to higher purity silicon than is obtainable otherwise. Data for the adsorption efficiency of various materials are presented using infrared spectroscopy and radioactive tracer techniques as the basis of comparison.

Diffusion of Impurities in Gallium Antimonide - See 6069.

6018 INTERACTION BETWEEN ARSENIC AND ALUMINUM IN GERMANIUM by J. O. McCaldin (Hughes); J. Appl. Phys., Vol. 31, pp. 89-94, Jan. 1960

The behavior of As in Ge containing regions doped with ~5×10^{20}/cc Al is discussed. The solubility of As is enhanced tenfold or more by the heavy Al doping, on the basis of (1) measurements of conductivity type and (2) the negative results of a search for compounds by x-ray diffraction. The behavior of As diffusion fronts was studied by observing the progress of the p-n junction formed in Ge containing 10^{17}/cc In. When a region of heavy Al doping was added, the p-n junction was displaced. The displacements indicate that the diffusing As is attracted to regions of heavy Al doping. These results are similar to those of Reiss, Fuller, and others for Li in Si, though a detailed understanding is not yet available in the present case.

6019 Li-B PAIRING IN Si BY ION DRIFT IN NP JUNCTIONS by E. M. Pell (GE Res. Lab.); Bull. Am. Phys. Soc., Ser. II, Vol. 5, p. 78 (A), Jan. 27, 1960

The Li-B ion pairing reaction has been investigated in Si by measuring its effect on the diffusion constant of Li, using the method of ion drift in an n-p junction. The distance of closest approach, determined by the best fit of the data to the Reiss model, is about 2.6 A. The relaxation time for ion pairing was measured by the same technique at 0°C and yields a reasonable value for the capture radius.

6020 THEORY OF SOLUBILITY OF INTERSTITIAL IMPURITIES IN SEMICONDUCTORS by K. Weiser (IBM Res. Lab.); Bull. Am. Phys. Soc., Ser. II, Vol. 5, p. 61 (A), Jan. 27, 1960

For a given concentration of impurity in the gas phase, the solubility is largely determined by the energy needed to transfer the impurity to an interstitial site in the host crystal. Formulas for this energy are given for both neutral and ionized impurities in terms of the polarizabilities, the ionization potential, the work function, a characteristic absorption energy of the host crystal, two overlap parameters, the distance from the impurity to the nearest host atom, and the polarization energy. A theory pertaining to the solubility of interstitial impurities in semiconductors was applied to hydrogen and copper to predict whether the impurity will be neutral or ionized, and to predict relative solubilities.

Effects of Oxygen in Germanium - See 6179.

6021 BEHAVIOR OF InSb SURFACES DURING HEAT TREATMENT by D. Haneman (Brown U.); J. Appl. Phys., Vol. 31, pp. 217-218 (L), Jan. 1960

It is reported that flat-topped, mobile hillocks form on the surfaces of InSb crystals which are heated to about 400°C. Detailed observations made on two different $(11\bar{1})$ surfaces are discussed and three photographs of the formation and migration of these hillocks on one of the surfaces are presented. It is suggested that the hillocks form as a result of the preferential evaporation of antimony from the heated surface. No hillocks were noticed in the vicinity of chemical etch pits produced where dislocations emerge.

Structure of Silicon Carbide Surfaces - See 6048.

6022 INTERFEROMETRIC DETERMINATION OF TWIST AND POLYTYPE IN SILICON CARBIDE WHISKERS by D. R. Hamilton (Westinghouse Res. Labs.); J. Appl. Phys., Vol. 31, pp. 112-116, Jan. 1960

Observation of a twist in the $\{1\bar{1}00\}$ faces of hexagonal SiC whiskers by means of optical interference techniques is reported. The whiskers were grown in a graphite tube furnace by sublimation of SiC in hydrogen and were deposited at temperatures about 2000°C as acicular crystals of hexagonal section with [0001] along the whisker length. The Eshelby for-

mula for twist caused by a screw dislocation has been used to estimate the strength of the associated Burgers vector. It is found that, within the experimental error, the estimated Burgers vector is equal to, or is an integral multiple of the unit cell of the SiC polytype 4H. It is concluded that these twisted whiskers grow by means of a screw dislocation of integral strength parallel to the axis, and that they are of polytype 4H.

6023 CRYSTAL STRUCTURE OF SILICON CARBIDE OF 174 LAYERS by T. Tomita (Saitama U.); J. Phys. Soc. Japan, Vol. 15, pp. 99-105, Jan. 1960

A new modification of silicon carbide having rhombohedral symmetry and a unit cell composed of 174 layers is reported. The cell size and symmetry were determined by the method employed by Honjo et al. to study silicon carbide of 594 layers. The structure, namely the stacking order of Si-C layers, of the new modification was determined by comparing the intensity of x-ray reflections with those calculated for a number of models. The structure is represented by $\{C(CCH)_7C_3(CCH)_{11}\} \times 3$ in Wyckoff's notation.

CRYSTAL GROWTH

6024 GROWING SINGLE CRYSTALS WITH CONSTANT RESISTIVITY BY FLOATING CRUCIBLE TECHNIQUE by J. Goorissen, F. Karstensen, and B. Okkerse (N. V. Philips); Solid State Phys. Electronics and Telecommun., Vol. 1, Part 1, pp. 23-27, 1960

Use of the floating crucible technique to grow single crystals of germanium with a constant impurity concentration is described. The crystal is pulled from a small crucible which contains the desired impurity and which floats on molten germanium in a large outer crucible. The two crucibles are connected by means of a capillary. The crystal is grown at a constant speed and the floating crucible lowers itself with a corresponding velocity due to the force of gravitation. Typical resistivity curves for crystals doped with Sb, In, and P which have been grown by this technique are presented. The yield in each case is between 70 and 75%. Other impurities have been utilized with equal success.

6025 THE EFFECTS OF SEED ROTATION ON SILICON CRYSTALS by A. J. Goss and R. E. Adlington (Marconi's Wireless); Solid State Phys. Electronics and Telecommun., Vol. 1, Part 1, pp. 28-43, 1960

The effects of seed rotation of up to 200 rpm on the physical and electrical properties of silicon single crystals are described. As a result of changes in the rotation rate, the shape and size of the ingot are altered. In addition, there is an important change in the growth interface. The relation between interface curvature and rotation rate is presented graphically and the results are discussed in terms of temperature gradients in the system. The properties of crystals grown under these conditions are considered in terms of resistivity, dislocation density, and minority carrier lifetime. The importance of interface shape and size for the control of dislocation density is also discussed.

6026 GROWTH OF InSb CRYSTALS IN THE <111> POLAR DIRECTION by H. C. Gatos, P. L. Moody, and M. C. Lavine (Lincoln Lab.); J. Appl. Phys., Vol. 31, pp. 212-213 (L), Jan., 1960

Some observations made on the crystalline perfection of InSb crystals grown by the Czochralski technique using <111> seed crystals which terminate either in Sb atoms (B {111} surface) or in In atoms (A {111} surface) are explained by means of an atomic model of the two surfaces. Under identical growth conditions single crystals are grown when the B surface is used whereas twinning and large grain formation often occur in the initial stages of crystal growth when the A surface is used. The dislocation densities in the crystals grown in the two directions also differ. In the surface model, tetrahedrally bonded atoms of the B surfaces have an unshared pair of electrons and the atoms of the A surfaces have their fourth tetrahedral orbit unfilled. This model which accounts for differences in the chemical and electronic properties of the two surfaces, also applies to the other III-V compounds.

6027 THE CONTAMINATION OF SILICON BY THE CRUCIBLE by S. E. Bradshaw (GE Ltd.); Solid State Phys. Electronic and Telecommun., Vol. 1, Part 1, pp. 44-60, 1960

An explanation of the pattern of observed impurities in single "pulled" crystals of silicon is presented. It has been found that boron and phosphorus impurities in the fused silica crucible have the most marked effect on crystal purity. It is demonstrated that the rate of contamination is a constant, the value of which is determined for crucibles containing a known concentration of boron, thus enabling the rate of dissolution of the silica to be estimated. The relative independence of the rate of crucible dissolution on the melt-crucible contact area appears to involve two rate-limiting factors: the diffusion rate of oxygen in molten silicon and the dissolution rate of silica in oxygen-free silicon.

6028 HIGH RESISTIVITY N-TYPE SILICON CRYSTALS GROWN FROM FUSED QUARTZ CRUCIBLES by P. Ransom (Brit. Thomson-Houston); Solid State Phys. Electronics and Telecommun., Vol. 1, Part 1, pp. 139-145, 1960

An expression giving the acceptor concentration at the top of a pulled silicon crystal caused by continuous contamination from the crucible is derived in terms of the solubility of the fused quartz in molten silicon, the impurity content of the quartz, the melting time of the Si, and the seeding-on time. From this the solubility of the fused quartz is estimated at 4.0×10^{-7} gm cm^{-2} sec^{-1} at 1420°C and its acceptor impurity content (most probably boron) as 1.0 ppm. Under typical operating conditions the conductivity of the pulled crystal changes at an average rate of 2.0×10^{-4} mho cm^{-1} min^{-1} because of the melting time and 1.4×10^{-4} mho cm^{-1} min^{-1} because of the seeding-on time. With careful manual control of the parameters of growth, a reproducibility of ±5 ohm-cm is reported in the region of 100 ohm-cm.

6029 RECENT ADVANCES IN THE PREPARATION OF SEMICONDUCTING MATERIALS by W. G. Pfann (Bell Labs.); Solid State Phys. Electronics and Telecommun., Vol. 1, Part 1, pp. 17-22, 1960

A new "compensation method" of preparing semiconducting materials by eliminating fluctuations in the electrical conductivity of extrinsic semiconducting crystals is described. Such fluctuations arise from variations in growth rate or stirrin while the crystal is being grown from the melt, and can be substantially eliminated by adding to the melt a critical concentration of a suitably chosen solute whose conductivity type is opposite to that of the major solute. Determination of the critical concentration ratio, the effects of deviation from the

ritical ratio, and properties of suitable solute combinations r utilization of this method are also discussed.

lectron Beam Zone Melting Apparatus - See 6305 (New Product Section).

030 HYDROTHERMAL PREPARATION OF TWO-COMPONENT SOLID SOLUTIONS FROM II-VI COMPOUNDS by . Kremheller and G. Gashurov (Sylvania Res. Labs.) and . K. Levine (Brooklyn Coll.); J. Electrochem. Soc., Vol. 07, pp. 12-15, Jan. 1960

he hydrothermal synthesis of binary solid solutions of inorganic hosphors and photoconductors is described. This method deends on the increased reactivity between the components and se of crystal growth in an aqueous solution maintained at high emperature under a confining pressure. The hydrothermal methd offers the advantages of a sealed system and easily reproducile experimental conditions. Solid solutions of ZnS-HgS, CdS-gS, and ZnS-CdS have been prepared by this method. Results optical absorption measurements, x-ray analysis, microscopic udies, and the spectral photo-response of the solid solutions rmed are presented.

031 DEVELOPMENT OF THE PERIODIC SHOCK WAVE TECHNIQUE AND ITS APPLICATION TO THE PREPARATION OF EMICONDUCTOR SILICON CARBIDE (Technical Res. Group); . S. Gov. Res. Rep., Vol. 33, p. 93 (A), Jan. 15, 1960 B 138 704

he development and application of the periodic shock wave echnique for preparing silicon carbide are discussed. The xperimental synthesis of silicon carbide (a) from silicon tetrahloride and hydrocarbon and (b) from methyltrichlorosilane are iscussed.

032 THE FORMATION OF THIN FILMS OF GERMANIUM BY HE DISPROPORTIONATION OF GERMANIUM DI-IODIDE y R. C. Newman and J. Wakefield (Assoc. Elect. Industries, ngland); Solid State Phys. Electronics and Telecommun., ol. 1, Part 1, pp. 160-170, 1960

detailed investigation of the thermodynamics of germanium rowth by the disproportionation of gaseous GeI_2 over a Ge ngle-crystal substrate heated to approximately 400°C is reorted. When the pressure of the GeI_2 is increased to a certain evel, the combined rate of solid disproportionation plus the te of reevaporation balance the rate of condensation and olid GeI_2 crystallizes from the vapor. Germanium deposits rmed on Ge [111] and [100] substrates are correlated with the ree growth conditions indicated by the thermodynamic analys. The greater ease of Ge growth on a substrate with a [111] rientation than on substrates with other orientations is demonrated by comparison with [100] specimens.

rmation of Cesium Antimony Films - See 6070.

033 ON THE GROWTH OF GERMANIUM DENDRITES by R. Wagner (Bell Labs.); Acta Met., Vol. 8, pp. 57-60 (L), an. 1960

is shown that the growth of germanium crystals in contact with supercooled melt can be either slow (polyhedral) or very rapid endritic) depending on the crystallographic nature of the seed. mechanism for the dendritic growth process is proposed and experimental evidence for it presented. The essence of the mechanism is that the two twin planes which bound the lamella produce in the sides of the growing dendrite a self-perpetuating system of grooves in which nucleation and growth readily occur. If only one, or no, twin plane is present, growth is slow and polyhedral.

6034 NOVEL MECHANISM FOR MASS TRANSPORT DURING WHISKER GROWTH - CESIUM CHLORIDE FROM AQUEOUS FILMS by W. W. Webb and N. P. Bertolone (Union Carbide Metals); J. Appl. Phys., Vol. 31, pp. 207-209, Jan. 1960

It is reported that capillary rise of a saturated solution within a hollow whisker provides a mechanism yielding growth at the tips of cesium chloride whiskers on a moist substrate in air at room temperature. The driving force for crystal growth is local supersaturation due to evaporation of water from solution at the tip of the capillary pore in each whisker. Screw dislocations provide the lattice steps on the whisker tips.

6035 THE PREPARATION OF TRANSISTOR-GRADE SILICON by B. Rubin (U. S. Air Force Cambridge Res. Ctr.); Solid State Phys. Electronics and Telecommun., Vol. 1, Part 1, pp. 9-16, 1960

A physico-chemical approach to the preparation of semiconductor grade silicon through synthesis of the intermediate silicon tetraiodide; purification of this compound by crystallization, sublimation, and zone purification; and decomposition into elemental Si is described. The SiI_4 is prepared by direct combination of 98% silicon with resublimed iodine at 810°C in a horizontal quartz furnace heated electrically. To minimize the ultimate concentration of impurities in the zone purification step, low concentrations are desirable initially; the crude SiI_4 is therefore recrystallized from toluene and sublimed in a stepwise process. The product is then encapsulated, densified, refrozen, and zone refined. Decomposition of the SiI_4 is effected in vacuo by passing the vapor over a single-crystal Si ingot heated inductively to a temperature of 1100°C.

Growth of Silicon Single Crystals - See 6013.

6036 SEMICONDUCTORS AND PHYSICAL ELECTRONICS (Chicago Mid. Labs.); U. S. Gov. Res. Rep., Vol. 33, p. 45 (A), Jan. 15, 1960 PB 138 623

Abstracts of published papers on the preparation of large InSb and InAs crystals, secondary electron emission, an image amplifier, a thermal image tube, and infrared detectors are presented. Growth of large single crystals by pulling from the melt has been on a routine basis. The purity of pulled crystals is always below that of the zone-refined material from which they are made. Distribution coefficients of four common impurities -- cadmium, zinc, selenium, and tellurium--in single crystals of InSb pulled from the melt have been determined by electrical measurements.

6037 SILICON CARBIDE AND ITS USE IN HIGH TEMPERATURE RECTIFIERS by H. C. Chang (Westinghouse); Semicon. Prod., Vol. 3, pp. 29-34, Jan. 1960

A detailed description of the preparation of semiconductor grade silicon carbide crystals in a Lely-type furnace is presented and the fabrication of silicon carbide rectifiers is discussed briefly. The purification of silicon carbide by zone melting is extremely difficult; however pure crystals can be prepared by using extremely pure silicon and carbon. N-type platelets with room temperature resistivities ranging from 10^6 to 10^7 ohm-cm have

been prepared. Uniform doping can be achieved by utilizing vapors of volatile compounds such as BCl_3, $AlCl_3$, and PCl_3 mixed with argon gas. Several physical constants of α-SiC at 650°C are listed.

6038 SYNTHESIS OF AlN CRYSTALS by T. Matsumura and Y. Tanabe (Tohoku U.); J. Phys. Soc. Japan, Vol. 15, p. 203 (L), Jan. 1960

Two techniques for synthesizing AlN crystals are discussed. In the Frerichs method a crucible containing pure aluminum and argon gas is heated for 24 hours at 1500°C in a tube containing a nitrogen atmosphere. The Al vapor reacts with the nitrogen and pale gray, felt-like crystals and transparent, colorless rod- and plate-like crystals grow at spots on the tube wall where the necessary conditions for their respective growth exist. Photographs of both the rod-like and plate-like crystals are presented. In the sublimation method a crucible filled with AlN powder is heated to 1500°C in a tube through which nitrogen gas is passed. After 24 hours rod-like crystals smaller than those produced by the Frerichs method grow on the tube wall. The apparatus and techniques are being improved so that large crystals can be grown.

Preparation of Tin Selenide - See 6132.

Preparation of $CdSnAs_2$ by Directional Freezing - See 6108.

Growth of Peritectic Compounds Using Zone Refining Equipment - See 6015.

6039 SOME PROPERTIES OF ZINC SULFIDE CRYSTALS GROWN FROM THE MELT by A. Addamiano and M. Aven (GE) J. Appl. Phys., Vol. 31, pp. 36-39, Jan. 1960

The growth of hexagonal zinc sulfide crystals by controlled cooling of melted luminescent grade zinc sulfide powders is discussed. Both pure and activated zinc sulfide powders were used. The density of pure melt grown crystals was found to be higher than that of natural zinc blende crystals or crystals grown by evaporation. The stability of the pure hexagonal crystals towards transformation to the cubic zinc-blende structure in the interval of temperature 700-1150°C was investigated and a full conversion to the cubic phase was never observed. The experimental evidence indicates the transition point to be above 1150°C.

Preparation of Alkaline Earth Pyrophosphate Phosphors - See 6189.

6040 GROWTH OF SINGLE CRYSTALS OF INCONGRUENTLY MELTING YTTRIUM IRON GARNET BY FLAME FUSION PROCESS by R. G. Rudness and R. W. Kebler (Union Carbide); J. Am. Ceram. Soc., Vol. 43, pp. 17-22, Jan. 1960

It is reported that single crystals of yttrium iron garnet ($Y_3Fe_5O_{12}$) have been grown using the flame fusion process, even though the compound is reported to melt incongruently. The growth of these single crystals involves a mechanism different from that which has been proposed for the growth of single crystals of incongruently melting mullite. Crystal boules were grown at varying linear growth rates and analyzed with chemical, X-ray, and metallographic techniques. With high linear growth rates, the samples are uniformly polycrystalline and three-phase, containing Fe_2O_3, $YFeO_3$, and $Y_3Fe_5O_{12}$. When slow linear growth rates are used, single-crystal $Y_3Fe_5O_{12}$ can be grown. The mechanism is as follows: at the beginning of growth the first phase to precipitate is $YFeO_3$, and during this stage in growth the molten cap becomes enriched in Fe_2O_3 compared with the $Y_3Fe_5O_{12}$ composition. The liquid cap composition thus changes to the limit of the peritectic on the Fe_2O_3-rich side, and $Y_3Fe_5O_{12}$ then crystallizes from the bottom of the melt as $Y_3Fe_5O_{12}$ powder is added to the top of the molten cap. The central sections of these boules are single-crystal yttrium iron garnet.

Preparation of Manganese Chromite-Aluminates - See 6157.

Preparation of the Ternary Alloy $Mn_{1.75}Co_{2.25}C$ - See 6153.

6041 PRODUCTION OF FERROELECTRIC MONOCRYSTALS ZONE RECRYSTALLIZATION by O. P. Kramarov (Rostov-on-D State U.); Soviet Phys.-Cryst., Vol. 4, pp. 101-104, Jan. 19

The growth of large single crystals of $BaTiO_3$ by zone recrystallization is discussed. A vertical oven with a large temperatur gradient is employed. A polycrystalline rod up to 50 mm long and 3-5 mm in diameter is centered in the oven by means of platinum holders and after stable temperature conditions are achieved the sample is moved at a rate of 1 to 20 mm/hour. After an appropriate number of cycles, the oven and sample are cooled together. The nucleation kinetics have also been examined by heating the samples without moving them. Three sharply defined regions have been found. Single crystals of (Ba, Pb) TiO_3 have been grown and the method can be used to grow single crystals of materials such as corundum.

6042 METHOD OF FORMING THIN FILMS OF BARIUM TITANATE by C. Feldman (USA); U. S. Pat. 2,922,730, Issued Jan. 26, 1960

An evaporative technique for forming films of ferroelectric barium titanate ($BaTiO_3$) 1 to 2 microns thick which have a dielectric behavior similar to that of bulk barium titanate is described. A source of barium oxide (BaO) and titanium dioxide (TiO_2) such as a tungsten filament coated with $BaTiO_3$, is heated in a vacuum above the vaporization temperature of $BaTiO_3$. The BaO constituent vaporizes first and deposits on a refractory substrate such as platinum, alumina, or silicon carbide. When the vaporization is carried to completion, the coating consists of BaO at the substrate-film interface and TiO_2 at the film-air interface with varying compositions in between. The coated substrate is then heated in an oxygen atmosphere at some temperature between 1000 and 1500°C, preferably 1200 to 1300° for a time sufficient to cause the constituents to react and for $BaTiO_3$. A device which can be used as a memory element, a thermal detection element, a dielectric amplifier, a non-linear electrical circuit element, or as a condenser can be made by evaporating the $BaTiO_3$ film on an electrically conductive substrate and then applying an electrode to the other surface.

6043 THE PREPARATION OF CRYSTALS OF TRIGLYCINE SULFATE AND THEIR PHYSICAL PROPERTIES by V. P. Konstantinova, I. M. Sil'vestrova, and K. S. Aleksandrov (Inst. Cryst.); Soviet Phys. - Cryst., Vol. 4, pp. 63-67, Jan. 196

The growth of large single crystals of the ferroelectric triglycine sulfate from aqueous solutions by the method of temperature lowering is discussed. Measurements of the piezoelectric modeli, elastic constants, and dielectric susceptibilities of these crystals are presented and the measuring techniques employed are described.

6044 ARC-IMAGE FURNACE FOR GROWTH OF SINGLE CRYSTALS by R. E. deLaRue and F. A. Halden (Stanford Res. Inst.); Rev. Sci. Instr., Vol. 31, pp. 35-38, Jan. 1960

A carbon arc-image furnace for growing single crystals of refractory compounds is described. The image furnace is unique for this application since it provides a sharply defined hot zone, excellent atmosphere control, and complete freedom from contamination during crystal growth. General operating and performance characteristics of the furnace are given. Single crystal boules of rutile, varying from 3 to 6 mm in diameter and from 18 to 50 mm in length have been grown in both argon and pure oxygen atmospheres.

6045 BERYLLIUM OXIDE "FLAGPOLE" WHISKERS by P. L. Edwards and R. J. Happel, Jr. (U. S. Nav. Ord. Lab.); Bull. Am. Phys. Soc. Ser. II, Vol. 5, p. 49 (A), Jan. 27, 1960

The growth of beryllium oxide whiskers with a sphere at the end, called "flagpole" whiskers, by heating beryllium metal to 1450°C in the presence of hydrogen or helium containing traces of water vapor was reported. Some of the flagpole whiskers have straight sides with diameters of 1μ and greater, lengths to 1 mm, and are topped with balls of 10-100μ diam. Other whiskers are tapered toward the base. As seen in the microscope, the spheres appear to be oxide-covered beryllium, but are hollow on the tapered whiskers, and apparently are also hollow on the others. It was suggested that the whiskers are grown as follows: the beryllium vapor condenses forming a molten ball, the surface of which then oxidizes. At the interface between the ball and the substrate oxidation is assumed to occur in such a manner, perhaps by the formation of a screw dislocation, as to promote the growth of an oxide whisker which pushes the ball away from the container. The growth takes place at the ball-whisker junction utilizing beryllium from the ball and oxygen from the water in the wet atmosphere. As the beryllium is used from the sphere, the sphere is prevented from collapsing by the oxide on its surface. It is possible in this way to account for the empty sphere at the top of the whiskers.

CRYSTAL SURFACES

Properties of Solid Oxides - See 6057.

6046 MASS-SPECTROMETRIC DETERMINATION OF THE AMOUNT AND COMPOSITION OF GASES ADSORBED ON THE SURFACE OF GERMANIUM AND SILICON MONOCRYSTALS by V. M. Kozlovskaya; Soviet Phys. - Solid State, Vol. 1, pp. 940-946, Jan. 1960

Studies of the nature, amount, and composition of gases evolved by silicon and germanium are discussed. The effect of etching on the adsorption of gases was also investigated. It was found that the mass-spectrometric technique can be used to make detailed studies of the adsorption properties of semiconductor surfaces.

Effect of Ion Adsorption on Long Term Relaxation Processes in the Field Effect in Germanium - See 6128.

Gas Absorption by Vacuum Evaporated Magnetic Films - See 6149.

Crystal Wafer Slicer - See 6306 (New Product Section).

6047 SHAPES OF ETCH HILLOCKS AND PITS AND THEIR CORRELATION WITH MEASURED ETCH RATES by B. A. Irving (Assoc. Elec. Ind.); J. Appl. Phys., Vol. 31, pp. 109-111, Jan. 1960

The factors which govern the occurrence and stability of etch hillocks and pits are discussed. Batteman's original analysis (see 1439) has been reconsidered and extended to account for all the crystallographic facets of etch hillocks and pits produced by a dilute hydrogen peroxide-hydrofluoric acid etchant on germanium surfaces. The treatment should be valid for other etchants and materials but suitable data are not available.

6048 RESEARCH DIRECTED TOWARD THE INVESTIGATION OF SILICON AND SILICON-CARBIDE SURFACES by J. A. Dillon, Jr. and R. M. Oman (Brown U.); U. S. Gov. Res. Rep, Vol. 33, p. 91 (A), Jan. 15, 1960 PB 143 632

An investigation of the properties of SiC surfaces following chemical treatments is discussed. Differences in etching are presumably due to the asymmetry in atomic species on opposite faces. There appeared to be no correlation between this etching behavior and such gross surface properties as defect density and stepped structure.

6049 ION-BOMBARDMENT ETCHING OF SILICON AND GERMANIUM by J. A. Dillon, Jr. and R. M. Oman (Brown U.); J. Appl. Phys., Vol. 31, pp. 26-28, Jan. 1960

Ion-bombardment-induced etch pits on silicon and germanium surfaces are discussed. Electron-microscope photographs of a germanium single crystal surface subjected to prolonged argonion bombardment under conditions used for surface cleaning disclosed etch patterns of a type completely different from those observed after chemical etching alone. The dimensions and distribution of the bombardment-induced pits were such that the patterns were not detectable either with an optical microscope or by low-energy electron diffraction. Approximately 95 percent of the surface remained undamaged. Bombardment of silicon and germanium at 500 ev for prolonged periods at higher current densities produced a different type of etching which may be associated with screw-type dislocations.

Sputtering of Semiconductors and Metals by Low Energy Argon Ions - See 6052.

ENVIRONMENTAL EFFECTS

Behavior of InSb Surfaces During Heat Treatment (Preferential Evaporation of Sb) - See 6021.

Alpha Particle Bombardment of Rhombic Sulfur - See 6113.

6050 INFRARED STUDIES OF ELECTRON IRRADIATED SILICON I. by J. W. Corbett, G. D. Watkins, and R. M. Chrenko (GE Res. Lab.); Bull. Am. Phys. Soc., Vol. 5, Ser. II, pp. 25-26 (A), Jan. 27, 1960

The IR absorption spectrum (1.4-14μ) of silicon irradiated at room temperature with 1.5 mev electrons was discussed. A sharp band at 12μ with an intensity roughly proportional to the concentration of dissolved oxygen originally in the silicon has been observed. The production rate of this band vs. irradiation correlates with that of the defect previously studied in spin resonance (A center) and in electrical measurements (net acceptor at E_c-0.17 ev), which has been shown to be strongly depend-

ent upon oxygen content. The annealing behavior of the 12μ band is similar to that of the other measurements, again suggesting that they arise from the same defect. In a sample enriched with 14 percent O^{18}, a small subsidiary peak is observed which identifies the 12μ absorption as arising from the vibration of a single oxygen atom. These data lend support to the model proposed from spin resonance studies that the A center, which is the dominant defect produced by irradiation in pulled silicon, involves an oxygen atom trapped in a lattice vacancy.

6051 INFRARED STUDIES OF ELECTRON IRRADIATED SILICON II. by G. D. Watkins, J. W. Corbett, and R. S. McDonald (GE Res. Lab.); Bull. Am. Phys. Soc., Vol. 5, Ser. II, p. 26 (A), Jan. 27, 1960

The annealing of the 12μ band produced in silicon by room temperature irradiation with 1.5 mev electrons (see 6050) was discussed. The first stage (~300°C) consists of the disappearance of the 12μ band and the emergence of a new band at 11.3μ of approximately the same intensity. It is primarily in this stage that the spin resonance center anneals and electrical properties recover. It is clear, however, that the sample has not been returned to its initial state. During subsequent higher temperature annealing (~500°C), the 11.3μ band disappears and a succession of bands between 11.3 and 9μ band emerge and disappear. During the second stage the 9μ band associated with oxygen in its original state is also observed to diminish. A model of these annealing stages which is also consistent with the identification of the 12μ band as arising from an oxygen trapped in a lattice vacancy was presented.

6052 SPUTTERING OF METALS AND SEMICONDUCTORS BY LOW ENERGY ARGON IONS by N. Laegreid and G. K. Wehner (Gen. Mills); Vacuum, Vol. 9, p. 300 (A), Nov. 1959/Jan. 1960

Measurements of sputtering yields for polycrystalline semiconductor and metal targets under normally incident A^+ ion bombardment in the energy range from 30 to 800 ev in a low pressure (2-5μ) high density argon plasma created in a demountable low voltage hot cathode discharge tube were reported. The yields, determined by measuring the weight loss of spherical targets immersed like large Langmuir probes in the plasma, are independent of gas pressure (below p = 30μ), ion current density, and target temperature. At 100 ev ion energy, the yields range from 0.06 atoms/ion for Si to 0.6 atoms/ion for Ag.

6053 RANGE OF 1-10 KEV ELECTRONS IN SOLIDS by C. Feldman (U. S. Nav. Res. Lab.); Phys. Rev., Vol. 117, pp. 455-459, Jan. 15, 1960

Measurements of the range of 1-10 kev electrons in metals and phosphors obtained by recording the light output as a function of energy from a sample consisting of a metallic layer deposited on a transparent phosphor layer are reported. The measurements lead to the development of the following range-energy expression: $R = 250(A/\rho Z^{n/2})E^n$, where $n = 1.2/(1-0.29 \log_{10} Z)$, E = energy in kev, R = range in angstroms, and A, ρ, Z have their customary meaning. This differs from the usual range expression in the dependency of n on Z. Usually n is assumed to be independent of material. This dependency can be justified on the basis of Bethe's theory of electron stopping power.

6054 ELECTRON-ELECTRON COLLISION INTERPRETATION OF CHARACTERISTIC ENERGY LOSSES IN SOLIDS by E. J. Sternglass (Westinghouse Res. Labs.); Bull. Am. Phys. Soc., Ser. II, Vol. 5, pp. 68-69 (A), Jan. 27, 1960

The dependence of the principal electron energy losses on ang of scattering θ has been regarded as conclusive evidence for t excitation of plasma oscillations in solids. However, it was demonstrated that the same behavior is to be expected if these losses are assumed to accompany the ionization of electrons in shells next to the outermost, bound with an energy of the orde of the theoretical plasmon energy. For example it was shown that measurements on Al films are consistent with either interpretation. The remaining aspects of the characteristic losses can also be explained in terms of individual excitation and ionization processes, so that this phenomenon may be understood without introducing any collective interactions.

6055 RELATION BETWEEN ELECTRON ENERGY DISSIPATIO AND SECONDARY EMISSION IN SOLIDS by H. Kanter (We inghouse Res. Labs.); Bull. Am. Phys. Soc., Ser. II, Vol. 5 p. 69 (A), Jan. 27, 1960

Determination of electron energy dissipation as a function of depth by means of electron penetration experiments on thin fi of C and Al at energies below 10 kev and by similar measurements in the backward direction was discussed. While at low primary energies, the rate of energy loss per unit foil thickne dE/dx, is roughly constant in the first half of the practical ra with increasing energy dE/dx shows an increasingly pronounc maximum at about one-half the practical range. A direct pro portionality exists between dE/dx at the surface and the yield of secondary electrons (SE). Per SE emitted, dx/dE is 2.7 ev in Al and 4 ev/A in C. The actual energy expended per SE formed in the solid calculated from this data depends on SE es cape depth and surface transmission. For sufficiently high en gies, the energy dependence of the yield of SE was found to approach that of the rate of energy loss per unit path-length calculated from the Bohr-Bethe theory. With decreasing ene gies, the SE yield increases more rapidly, revealing the importance of primary scattering in SE production.

Characteristic Energy Losses In Metal Films - See 6177.

6056 ANNEALING OF γ-RAY DAMAGE IN GERMANIUM by T. Asada, H. Saito, K. Omura, and T. Oku (Osaka U.); and M. Oka (Shimane U.); J. Phys. Soc. Japan, Vol. 15, pp. 93-94, Jan. 1960

The isothermal annealing, in the temperature range 10-55°C germanium single crystals irradiated with γ-rays from Co-60 i discussed. The variation of conductance with time was measu and it was found that, at a given annealing temperature, the conductance initially increased, then decreased to a certain value, and finally increased asymptotically to a final value. A modification of the model proposed by Fletcher and Brown may be used to explain these observations. From an analysis these curves, the activation energies for direct recombinatio of vacancy-interstitial pairs, for the diffusion of interstitial atoms, and for diffusion of vacancies are found to be 0.765 e 0.741 ev, and 1.250 ev, respectively.

SOLID STATE PHYSICS

GENERAL

057 PROPERTIES OF SOLID OXIDES by C. G. Harman (Battelle Mem. Inst.); U. S. Gov. Res. Rep., Vol. 33, p. 91 (A), Jan. 15, 1960 PB 143 943

A literature survey of the properties of all known solid oxides is presented. The data are arranged in the order in which the elements appear in the periodic table. Some of the data are very old, and are of limited usefulness, but are included for the sake of completeness. It is pointed out that, even after inclusion of all published data without regard to reliability, many important gaps exist in the literature on the properties of many of the materials.

CRYSTAL PHYSICS

(Including Energy Band Structure)

058 APPLICATION OF THE EQUIVALENT ORBITAL METHOD TO THE STUDY OF BAND STRUCTURE IN $A^{III}B^{V}$ COMPOUNDS by A. I. Gubanov and A. A. Nran'yan (Physico-technical Inst.); Soviet Phys. - Solid State, Vol. 1, pp. 956-963, Jan. 1960

The tight-binding method and the method of equivalent orbitals for studying band structure are compared and use of the latter to obtain analytical expressions representing the dependence of the energy of the wave vector of the four-valence bands and the four conduction bands in $A^{III}B^{V}$ compounds, correct to coefficients, is described. The data obtained are analyzed to determine the characteristics of the band structure for all $A^{III}B^{V}$ compounds; in particular, it is established that on passing from Group-IV elements to $A^{III}B^{V}$ compounds, an additional forbidden zone separating the third and fourth bands is created both inside the four-valence bands and inside the four conduction bands.

059 GENERALIZATION OF BAND THEORY TO INCLUDE SELF-ENERGY CORRECTIONS by G. W. Pratt, Jr., (Lincoln Lab.); Bull. Am. Phys. Soc., Ser. II, Vol. 5, pp. 59-60 (A), Jan. 27, 1960

A one-particle Schrödinger-like equation whose eigenvalues in certain cases are identical with the energies of the many electron states of a semiconductor or insulator, including self-energy corrections, was described. The one-particle Hamiltonian is expressed in terms of the Coulomb interaction as modified by polarization processes. The relation between the modified Coulomb interaction and the dielectric function, which is the generalization of the classical dielectric constant, was given. It was suggested that the one-particle equation including self-energy effects might be solved in practice by the pseudopotential method of Phillips.

060 EXPERIMENTAL INVESTIGATION OF CONDUCTION BAND OF GaSb by A. Sagar (Westinghouse Res. Labs. and U. Pittsburgh); Phys. Rev., Vol. 117, pp. 93-100, Jan. 1, 1960

The conduction band of GaSb has been investigated by making the following measurements on a number of n-type samples with different carrier concentrations: (1) Hall effect and conductivity between 1.5°K and 370°K; (2) the change of resistance and Hall effect of the samples under hydrostatic pressure (up to 14×10^9 dynes/cm^2) at room temperature; and (3) the change of resistance due to uniaxial stress between 77°K and 370°K. The data can be explained on the basis of a double conduction band for this material with the lowest band-minimum in the center of the Brillouin Zone characterized by spherical constant-energy surfaces and the next minima along [111] directions in k-space characterized by ellipsoidal constant-energy surfaces. The data can be further interpreted by assuming that the deformation potentials for the two bands in GaSb are similar to those of the corresponding bands in n-type germanium. The energy separation of the two bands at room temperature is estimated to be about 0.08 ev. The observed temperature dependence of the piezoresistance could be explained by assuming that the energy separation, ΔE, changes with temperature at a rate $(d\Delta E/dT) \approx -3 \times 10^{-4}$ ev/°C. Throughout the analysis, the relaxation times for the electrons in the two bands are assumed to be independent of energy.

6061 OBSERVATION OF THE ENERGY GAP BY LOW-TEMPERATURE PENETRATION DEPTH MEASUREMENTS IN LEAD by M. P. Sarachik, R. L. Garwin, and E. Erlbach (IBM); Phys. Rev. Lett., Vol. 4, pp. 52-55 (L), Jan. 15, 1960

Sensitive measurements made in the temperature range 1.35 to 4.2°K of the penetration of a 2.2 mc magnetic field through thin lead films which vary in thickness by a factor of three are analyzed. Energy gaps of 4.93 kT_c and 5.4 kT_c have been found by comparing the experimental data with the Bardeen-Cooper-Schrieffer (BCS) predictions of $\lambda_L(T)/\lambda_L(0)$ and with the BCS predictions of $\lambda_\infty^{3/2}(T)/\lambda_\infty^{3/2}(0)$ for various energy gaps. Better agreement with the experimental data is found for the 4.93 kT_c value.

6062 VALLEY-ORBIT SPLITTING IN GERMANIUM FROM EFFECT OF STRAIN ON THE ELECTRON SPIN RESONANCE by D. K. Wilson and G. Feher (Bell Labs.); Bull. Am. Phys. Soc., Ser. II, Vol. 5, p. 60 (A), Jan. 27, 1960

Electron spin resonance experiments performed at 1.2°K and 9000 mc on localized electrons in germanium subjected to elastic strains up to 10^{-3} were described. Assuming a value for the deformation potential of 18 ev, the valley-orbit splitting (i.e., singlet-triplet spacing) for arsenic is 4.2 ± 0.2 milli-ev in agreement with piezoresistance measurements; and for phosphorus 2.9 ± 0.2 milli-ev. From the g anisotropy in an arsenic-doped sample under strain, for H perpendicular to the valley axis, $g_\perp = 1.92 \pm 0.05$, and for H parallel to the valley axis, $g_{||} = 0.87 \pm 0.05$.

6063 VALLEY-ORBIT SPLITTING IN GERMANIUM FROM STRAIN-INDUCED SHIFT OF LYMAN SPECTRUM by G. Weinreich and H. G. White (Bell Labs.); Bull. Am. Phys. Soc., Ser. II, Vol. 5, p. 60 (A), Jan. 27, 1960

An elastic strain applied to a germanium crystal splits all the donor states; but the ground state behaves differently from the p states due to the appreciable valley-orbit interaction, and as a result the absorption lines of the Lyman series (which are in the region of 100 cm^{-1}) also split. The line shifts become nonlinear with strain at sufficiently high strains because of interaction between the singlet and triplet components of the ground state, and from the amount of this nonlinearity the energy separation between the singlet and the triplet can be calculated. Applied compressions up to about 3×10^{-4} split the lines by up to six times the line width without broadening. For the total singlet-triplet splitting values of 3.0 ± 0.3 Mev for phosphorus donors and 3.9 ± 0.6 Mev for arsenic donors were obtained.

6064 ENERGY LEVELS IN GOLD-DOPED P-TYPE GERMANIUM by P. P. Debye, C. A. Klein, and G. Rupprecht (Raytheon); Bull. Am. Phys. Soc., Ser. II, Vol. 5, p. 62 (A), Jan. 27, 1960

Hall- and pulsed-field effect studies on p-type Ge samples with Au concentration ranging from 10^{14} to almost 10^{16} cm^{-3} as a function of temperature were described. The program aimed at providing a better description of the donor level at $E_V + 0.041$ ev as well as the acceptor level at about $E_V + 0.14$ ev, and at improving the accuracy of evaluating the concentration of both the gold and the counter-doping. A correct appreciation of the statistical factors g_D and g_A associated with the two levels appears to be critical. Hall-effect experiments appear able to lead to this information, if care is taken in estimating the Hall coefficient factor $\mu H/\mu$ and applying adequate statistics to the multilevel situation in Au-doped Ge. Presently available results point towards $g_D \sim 1/2$, indicating that the valence electron of substitutional Au in the Ge lattice has an S-state character, as might be expected on the basis of the tetrahedral bonding model. Besides yielding accurate majority carrier capture cross sections, the pulsed field effect approach provides straightforward indications on the level's position and density.

6065 INTERNAL IMPURITY LEVELS IN P-TYPE SILICON by S. Zwerdling, K. J. Button, and B. Lax (Lincoln Lab.); Bull. Am. Phys. Soc., Ser. II, Vol. 5, p. 62 (A), Jan. 27, 1960

New transitions to discrete impurity levels within the valence bands associated with the split-off $p_{1/2}$ band were described. Infrared measurement of the spin-orbit splitting of this band gave a value $\Delta = 0.044$ ev and a hole mass $m^* = 0.21m_0$ for the $p_{1/2}$ band at $k = 0$. Observations were made for both boron and aluminum impurities of $\sim 5 \times 10^{15}/cm^3$. The levels fit the Rydberg formula $E_n = 13.6m^*/n^2\kappa^2m_0$, yielding the effective mass and the series limit E_I^* for hole excitation from the gap ground state to the band maximum. The spin-orbit splitting is therefore $\Delta = E_I^* - E_I$, where the E_I values are known. Linear Zeeman splitting was also observed from the 2p', 3p', and 4p' levels. The effective mass calculated from the $\bar{E} \perp \bar{B}$ Zeeman spectrum for the 2p' level was in good agreement with the Rydberg effective mass. The unexpected splitting for $\bar{E} \parallel \bar{B}$ for a simple spherical band reflects the complexity of the ground state. Transitions to bound Landau states above E_I^* were also found. The $p_{1/2}$ band mass differs from the value deduced from cyclotron resonance, $m^* = 0.25m_0$.

Surface States on Germanium - See 6129

6066 CRYSTAL POTENTIAL AND ENERGY BANDS OF SEMICONDUCTORS. II. SELF-CONSISTENT CALCULATIONS FOR CUBIC BORON NITRIDE by L. Kleinman and J. C. Phillips (U. Calif.); Phys. Rev., Vol. 117, pp. 460-464, Jan. 15, 1960

A self-consistent crystal potential is constructed for cubic BN. Exchange is included according to the Slater free-electron approximation. The effect of the heteropolar character of the potential is included explicitly in an approximately self-consistent treatment of the valence-electron charge density. The energy gap is found to be about twice that of diamond, consistent with the results of other zincblende crystals and their diamond-type analogs. The maximum of valence band and the minimum in the conduction band are at the center and (100) face of the Brillouin zone, respectively. It is suggested that the heteropolar potential splits the valence band into two sub-bands. The lower sub-band width is about 5 ev, while the higher (which contain three times as many states) has a band width of about 4 ev. The energy gap between the sub-bands is about 10 ev. The effect should be common to all zincblende crystals and may be observable by soft x-ray emission.

Energy Band Structure of Tellurium - See 6178.

Energy Band Structure of Gallium Antimonide - See 6068.

Energy Band Structure of Indium Phosphide - See 6111.

Energy Band Structure of the Cuprous Halides - See 6067.

Scattering of Phonons by Lattice Defects - See 6200.

6067 ELECTRONIC STRUCTURE OF THE CUPROUS HALIDES by F. Herman and D. S. McClure (RCA Labs.); Bull. Am. Phys. Soc., Ser. II, Vol. 5, p. 48 (A), Jan. 27, 1960

The optical absorption spectra of CuCl, CuBr, and CuI have been interpreted with the aid of crystal field theory and energy band theory. According to this interpretation, the weak absorption peak in the spectra of each of these compounds lying at about 3 ev is due to a $3d^{10}$ to $3d^9$ 4s transition within the Cu^+ ion; the strong absorption peak occurring in CuCl at 6.5 ev, in CuBr at 5.6 ev, and in CuI at 4.9 ev is due to the transfer of an electron from the halide to the Cu^+ ion. In the language of energy band theory, the lowest conduction band and the highest valence band arise from the 4s and 3d states of the Cu^+ ion, respectively, while the next lowest valence band arises from the 3p Cl^-, 4p Br^-, and 5p I^- states. There are two forbidden bands, one between the 4s and 3d Cu^+ bands, and another between the 3d Cu^+ and the p halide bands; the optical energy gap is determined by the width of the former. The previous inability to reconcile the optical gap of CuBr with those of the other members of the isoelectronic sequence Ge-GaAs-ZnSe-CuBr results from the reversal in order of the cation 3d and anion 4p bands. (In Ge, GaAs, and ZnSe, the 3d bands of Ge, Ga, and Zn appear to lie below the 4p bands of Ge, As, and Se.).

ELECTRICAL PROPERTIES - GENERAL

6068 EFFECTS OF HIGH HYDROSTATIC PRESSURE ON THE ELECTRIC PROPERTIES OF N-TYPE GaSb by A. Sagar, M. Pollak, and R. W. Keyes (Westinghouse Res. Lab.); Bull. Am. Phys. Soc., Ser. II, Vol. 5, p. 63 (A), Jan. 27, 1960

Measurements of the electrical conductivity, Hall constant, and piezo-resistance tensor Π of several samples on n-type GaSb (2 to 80 x 10^{17} donors/cm^3) as functions of hydrostatic pressure up to 12000 kg/cm^2 at 300°K were presented. The results are roughly as follows, with details depending considerably on the impurity content. The conductivity decreases rapidly at first, and at high pressures levels off at about one-third of the initial conductivity. The Hall constant passes through a flat maximum and then decreases to one-half or less of its initial value at high pressures: $(\Pi_{11} + 2\Pi_{12})$ decreases rapidly initially and approaches zero at high pressure. Π_{44} is about 80 at atmospheric pressure, increases with increasing pressure, and approaches a value of about 200 at high pressures (in units 10^{-12} cm^2/dyne). $\Pi_{11} - \Pi_{12}$ is small throughout the entire pressure range. These results can be understood in terms of a recently proposed model of the band structure. According to this model there are electrons in both the (000) and (111) conduction band extrema at atmospheric pressure; the (000) energy increases much more rapidly with increasing pressure than the (111) energy.

6069 SOME RESULTS ON THE DIFFUSION OF IMPURITIES AND THEIR EFFECT ON THE ELECTRICAL PROPERTIES OF GALLIUM ANTIMONIDE By B. I. Boltaks and Yu. A. Gutorov

(Inst. for Semicon.); Soviet Phys. - Solid State, Vol. 1, pp. 930-935, Jan. 1960

Studies of the effect of In, Sb, Se, and Te on the electrical properties of GaSb are reported. Measurements were carried out at temperatures from -120 to +680°C. The diffusion of In, Sn, Sb, Se, and Te in GaSb which had been diffusion-annealed at various temperatures was also studied. The results show that there is a definite correlation between the diffusion-activation energy of these impurities and their effect on the electrical properties of gallium antimonide.

6070 FORMATION OF CESIUM ANTIMONIDE. I. ELECTRICAL RESISTIVITY OF THE FILM OF CESIUM-ANTIMONY SYSTEM by K. Miyake (Nippon Tel. and Tel. Pub.); J. Appl. Phys., Vol. 31, pp. 76-81, Jan. 1960

The preparation of Cs-Sb films in which the atomic ratio of Cs to Sb varied from 0.91 to 4.86 and measurements made on these films are reported. The electrical resistance was reproducible for all the samples except $Cs_{3.30}Sb$, and the temperature coefficients of resistance were negative for all the samples except $Cs_{0.91}Sb$. It was found that four compounds, CsSb, Cs_3Sb_2, Cs_2Sb and Cs_3Sb, having a remarkably high resistance could be formed. The observed values of the electrical resistivity at 20°C and the thermal activation energy associated with conductivity were 1.84×10^3 ohm-cm, 0.61 ev for $Cs_{1.02}Sb$; 1.82×10^3 ohm-cm, 0.76 ev for $Cs_{3.02}Sb_2$; 2.85×10^3 ohm-cm, 0.62 ev for $Cs_{2.02}Sb$; and 1.95×10^3 ohm-cm, 0.77 ev for $Cs_{3.33}Sb$. Alloys with atomic ratio above 5 were not formed.

6071 ANISOTROPY OF CARRIER TRANSPORT IN SEMICONDUCTOR BICRYSTALS by H. F. Matare (Sylvania Res. Labs.); Solid State Phys. Electronics and Telecommun., Vol. 1, Part 1, pp. 73-96, 1960

An extensive study of the electrical effects of dislocation in semiconductor bicrystals grown with a known orientation is presented. Characteristics of the dangling bonds introduced by lattice misfit in the dislocation are enumerated. The temperature-independent low sheet resistivity is due to an overlap of the wave functions of the dangling bonds. The valence band at the grain boundary approaches the Fermi level for the cases of conductivity in the dislocation pipes, and perpendicular to the tilt axis. Measurements show clearly that the dangling bond levels primarily contribute to hole transport, since they give almost constant values of conductance over a wide range of impurity values.

6072 ELECTRICAL AND PHOTOELECTRICAL PROPERTIES OF GRAIN BOUNDARY LAYERS BY O. Weinreich, H. F. Matare, and B. Reed (Sylvania Res. Labs.); Solid State Phys. Electronics and Telecommun., Vol. 1, Part 1, pp. 97-108, 1960

Two properties of natural grain boundaries in germanium crystals are discussed: the photoeffect transverse to the boundary and the conduction along the grain boundary region (sheet conductance). Measurements were made on bicrystals grown with [100] seeds symmetrically tilted about the [001] axis at angles of 15 to 30°. Two important experimental results were obtained: (1) the existence of a $p\text{-}p^+\text{-}p$ structure across the grain boundary in p-type Ge, and (2) the independence of the grain boundary sheet conductance with respect to impurity concentration. These strongly support the belief that it is not segregation of impurities but lattice misfit at the grain boundary which is the predominant factor in the presence of acceptor levels in Ge bicrystals.

6073 THE INFLUENCE OF GRAIN BOUNDARIES ON THE DIFFUSION OF MINORITY CARRIERS by T. Figielski and L. Sosnowski (Polish Acad. of Sci.); Solid State Phys. Electronics and Telecommun., Vol. 1, Part 1, pp. 109-116, 1960

The two types of behavior of grain boundaries in n-type germanium and n-type silicon in which holes were generated by a small light spot are described. The first type of boundary introduces a discontinuous drop in the hole concentration because of the increased rate of recombination at the boundary and no photo-emf is observed. The second type of boundary is related to the occurrence of a maximum on the hole concentration vs. distance curve; the boundary does serve as a source of photo-emf and has abnormally large diffusion lengths. X-ray investigations as to physical differences between the two types of boundaries are correlated with their properties.

DIELECTRIC PROPERTIES

(Including Ferroelectric Properties)

6074 ELECTROMAGNETIC PROPERTIES OF INSULATORS. I. by V. Ambegaokar and W. Kohn (Carnegie Inst. Tech.); Phys. Rev., Vol. 117, pp. 423-431, Jan. 15, 1960

The response of a perfect insulator to weak external electromagnetic fields of long wavelength is discussed from a many-particle point of view. The Coulomb interaction between all electrons is treated to all orders of perturbation theory and the structure of the corresponding Feynman graphs is analyzed. As a result of this graphical analysis it is shown that the response of the many-particle system to long-wavelength external fields of arbitrary polarization is completely described by a single frequency-dependent dielectric constant. In the limit of long wavelengths as well as low frequencies the magnetic effects of an external field on the system are included in terms of a magnetic permeability.

6075 DIELECTRIC CONSTANT MEASUREMENTS IN GERMANIUM AND SILICON AT RADIO FREQUENCIES AS A FUNCTION OF TEMPERATURE AND PRESSURE by M. Cardona, W. Paul, and H. Brooks (Harvard U.); Solid State Phys. Electronics and Telecommun., Vol. 1, Part 1, pp. 206-214, 1960

Measurements of the variation of the r-f dielectric constant in silicon and germanium crystals with pressure up to 10,000 kg/cm^2 for Si and up to 6000 kg/cm^2 for Ge are reported for Si at 263°K and Ge at 77°K. The corrected residual variation is a decrease of 1% ± 0.2% in 10,000 kg/cm^2 for Si and 0% ± 0.8% in 10,000 kg/cm^2 for Ge. The variation of the dielectric constant of Si has been measured between 4°K and 300°K, and of Ge between 4°K and 77°K; the results cannot be interpreted fully in terms of a lattice-expansion effect but show a large explicit temperature dependence.

6076 ON THE MICROWAVE DIELECTRIC DISPERSION AND LOSS IN HIGH-PERMITTIVITY FERROELECTRICS by H. Diamond (U. Mich.); Bull. Am. Phys. Soc., Ser. II, Vol. 5, p. 83 (A), Jan. 27, 1960

Measurements of complex permittivity vs. frequency made on several ferroelectrics from 0.5 mc to 4000 mc were reported. Dynamic permittivity spectra of $BaTiO_3$ crystals with the polar axis aligned with, and also transverse to, the high-frequency fields show a complex dimensional resonance spectrum in the 1-mc to 20-mc frequency range. For frequencies higher than 20 mc both the parallel and transverse permittivity is reduced to about one-half of that at the low frequency limit, consistent with the Devonshire theory for the clamping of single crystals. Microwave data to 4000 mc fail to reveal further dispersion. On the other hand, data on several polycrystalline ferroelectric compositions including $BaTiO_3$, $Ba_xSr_{1-x}TiO_3$, $Pb_xSr_{1-x}TiO_3$, $PbTiO_3$, and $Cd_2Nb_2O_7$ show substantial reductions in permitivities at microwave frequencies. The disparity between the single crystal and polycrystal data is ascribed directly to the effects of electrostrictive and piezoelectric interactions at grain boundaries and domain walls. The effect of such loss mechanisms on reducing the apparent permittivity at high frequencies is shown to be more pronounced the higher the permittivity of the dielectric. Data on the change in incremental permittivity and loss at microwave frequencies for polycrystalline ferroelectrics under static and low-frequency biasing fields were also presented.

6077 THEORY OF THE ELECTRIC FIELD VARIATION OF INCREMENTAL PERMITTIVITY IN PEROVSKITE-TYPE FERROELECTRICS by H. Diamond (U. Mich); Bull. Am. Phys. Soc., Ser. II, Vol. 5, p. 57 (A1, Jan. 27, 1960

A model for the case of polycrystalline ferroelectrics in which each crystallite is presumed to behave according to Devonshire's free energy functions was considered. The Curie temperatures for the individual grains are taken in a Gaussian distribution about some chosen temperature. The permittivity is obtained by averaging with this distribution over all of the crystallites. In accordance with the free energy function, it is assumed that the electric field induces a ferroelectric axis along the field direction in those crystallites of the distribution which are not ferroelectric at a given temperature. On the basis of experimental evidence, domains in the ferroelectric part of the distribution are presumed to be immobile. Despite the seemingly severe restriction imposed by the latter assumption, a large field sensitivity is predicted. Agreement between the theory and the experimental data is excellent for both parallel and transverse fields. It is concluded that the variation of incremental permittivity is associated with an induced ferroelectric state rather than being directly a property of domain processes, and that a large variation with field must necessarily be accompanied by strong thermal sensitivity.

6078 INFLUENCE OF X-RAYS ON THE ELECTRIFICATION OF NaCl CRYSTALS by A. Szaynok (Inst. Tech., Warsaw); J. Appl. Phys., Vol. 31, pp. 211-213 (L), Jan. 1960

It is reported that the electrical charges which are produced by the x-ray irradiation of pulverized NaCl crystals are predominantly positive. The pulverized salt particles were introduced from the top into a thermally isolated column, were made to fall through an electric field set up between a vertical pair of plane parallel condenser plates, and their paths were photographed. Particles which were not irradiated exhibited a symmetrical charge distribution and a mean charge per unit surface of 0.441 electron/sqμ. Mean charges of 5.84 electron/sqμ and 0.668 electron/sqμ were measured before and after photo-emission of electrons, respectively, in irradiated crystals with an F-center concentration of about 10^{16} cm^{-3}. Causes for the positive shift of the charge are discussed and it is suggested that the increase of mean charge in the dust clou is caused by the increase of lattice defects in the crystals as a result of the x-ray irradiation.

6079 THE NATURE OF SPACE CHARGE AND CURRENT FLO IN DIELECTRIC LAYERS BETWEEN CYLINDRICAL ELECTROD by R. D. Barnard (Case Inst. Tech.); Diss. Abstr., Vol. 20, p. 2862 (A), Jan. 1960

Steady state flow of single (majority) charge carriers in insulator media between cylindrical electrodes is analyzed. Appropriate boundary conditions for carrier density in metal and semiconductor electrodes are applied, and accurate general solutions of the nonlinear conduction-diffusion equation are developed. Because of transcendental complexity, and since current values in insulators are small, the problem is treated b perturbation theory as a zero-current electrostatic state with small current perturbations. Practical expressions, valid for large and small radii of curvature, for the inner potential, electric intensity, carrier density, charge transfer, and radia electric field stress within the dielectric are developed to zer and first order. Electron atmosphere distributions and adhesio stress phenomena, namely, the equilibrium charge transferred across cylindrical junctions (phase boundaries), electrical stresses at electrode-dielectric interfaces, and criteria for zer electric stresses at junctions, are investigated. Rectification resulting from space charge accumulation in insulators is also considered; the applied potential-resulting current relationshi is derived and the dependence of rectification characteristics on curvature and on electrode work functions is analyzed quan titatively. Finally, expressions exhibiting the dependence of barrier layer resistance and capacitance on curvature and on the chemical nature of electrodes are derived.

6080 IONIC PROPERTIES OF ELECTROLUMINESCENT ZINC SULFIDE by M. Ratner (IBM); Bull. Am. Phys. Soc., Ser. II, Vol. 5, p. 70 (A), Jan. 27, 1960

By the use of a photographic technique, simultaneous measurements of the instantaneous capacity and conductivity as functions of temperature (T), the maximum value of the applied voltage (V_m), and the frequency (f) have been made on dielectric cells of electroluminescent ZnS:Cu:Cl. This material behaves like a highly ionic semiconductor. The conductivity (σ follows the high-field ionic relationship: $\sigma = [N(ea)^2 \nu/kT \times \exp(-E/kT)] \cosh\{(ae/2lkT) V_m \sin(2\pi ft)\}$, where N is the concentration of lattice defects, a is the jump distance, ν is the characteristic lattice frequency, e is the electronic charg and l is the effective thickness of the cell. Experimentally found values are in agreement with those determined by other investigators: $\sigma \sim 10^{-9}$ ohm^{-1} cm^{-1}; $N \sim 10^{17}$ per cm^3, $\nu = 7 \times 10^7$ cps; E = 0.28 ev; a = 2×10^{-6} cm. The energy of the defects is ~5kT at high fields for these cells. Dielectric relaxation peaks are present at 1.5 and 30 kc, and in the neighborh of 1-10 cps. The low-frequency peak is ascribed to the actio of ultra-violet light, and the 1.5-kc peak is associated with the emission of green light. The mechanism responsible for th 30-kc peak has not been identified.

6081 ANOMALOUS DIELECTRIC LOSS IN AL_2O_3 by N. M. Tallan and D. P. Detwiler (Alfred U.); Bull. Am. Phys. Soc. Ser. II, Vol. 5, p. 49 (A), Jan. 27, 1960

Measurements of the dielectric loss of Linde flame-fusion grow single crystal Al_2O_3, made in vacuum between - 160°C and

DIELECTRIC PROPERTIES (Cont'd)

400°C at frequencies between 100 cps and 100 000 cps were reported. A characteristic loss peak whose activation energy and position on the temperature scale are dependent upon the previous treatment of the specimen is found in this region. Exposure to moist air, dry hydrogen, or HCl solution results in a large, broad loss peak near 400°C with an activation energy of approximately 0.5 ev. Heating in vacuum at 400°C results in a gradual sharpening of the loss maximum, together with a progressive shift to lower temperature, diminution of amplitude, and decrease of activation energy to a final value of about 0.3 ev. These changes are reversible. This behavior is attributed to the penetration of hydrogen along dislocation lines and its binding in the strained regions of the lattice surrounding the dislocation.

6082 SYSTEM $(Ba_{6-2x}R_{2x}^{+3})$ $(Nb_{9-x}M_{1+x}^{+3})$ O_{30}. III. STRUCTURAL DATA by R. S. Roth and P. H. Fang (NBS); Bull. Am. Phys. Soc., Ser. II, Vol. 5, p. 58 (A), Jan. 27, 1960

Compositions in the system $(Ba_{6-2x}R_{2x}^{+3})$ $(Nb_{9-x}M_{1+x}^{+3})$ O_{30} were described for the situation where x = 0, i.e., there is no R component, and M is any trivalent ion. A single phase can be prepared for M varying in size from Mn through Yb. For Y, Ho, and Dy this structure type apparently is only metastable, while for the larger M ions the structure does not occur at all. When R^{+3} is one of the larger rare earth ions from La^{+3} to Gd^{+3}, M is Fe^{+3}, and x varies from 0 to 1, the tungsten bronze structure occurs and ferroelectric and ferrimagnetic properties are observed. The tetragonal potassium tungsten bronze structure is based on a ratio of 6 large cations to 10 smaller (octahedrally coordinated) cations and 30 oxygen ions. The space group is P4/mbm and contains two large ions and two small ions in two-fold special positions 000, $\frac{1}{2}\frac{1}{2}$ 0 and 0 $\frac{1}{2}\frac{1}{2}$, $\frac{1}{2}$ 0 $\frac{1}{2}$, respectively, while the remaining four large ions are in $x\frac{1}{2}\frac{1}{2}$ + $x\frac{1}{2}$0 and the eight smaller ions in $xy\frac{1}{2}$. The hypothesis that the ferrimagnetic properties arise from the rare earth and iron ions occupying the two-fold special positions and that the ferroelectric properties arise from the Ba and Nb ions occupying the remaining cation positions in the structure was evaluated by comparison of calculated and observed x-ray powder diffraction data.

6083 EFFECT OF HYDROSTATIC PRESSURE ON THE FERROELECTRIC PROPERTIES OF TRI-GLYCINE SULFATE AND SELENATE by F. Jona and G. Shirane (Westinghouse Res. Labs.); Phys. Rev., Vol. 117, pp. 139-142, Jan. 1, 1960

The transition temperatures T_c of tri-glycine sulfate and isomorphous tri-glycine selenate are raised by the application of hydrostatic pressure. Up to 2700 atmos, the dependence of T_c on pressure is linear with a slope of 2.6×10^{-3} degrees/atmos for the sulfate and 3.8×10^{-3} degrees/atmos for the selenate. The Curie-Weiss law, $\epsilon_b \cong C/(T - T_c)$, is unaffected by pressure except for the shift in transition temperature. The curve of the spontaneous polarization is shifted accordingly along the temperature axis; in the vicinity of the transition point, the square of the spontaneous polarization depends linearly on temperature and pressure. The results are discussed in terms of the thermodynamic theory of ferroelectrics.

6084 SYMMETRY OF THE LOW-TEMPERATURE PHASE OF BARIUM TITANATE by E. Sawaguchi and M. L. Charters (Rutgers); Phys. Rev., Vol. 117, pp. 465-469, Jan. 15, 1960

In order to find the crystal symmetry of $BaTiO_3$ below -80°C, the domain patterns and optical properties have been examined using thin (111) plates specially prepared for this purpose. Four kinds of domains have been differentiated; these domains are optically uniaxial. The crystal symmetry proved to be rhombohedral. The effect of a d-c field on the domain configuration has been studied. Explanations for the strange dielectric and optical behavior which had been thought paradoxical are given.

6085 VARIATION IN FERROELECTRIC CHARACTERISTICS OF LEAD ZIRCONATE TITANATE CERAMICS DUE TO MINOR CHEMICAL MODIFICATIONS by R. Gerson (Clevite); J. Appl. Phys., Vol. 31, pp. 188-194, Jan. 1960

It is reported that lead zirconate titanate ceramics with certain 3- or 5- valent additions (lanthanum, neodynium, tantalum, and niobium) exhibit low aging of electrical and mechanical properties, a well-defined hysteresis loop, and high electrical and mechanical losses. Electron microscopic and electrical investigations on plain lead zirconate titanate and on a low-aging niobium modification are reported. As a result of the study, the changed properties of the substituted material have been explained as being due to domain wall motion under low electric field. The results of electrical measurements supporting this conclusion and a hypothesis accounting for the effects in terms of lattice vacancies are presented. The observation that the 3- or 5-valent additives cause greatly increased volume resistivity in the ceramic has not been satisfactorily explained.

6086 SYSTEM $(Ba_{6-2x}R_{2x})$ $(Nb_{9-x}Fe_{1-x})O_{30}$. I. FERROELECTRIC PROPERTIES by P. H. Fang, R. S. Roth, and H. S. Schofer (NBS); Bull. Am. Phys. Soc., Ser. II, Vol. 5, p. 57 (A), Jan. 27, 1960

Observation of ferroelectric properties in the system $2BaNb_2O_6$ + P where P denotes materials with perovskite structures, such as $BaZrO_3$, hybrid perovskite, such as Ba (Nb, Fe) O_3, or one of the rare earth ferrites of perovskite structure, such as compounds of the composition $(Ba_{6-2x}R_{2x})$ $(Nb_{9-x}Fe_{1+x})O_{30}$, was reported. Both ferroelectric and ferrimagnetic properties are found in the latter system in which R is one of the rare earth ions Nd, Sm, Eu, and Gd. Ferroelectric hysteresis loops were observed at room temperature for R = Nd. On heating and cooling, the dielectric constant and the spontaneous polarization show large temperature hysteresis near the critical temperatures where the dielectric constant shows a maximum or the spontaneous polarization vanishes. For Gd, Eu, and Sm the critical temperatures are about 180 and 120°C. For Nd, they are about -5 and +70°C. When R = Gd and x varies from 0 to 1, there is an increase of the critical temperatures for heating from -160 to +170°C. The data indicate a single phase region with both ferroelectric and ferrimagnetic properties in the system $BaNb_2O_6$ - Ba $(Nb_{0.5}, Fe_{0.5})$ O_3 - $GdFeO_3$.

6087 MODEL FOR SWITCHING AND POLARIZATION REVERSAL IN COLEMANITE by H. H. Wieder (U. S. Naval Ord. Lab.); J. Appl. Phys., Vol. 31, pp. 180-187, Jan. 1960

The characteristic properties of the displacement current transients obtained from ferroelectric colemanite crystals during polarization reversal are presented in detail and a phenomenological and semiempirical model of the switching mechanism is proposed. The model yields good agreement with the switching current dependence upon time, field amplitude, and ambient temperature. It is based upon random nucleation followed by extensive sidewise displacement of the nucleated 180° domains. A model based upon three dimensional growth of nucleated domains is shown to be in poor agreement with experiment.

Paramagnetic Resonance in Ferroelectric Materials - See 6166, 6167.

6088 DETERMINATION OF PIEZOELECTRIC PROPERTIES AS A FUNCTION OF PRESSURE AND TEMPERATURE by J. E. McKinney and C. S. Bower (NBS); J. Acoust. Soc. Am., Vol. 32, pp. 56-61, Jan. 1960

The determination of piezoelectric data for a mixed titanate system (82.0% $BaTiO_3$, 9.1% $CaTiO_3$, 3.6% $PbTiO_3$, and 4.4% TiO_2) by means of an apparatus intended to measure the dynamic compressibility of materials is described. The colibration constant, determined from measurements on specimens of known compressibility, involves the piezoelectric and dielectric constants of the ceramics used as transducers. The method is discussed and an operating equation for the apparatus is derived. Piezoelectric and dielectric constants have been measured as a function of temperature and pressure over the ranges -25 to 37.5°C and 0 to 1000 kg/cm^2. An apparent phase transition was observed near 5°C. The results are discussed qualitatively.

6089 EXPERIMENTAL INVESTIGATIONS IN THE SEARCH FOR NEW PIEZOELECTRIC SUBSTANCES by I. S. Rez, A. S. Sonin, E.E. Tsepelevich, and A. A. Filimonov (Central Sci. Res. Lab. for Piezoelectricity); Soviet Phys.-Cryst., Vol. 4, pp. 59-62, Jan. 1960

An investigation of the piezoelectric properties of 356 compounds is summarized. The compounds which were investigated are listed under the following headings: (1) Inorganic and complex compounds having a marked piezo effect; (2) Inorganic and complex compounds having a slight piezo effect; (3) Organic compounds having a marked piezo effect; and (4) Organic compounds having a slight piezo effect.

Piezoelectric Properties of Barium Titanate - See 6307 (New Product Section).

Dielectric Properties of Triglycine Sulfate - See 6043.

CARRIER PROPERTIES

(Including Recombination, Mobility, Etc.)

6090 MICROWAVE HEATING OF ELECTRONS IN SEMICONDUCTORS by B. V. Paranjape (La. State U.); Bull. Am. Phys. Soc., Ser. II, Vol. 5, pp. 60-61 (A), Jan. 27, 1960

Calculations of electron temperature as a function of the applied microwave field and its frequency were presented. The calculations are based on a simplified model which assumes that under the influence of a strong external electric field, electrons are at a temperature T much higher than that of the lattice. Neglecting interaction of electrons with optical modes, it was shown that at high frequencies ($\omega > \omega_c$) of the microwave field the electronic temperature always stays a finite distance above the lattice temperature T_0. The critical frequency ω_c is given by $2\,(kT_0/m^*s^2)\,\omega_c\tau \sim 1$ where τ is the mean collision time at the highest electronic temperature, and s is the speed of sound in the medium. Properties associated with electrons heated by microwaves can be calculated from these results.

Scattering of Hot Carriers in Germanium - See 6109.

6091 WAVE FUNCTIONS AND EFFECTIVE HAMILTONIAN FOR BLOCH ELECTRONS IN AN ELECTRIC FIELD by G. H. Wannier (Bell Labs.); Phys. Rev., Vol. 117, pp. 432-439, Jan. 15, 1960

Wave functions which satisfy the Schrödinger equation for a potential which is a sum of a periodic and a uniform field term are constructed. The wave functions are Houston modifications of Bloch type functions; the Bloch functions form an orthogonal set whose members are fully determined except for phase. The theory exhibits them in the form of power series in the field strength; the unmodified Bloch band functions form the zero order term of that series. The solutions themselves do not allow for a Zener effect, but the fact that they are only given as power series in E may imply that there is a remainder term causing interband transitions; it would have to be asymptotically smaller than any power of E. Instead of constructing time dependent solutions of the Schrödinger equation one can take the time independent functions to construct an effective Hamiltonian for electrons in one band. Certain indeterminacies are attached to this form of representation; it is shown, however, that final physical answers are unique. The study furnishes an incidental proof that k-space is a finite space consisting in its entirety of what is customarily called the first Brillouin zone.

6092 A MORE PRECISE THEORY OF PLASMA RECOMBINATION by V. L. Bonch-Bruevich (Physicotechnical Inst.); Soviet Phys. - Solid State, Vol. 1, pp. 984-990, Jan. 1960

The plasma mechanism of carrier recombination in homopolar semiconductors is examined on the basis of a more precise theory of electron plasmas in solids. Recombination coefficients are calculated for two models, i.e., for deep traps and for third- and fifth-group impurity traps in germanium and silicon.

6093 DETERMINATION OF THE MINORITY CARRIERS LIFETIME IN SEMICONDUCTORS by Z. Bodo (Industrial Res. Inst. for Telecommun. Tech., Budapest); Solid State Phys. Electronics and Telecommun., Vol. 1, Part 1, pp. 194-198, 1960

Investigations aimed at determining the carrier and potential distribution in the interior of an infinite semiconductor, for the case in which electron-hole pairs are generated in an arbitrary distribution on the surface, are reported. The minority carrier concentration and the potential at the midpoint of a circular light spot caused by the homogeneous irradiation of the semiconductor surface are calculated for small light intensities. The dependence of various surface and bulk recombinations on the light-spot radius is calculated, then checked by measurements which prove that the method is adapted for the separation of surface and bulk recombinations.

Measurement of Carrier Lifetime Using Transients in Junction Diodes - See 6223.

6094 THE EFFECT OF AN ELECTRIC FIELD ON THE DECAY OF EXCESS CARRIERS IN SEMICONDUCTORS by B. K. Ridley (Mullard); Proc. Phys. Soc., Vol. 75, pp. 157-161, Jan. 1960

Effects of transient sweep-out on the decay rate of excess charge carriers in semiconductors are analyzed. It is shown that the transient sweep-out effects increase the decay rate and, if great enough, can affect the form of the decay. Good agreement has been found between the theoretical and experimental results in one sample. It is pointed out that measurement of the sweep-out effect is a sensitive technique for detecting small differences between hole and electron densities in near-intrinsic material since the sweep-out mobility depends upon this difference.

6095 FREQUENCY FACTOR OF SHALLOW TRAPS IN CdS by J. J. Brophy and R. J. Robinson (Armour Res. Found.); Bull. Am. Phys. Soc., Ser. II, Vol. 5, p. 63 (A), Jan. 27, 1960

Determination of the energy distribution and frequency factor of shallow traps in the range 0.3 to 0.5 ev below the conduction band by current noise and photoconductivity measurements taken under uniform 5200 A illumination of lightly CuCl-doped CdS single crystals was discussed. The current noise observed has been interpreted in terms of multiple retrapping in these levels and results in a new way of determining the trap escape probability. Both discrete states and a continuous distribution in energy are found in different crystals. The distributed states all have the same frequency factor, which may imply the traps are structurally similar. It is possible to account semiquantitatively for the 1/f noise spectrum observed in some crystals at high frequencies using the near-exponential trap distributions found from photoconductivity measurements and the constant frequency factor derived from low-frequency noise measurements.

Method of Determining the Ionization Energy of Traps - See 6190.

6096 RECOMBINATION THROUGH DISLOCATIONS IN TELLURIUM by J. S. Blakemore and K. C. Nomura (Honeywell Res. Ctr.); Bull. Am. Phys. Soc., Ser. II, Vol. 5, p. 62 (A), Jan. 27, 1960

The marked effect of dislocations on lifetime in tellurium single crystals, both at room temperature and in the liquid air range, was discussed. Tellurium as grown may have as few as $N_D \sim 10^3$ dislocations/cm^2, but since the material is very soft, slight flexural stress can easily introduce as many as 10^6cm^{-2}. For samples whose lifetime is dominated by the presence of dislocations, the room temperature recombination rate (in sec^{-1}) is about equal to N_D (in cm^{-2}). It also appears that dislocations contribute to the minority electron trapping seen at low temperatures in tellurium. Dislocation densities can readily be measured from counts of etch pits on the cleavage $10\bar{1}0$ planes. A fast acting etch such as CP4 yields pits of poorly defined shape; but when Te is slowly attacked with sulfuric acid, the pits have well-defined planar surfaces corresponding to $\bar{1}100$, $10\bar{1}3$, $01\bar{1}1$, and $0\bar{1}1\bar{1}$ faces.

6097 ELECTRON CAPTURE BY A LATTICE VACANCY IN Si by A. Morita (Purdue U.); Phys. Rev., Vol. 117, pp. 84-89, Jan. 1, 1960

The electron-capture cross section of the deep trap due to a lattice vacancy in Si is calculated by taking into account the distortion of the lattice vibrations by the lattice vacancy. It is assumed that the trap is a neutral center for electron capture. The results show that although the distortion effect enlarges the calculated cross section by three orders of magnitude at 300°K, it is not enough to explain the magnitudes of observed cross sections.

Recombination Centers in Germanium - See 6196.

Carrier Lifetime in Silicon - See 6104.

Effective Mass of Electrons in InSb and HgSe - See 6130.

Effective Masses in Silicon - See 6123.

6098 SIMPLIFIED THEORY OF TWO-CARRIER, SPACE-CHARGE-LIMITED CURRENT FLOW IN INSULATORS by M. A. Lampert (RCA Labs.); Bull. Am. Phys. Soc., Ser. II, Vol. 5, p. 60 (A), Jan. 27, 1960

Two-carrier, space-charge-limited currents were analyzed by an extension of the simple but effective method introduced by Rose to treat the one-carrier problem. The lifetime-to-transit-time ratio for free carriers is used to relate the total injected-carrier density, which is largely electrically neutral, to its small unneutralized portion, the space charge. The latter is, in turn, related to the applied voltage via the geometric capacitance. The analysis has been carried out for both monomolecular and bimolecular recombination in cases where the injected carriers are free and the currents are field driven (diffusion neglected). Because of neutralization, far larger currents can result from two-carrier flow than from one-carrier flow at the same voltage. The simplified theory very closely checks previous results for the bimolecular recombination, field-independent mobility (low field) case.

6099 CHANGING SPACE CHARGE AND ADDED CARRIER CONCENTRATIONS IN SEMICONDUCTORS by M. Green (USASRDL); Bull. Am. Phys. Soc., Ser. II, Vol. 5, p. 60 (A) Jan. 27, 1960

The effects of transient concentration gradients on hole-current density and electron-current density in semiconductors were described. No displacement current can result in a circuit unless there is a changing space charge. Space charge in semiconductors results from charge carrier density gradients. The processes of generation and recombination of charge carriers, of themselves, are not space-charge producing mechanisms because the charges involved occur in equal and opposite quantities; but, since these processes constitute sources and sinks, they produce concentration gradients and hence space charge. Associated with transient concentration gradients, there occur time-varying components of the hole current density I_p and of the electron current density I_n that are both solenoidal and nonsolenoidal. The sum of the nonsolenoidal components of I_p and I_n just balance out the displacement current $\partial\epsilon E/\partial t$ so that the total current I is everywhere solenoidal, in agreement with Maxwell's equation Curl $H = 4\pi (I_p + I_n) + \partial\epsilon E/\partial t$.

6100 MICROWAVE METHODS OF MEASURING MOBILITY IN SEMICONDUCTORS by H. M. Barlow and J. Brown (Univ. College, London); Solid State Phys. Electronics and Telecommun., Vol. 1, Part 1, pp. 199-205, 1960

Measurement of the Hall mobility in semiconductors at microwave frequencies by means of the Hall effect, radiation pressure, and Faraday rotation is discussed. In the determination of the charge density of the current carriers, simultaneous measurements of radiation pressure and Hall emf permit allowance for the non-uniformity of the electric and magnetic fields throughout the semiconductor. A microwave mixer utilizing the Hall effect which provides a convenient method of measuring carrier mobilities is described.

6101 THE FIELD-DEPENDENCE OF CARRIER MOBILITY IN SILICON AND GERMANIUM by A. C. Prior (RRE); J. Phys. Chem. Solids, Vol. 12, pp. 175-180, Jan. 1960

The variation of mobility with electric field for n- and p-type silicon and germanium with fields up to 10^5 volts/cm is discussed. For p-type silicon the variation is found to depend on hole concentration. For the other materials any variation with concentration must be smaller, and these experiments are inconclusive as to its existence.

6102 MINORITY CARRIER CURRENT IN A LINEARLY GRADED DRIFT FIELD by D. P. Kennedy(IBM); J. Appl. Phys., Vol. 31, pp. 218-219 (L), Jan. 1960

The influence of a linearly graded drift field on the magnitude of the hole current in an n-type semiconductor is analyzed. The analysis is performed for four cases in which the field either aids

or opposes the diffusion current and a source of minority carriers is located either at the point of maximum or minimum drift field. The hole current which flows in the presence of an aiding field is considerably greater when the carrier source is at the point of maximum field than when it is at the point of minimum field. In an opposing field the magnitude of the minority carrier current is approximately the same for both cases.

6103 IMPURITY EFFECTS UPON MOBILITY IN SILICON by R. A. Logan and A. J. Peters (Bell Labs.); J. Appl. Phys., Vol. 31, pp. 122-124, Jan. 1960

Mobility measurements performed on highly purified n- and p-type silicon are discussed. In sufficiently pure n-type silicon, the carrier mobility follows a $T^{-1.5}$ law at low temperature and agrees well with Herring's theory of lattice scattering mobility. Similar results for p-type silicon give a T^{-2} law for the temperature dependence and are in disagreement with theory. In less pure samples, scattering is by ionized impurities and the magnitude of the mobility reduction agrees well with the theory of Herring and Brooks. Scattering by large concentrations ($\sim 10^{18}$ cm^{-3}) of dissolved neutral oxygen is negligible compared to that by other mechanisms.

6104 A COMPARISON OF DRIFT MOBILITY, CARRIER LIFETIME AND HALL EFFECT MEASUREMENTS ON P-TYPE SILICON by F. W. G. Rose, E. L. Heasell, and F. Paton (British Thomson-Houston); Solid State Phys. Electronics and Telecommun., Vol. 1, Part 1, pp. 230-239, 1960

The discrepancy between an experimental relation derived by Prince for the drift mobility as a function of the concentration of scattering centers in p-type silicon and the Brooks-Herring theory is discussed on the basis of combined drift mobility, lifetime, and Hall measurements. Experiments indicate that the low values of drift mobility sometimes measured in high-resistivity p-type materials are due to a high concentration of scattering centers, and bear no relation to the resistivity. An evaluation of the concentration of scattering centers, using the Brooks-Herring formula, yields values of 10^{15} to 10^{17} centers per cm^3. Lifetime measurements in the temperature range 300-500°K were made on adjacent parts of the same samples; good agreement of the measured lifetime vs. temperature curves with the Shockley-Read theory could be obtained if two types of recombination centers having activation energies of ~ 0.16 ev and 0.5 ev were assumed.

6105 EVIDENCE FOR A MOBILITY KILLER IN GaAs, InAs, AND InP by L. R. Weisberg and J. Blanc (RCA Labs.); Bull. Am. Phys. Soc., Ser. II, Vol. 5, pp. 62-63 (A), Jan. 27, 1960

Evidence which indicates the presence in n-type GaAs, InAs, and InP of a mobility "killer" that has little effect on electron concentrations was presented. Carrier mobilities in semiconductors heretofore have been interpreted mainly in terms of lattice scattering and ionized impurity scattering. However, considerable evidence has accumulated against such an interpretation: (1) Over 99 percent of all crystals prepared turn out n-type; (2) at given electron concentrations, curves of mobility versus temperature for different samples are observed to cross; (3) at 300°K there is no correlation between measured mobilities and carrier concentrations, while at 78°K a correlation exists; (4) erratic mobility variations observed along an ingot are percentagewise greater at 300°K than at 78°K; (5) purification of the elements causes changes in the mobility at 78°K with no corresponding change at 300°K and vice versa. All of these phenomena can be accounted for by assuming that the samples are actually uncompensated, but that a mobility "killer" is present. Analysis of the available data indicates that the mobility of this new scatterer varies with temperature roughly $T^{-3/4}$.

6106 HALL MOBILITY OF HOLES IN AgBr by R. C. Hanson and F. C. Brown (U. Illinois); J. Appl. Phys., Vol. 31, pp. 210-211 (L), Jan. 1960

Measurement of the Hall mobility of holes in high purity silver bromide (AgBr) over the temperature range 25 to 150°C is reported and the experimental techniques are described. At 27°C the best value of Hall mobility obtained from several runs on different crystals was $\mu_p = 1.7 \pm 0.5$ cm^2/volt sec. The results indicate that the increase in conductivity following absorption of excess bromine is due almost entirely to the presence of holes. It is pointed out that electrons have a mobility about 40 times larger than the mobility of the holes in this temperature range. This difference in mobility explains the previous difficulty in separating hole from electron currents in silver halides.

6107 CALCULATION OF MOBILITY IN N-TYPE GaAs by E. Arnold (Sylvania Res. Labs.); Bull. Am. Phys. Soc., Ser. II, Vol. 5, p. 62 (A), Jan. 27, 1960

Theoretical calculations of carrier mobility in n-type GaAs using the Fermi distribution function and incorporating lattice and impurity scattering were described. This type of calculation is necessary for determination of electron mobility at room temperature in typical GaAs samples having a carrier concentration of about 10^{17} cm^{-3} or larger because the small effective mass causes the Fermi level to be near the edge of the conduction band. The relaxation time was obtained by adding the reciprocals of the relaxation times for acoustical phonon scattering and for Brooks-Herring impurity scattering. It was assumed that the total ionized impurity concentration was equal to the free carrier concentration. Spherical constant energy surfaces were also assumed. The resultant scattering integrals were evaluated numerically. Three adjustable parameters were used: the reduced Fermi level η, the effective mass m^*, and the mean free path for acoustical mode scattering l. The ratio r of Hall to drift mobility and the relationship between μ/μ_L and μ_L/μ_I valid for different degrees of degeneracy were determined. In the nondegenerate limit the mobility is somewhat larger than that given by Conwell because, in the present calculation, the approximation of replacing the logarithmic term in the expression for the impurity relaxation time by a constant has not been made.

6108 PROPERTIES OF $CdSnAs_2$ by A. J. Rosenberg and A. J. Strauss (Lincoln Lab.); Bull. Am. Phys. Soc., Ser. II, Vol. 5, p. 83 (A), Jan. 27, 1960

Directional freezing of a stoichiometric melt of $CdSnAs_2$ leads to a single phase material crystallizing in the chalcopyrite structure with $a = 6.084$ A and $c = 11.916$ A, $c/a = 1.957$. The resistivity and Hall coefficient are 4.2×10^{-3} Ω-cm and -2.3 cm^3/coul, respectively, at room temperature and are virtually the same at 78°K. These values correspond to an electron mobility of 5600 cm^2/v-sec at a carrier concentration of 2.7×10^{18} cm^{-3}. The thermoelectric power at room temperature is -54 μv/degree. Therefore, despite an extremely small grain size (<1μ), the electron mobility is the highest value reported for any ternary compound, and is comparable to that of monocrystal InSb at the same carrier concentration.

6109 SCATTERING OF HOT CARRIERS IN GERMANIUM by E. M. Conwell (Sylvania); Bull. Am. Phys. Soc., Ser. II, Vol. 5, p. 61 (A), Jan. 27, 1960

Extension of the theory of scattering by acoustical lattice mode to cover carriers with energy many times the thermal value at lattice temperatures of 20°K and above was described. In the limit where the carriers interact mainly with lattice oscillators having only zero point energy, the relaxation time for acoustical mode scattering is proportional to the inverse square of the speed rather than to the inverse first power as it is for thermal carriers. Lattice mobility has been calculated as a function of average carrier energy for various values of the ratio of coupli

CARRIER PROPERTIES (Cont'd)

constants for acoustical and optical modes and various effective masses for lattice temperatures of 300, 78, and 20°K. The effect of dropping the assumption of equipartition of energy among the acoustical lattice oscillators is to increase the scattering effect of the acoustical modes. This increase is greater the lower the lattice temperature, the higher the carrier temperature, and the higher the mass of the carriers. The effect of impurity scattering in increasing hot-carrier mobility is generally smaller than expected.

Influence of Grain Boundaries on Minority Carrier Diffusion - See 6073.

Evidence for Neutral Energy Transport in CdS Obtained from Noise Measurements - See 6192.

Dipole Mode of Minority Carrier Diffusion - See 6214.

Effects of Transient Sweep - Out on the Decay Rate of Excess Carriers - See 6094.

Microwave Heating of Carriers in Semiconductors - See 6090.

CONDUCTIVITY (Resistivity)

6110 A TIME-FLUCTUATION METHOD APPLIED TO THE THEORY OF ELECTRICAL CONDUCTIVITY by R. Zigenlaub (Moscow State U.); Soviet Phys. - Solid State, Vol. 1, pp. 964-971, Jan. 1960

A method for calculating the electrical conductivity tensor which is similar to the damping method employed in quantum field theory is proposed. Within this frame-work the case where the interaction term in the Hamiltonian contains a small parameter is examined.

6111 PIEZORESISTANCE IN N-TYPE InP by A. Sagar (Westinghouse Res. Labs. and U. Pittsburgh); Phys. Rev., Vol. 117, p.101, Jan. 1, 1960

Piezoresistance measurements made on n-type InP at 77°K and 300°K are reported. The results suggest a spherical energy band for this material.

6112 NON-OHMIC ELECTRICAL CONDUCTIVITY OF CdS AT LOW TEMPERATURES by H. Shenker (U. S. Naval Res. Lab.); Bull. Am. Phys. Soc., Ser. II, Vol. 5, p. 63 (A), Jan. 27, 1960

Measurements of the electrical conductivity at liquid helium temperatures of CdS crystals which had no intentionally added impurities and which had room temperature conductivities in the range 0.1 to 10 ohm^{-1} cm^{-1} were reported. At liquid helium temperatures the dark conductivity increases rapidly with increasing electric field. A typical increase is three orders of magnitude for an increase of electric field from zero to 400 volts/cm. The conductivity appears to be mainly of the impurity band type since the Hall voltage was too small to be measured and the thermal activation energy for the conductivity is in the milli-electron-volt-range. The dependence of the conductivity upon electric field varies from sample to sample, but can generally be approximated by a sum of two or three exponentials in the first power of the electric field. In the range 350 to 450 volts/cm, several samples were found to exhibit a reversible breakdown effect somewhat similar to that in germanium. The breakdown field has a small dependence upon temperature and also upon applied magnetic field. The crystals also exhibit infrared photoconductivity with a cut-off at 32 microns.

6113 BOMBARDMENT CONDUCTIVITY AND PHOTOCONDUCTIVITY IN RHOMBIC SULPHUR by P. J. Dean, B. S. H. Royce and F. C. Champion (U. London); Proc. Phys. Soc., Vol. 75, pp. 119-135, Jan. 1960

Using pure single crystals of rhombic sulphur, of volume a few mm^3, conduction counting has been observed for α-particle bombardment but only in a region close to the negative electrode, indicating a barrier effect. If the applied voltage is increased there is an increase in the counting rate proportional to V^n where $n = 0.7$, but no increase in the maximum pulse height. Creation of a spcae charge barrier is essential before counting can begin, after which the counting rate decays with time. However, the crystal can be reactivated by light or other ionizing radiations. The primary photoconductivity between 4400 A and 9000 A down to 130°K has been examined and the photoconductive efficiency has been found to be about 1.5 μa/w. Comparing these results with von Hippel's interpretation for the alkali halides, a mean value of $N = 10^{13}$ cm^{-3} has been obtained for the donor density. Secondary currents have also been observed and breakdown pulses have been attributed to field emission at the electrodes. The free path w per unit field has been estimated as $\geq 5 \times 10^{-8}$ cm, and the lower limit of the mobility μ_e of the electrons which were the charge carriers, as about 10^{-1} cm^2 v^{-1} sec^{-1}. The energy per ion pair has been found experimentally to be about 32 ev which agrees with the value deduced from independent data on the electronic band structure of sulphur. The thickness of the barrier layer was approximately 10^{-2}cm with barrier field strength of the order of 10^5 vcm^{-1}. The conductivity pulse magnitude depends upon the position of the α-particle track inside the barrier and the excitation mechanism for conductivity pulses in a molecular crystal like sulphur differs considerably from that of a covalent crystal like diamond.

Resistivity of Erbium Single Crystals - See 6151.

SUPERCONDUCTIVITY

6114 A THERMODYNAMIC TREATMENT OF DILUTE SUPERCONDUCTING ALLOYS by R. E. Jones, Jr. (IBM Res. Lab.); IBM J. Res. and Dev., Vol. 4, pp. 23-27, Jan. 1960

The effect of adding small concentrations of an impurity to a superconducting metal is analyzed by thermodynamic methods. Two possible types of variation of the Gibbs free energy with compositions are then discussed, utilizing a number of simplifying assumptions. For the case in which alloys have a superconducting second-order transition, there is a long-range interaction among solute atoms, even in limits of high dilution.

6115 TRANSPORT PROPERTIES OF SUPERCONDUCTORS by L. P. Kadanoff and P. C. Martin (Harvard U.); Bull. Am. Phys. Soc., Vol. 5, Ser. II, p. 13 (A), Jan. 27, 1960

The transport properties of a system describe the flow of densities of conserved quantities when the system is perturbed from equilibrium. These properties may be discussed in terms of frequency and wave-number dependent transport coefficients, which are Fourier transforms of correlation functions of the conserved currents. The transport coefficients, together with the conservation laws, determine the hydrodynamical relaxation of deviations from equilibrium. The familiar transport coefficients of a degenerate Fermi gas may be obtained using a simple approximation for the two particle Green's function in which the finite lifetime of the single particle excitation is retained. Identical techniques may be employed with a superconductor. Using Green's functions which account for the binding of particles with opposite spin, the transport coefficients of pure superconductors have been evaluated. The thermal conductivity exhibits a

marked decrease in the neighborhood of the critical temperature. The sound wave and collective modes obtained at frequencies smaller than the inverse lifetime are significantly different from results derived using infinite lifetimes. Since the entire procedure preserves particles conservation, there are no difficulties with gauge invariance.

Possible Explanation of the "Coexistence" of Ferromagnetism and Superconductivity - See 6183.

6116 A METHOD FOR MEASURING MAGNETIC FIELDS IN SUPERCONDUCTORS by H. R. Lewis, J. F. Cochran, H. Frauenfelder, D. E. Mapother, and R. N. Peacock (U. Illinois); Z. Physik, Vol. 158, No. 1, pp. 26-34, 1960

A nuclear technique which permits local measurements of the variation of the magnetic field within a bulk superconductor is described. A radioisotope which decays through successive emission of γ-rays is embedded in the superconductor and the magnetic field is measured by observing its effect on the angular correlation pattern of the nucleus. By means of this technique, the Meissner effect has been observed in lead.

6117 INTERMEDIATE STATE IN CYLINDRICAL SUPERCONDUCTORS by C. A. Shiffman (NBS); Bull. Am. Phys. Soc., Vol. 5, Ser. II, p. 13 (A), Jan. 27, 1960

Measurement of the field variation along the axis of long circular cylinders of superconductors in the presence of a transverse magnetic field of sufficient magnitude to place the specimen in the intermediate stage was reported. A bismuth micro-probe technique is used to sense the field variations and hence the normal and superconducting domain distributions. Adequate resolution is guaranteed by the use of probes with effective dimensions of about 20μ, scanning the specimen surface at a separation of less than 20μ. The domain distribution has been measured as a function of specimen size, metallurgical state, magnetic field and temperature mainly in the case of tin, but to some extent for aluminum. The results were discussed in terms of the various models of the intermediate state and the theories of the surface energy between normal and superconducting phases.

6118 CRITICAL FIELDS OF THIN SUPERCONDUCTING TIN FILMS by W. B. Ittner III and R. H. Blumberg (IBM Res. Lab.); Bull. Am. Phys. Soc., Vol. 5, Ser. II, p. 14 (A), Jan. 27, 1960

The fabrication of tin films of thickness ranging from 500 A to 150 000 A in a manner designed to produce as nearly as possible a geometry corresponding to an "idealized" thin film was reported. Measurements have indicated that the critical magnetic fields of such films can be described by an equation of the type derived by London only if a penetration depth considerably greater than the bulk value of approximately 510 A is assumed. Consequently, calculations of the magnetic field penetration in a thin film were carried out for the non-local theories of Pippard and Bardeen using the equations obtained by Schrieffer. It was found that an effective penetration depth, which could be defined through a comparison of the local theory of London to the non-local theories, could be used to describe with reasonable accuracy the observed critical fields of the measured films.

6119 SUPERCONDUCTIVITY OF DILUTE INDIUM-MERCURY ALLOYS by M. D. Reeber (IBM Res. Lab.); Bull. Am. Phys. Soc., Vol. 5, Ser. II, pp. 13-14 (A), Jan. 27, 1960

Measurements of the critical magnetic field for the transition from the superconducting to the normal state in homogeneous polycrystalline rods of the substitutional solid solution In-Hg, containing 0-7 at. percent Hg were discussed. The transitions to the normal state were found to be similar to those for pure elemental superconductors. It was, moreover, possible to distinguish between properties that are characteristic of the ideal alloy system and properties which arise from structure within the specimen. The transition temperature in zero field was measured as a function of composition, and was found initially to decrease (up to a concentration of 1.75 at. percent Hg) after which it began to increase with added Hg concentration. The width of the transition to the normal state, as measured by the variation of specimen resistance in a longitudinal magnetic field was found to show a regular dependence upon composition, and also reached a minimum value at 1.75 at. percent Hg. The superconducting properties of pure indium were measured and used as a standard

BREAKDOWN

Breakdown in Cadmium Sulfide - See 6112.

GALVANOMAGNETIC PROPERTIES

(Including Hall Effect and Carrier Resonance)

6120 OSCILLATIONS IN THE THERMOMAGNETIC AND GALVANOMAGNETIC EFFECTS IN TIN AT LOW TEMPERATURES by J. M. Reynolds, K. S. Balain, and C. G. Grenier (La. State U.); Bull. Am. Phys. Soc., Ser. II, Vol. 5, p. 58 (A), Jan. 27, 1960

The observation of De Haas-van Alphen type oscillations in the Hall effect, Ettingshausen-Nernst effect, and thermoelectric power in tin was reported. With the magnetic field parallel to the tetragonal axis, the period of the oscillations in 1/H is 5.7 x 10^{-7} gauss^{-1} for each effect, which agrees well with previously reported periods for oscillations in the electrical and thermal magnetoresistance. The measuring apparatus was sufficiently sensitive that oscillation in each effect could be clearly seen at fields as low as 10 kilogauss. About one hundred oscillations were recorded in the range 10-17 kilogauss. Measurements made at several temperatures from 1.2°K to 4.2°K show the amplitude of the oscillations in each effect to be strongly dependent on temperature.

6121 HALL FIELD IN CADMIUM ARSENIDE by A. S. Fischler (IBM); Bull. Am. Phys. Soc., Ser. II, Vol. 5, pp. 77-78 (A), Jan. 27, 1960

Measurements of the Hall coefficients of oriented single crystals of $CdAs_2$ were reported. The measurements were made as a function of the angle between the applied magnetic field and the current and as a function of the magnetic field intensity. A finite Hall field, linear in the magnetic field H, was observed when H and the current were parallel along a principal crystal axis. The observed effect showed a strong dependence on sample purity. Although allowed by macroscopic crystal symmetry (C_4), the effect cannot be explained using the Boltzmann equation with the introduction of a momentum dependent relaxation time.

6122 NONEQUILIBRIUM CYCLOTRON RESONANCE OF NEGATIVE EFFECTIVE MASS CARRIERS by R. C. Williams and F. Herman (RCA Labs.); Bull. Am. Phys. Soc., Ser. II, Vol. 5, p. 61 (A), Jan. 27, 1960

Extension of the classical Boltzmann theory of cyclotron resonance for warped surfaces to cover the case of a nonequilibrium carrier distribution arising from generation and recombination

processes was described. As a specific application, the cyclotron resonance of optically-excited holes in Ge was examined with a circularly polarized rf electric field and a (100) - directed magnetic field. If the negative mass population is enhanced at the expense of the positive mass population (in the heavy hole band) to a degree of the order of the energy band warping, the power absorption is found to be negative for magnetic field values for which the negative mass holes are resonant. The type of nonequilibrium heavy hole distribution required to produce negative absorption is readily obtained by making physically plausible assumptions regarding the generation, recombination, and scattering terms.

6123 MILLIMETER CYCLOTRON RESONANCE IN SILICON by C. J. Rauch, J. J. Stickler, H. J. Zeiger, and G. S. Heller (MIT); Phys. Rev. Lett., Vol. 4, pp. 64-66 (L), Jan. 15, 1960

Cyclotron resonance absorption experiments performed on high-purity (3000 ohm-cm at room temperature) n-type silicon in a 2.1 mm cavity spectrometer are discussed. Measurements of $1/m_1^2 + 1/m_2^2 + 1/m_3^2$, $1/2\,(1/m_1^2 + 1/m_2^2)$, and $1/m_3^2$, where m_1, m_2, and m_3 are the effective masses for the individual ellipsoids in the conduction band of Si, were made as a function of sample orientation at 4.2°K. From this data it was found that $m_t = (0.192 \pm 0.001)\, m_o$ and $m_l = (0.90 \pm 0.02)\, m_o$, where m_o is the free electron mass, and m_t and m_l are the transverse and longitudinal components of the ellipsoids, respectively. The m_t value agrees with and the m_l value lies outside of the limits of error of previously reported values. Effective mass and line width were also measured as a function of temperature from 1.2°K to 50°K with the crystal oriented so that the static magnetic field was approximately along the 100 direction. A change in mass was not observed.

6124 SPIN RESONANCE OF CONDUCTION ELECTRONS IN InSb by G. Bemski (Bell Labs.); Phys. Rev. Lett., Vol. 4, pp. 62-64 (L), Jan. 15, 1960

The direct observation at 1.2 and 4°K of spin resonance of conduction electrons in n-type InSb having electron concentrations between 2×10^{14} cm^{-3} and 3×10^{15} cm^{-3} is reported. The g values varied between 48.8 and 50.7 depending upon electron concentration. It is believed that the shift of the g value with concentration is associated with the increasing mass of the electrons. No resonance was observed in a sample with 10^{16} electrons/cm^3.

6125 FLUCTUATIONS FROM THE NONEQUILIBRIUM STEADY STATE by M. Lax (Bell Labs.); Revs. Mod. Phys., Vol. 32, pp. 25-64, Jan. 1960

Noise (the spectrum of fluctuations) in a steady state possibly far from equilibrium is treated by assuming only that the physical system is, in an appropriate set of variables, Markoffian, stationary, and quasi-linear. The last restriction is partly removed by an analysis of slightly nonlinear systems and completely removed by a treatment of fluctuations in distribution functions. The equilibrium relations of Einstein, Onsager, and Nyquist are shown to exist in modified form in the nonequilibrium case. The Langevin noise-source viewpoint appears in this theory as a consequence rather than as an assumption. The validity of the circuit viewpoint based on Thevenin's theorem is derived for the equilibrium case and is shown to require modification in the nonequilibrium case. The meaning of fluctuations in intensive variables is clarified. A set of coupled oscillators is used as an example of a system possessing inertia and some variables that are odd under time reversal. The Hill-van Vliet treatment of ambipolar drift of carrier-concentration fluctuations is used to provide a continuous parameter example. The assumption that fluctuations at one time but at different places are uncorrelated is derived as part of a general treatment of fluctuations in distribution functions.

Spin Resonance of Impurity Ions in Silicon - See 6164.

OTHER ELECTRICAL PROPERTIES

Current noise in CdS due to Multiple Retrapping - See 6095.

6126 GENERATION-RECOMBINATION NOISE IN SEMICONDUCTORS -- THE EQUIVALENT CIRCUIT APPROACH by K. S. Champlin (U. Minnesota); IRE Trans., Vol. ED-7, pp. 29-38, Jan. 1960

Generation-recombination noise in semiconductors in thermal equilibrium is treated from the standpoint of thermal fluctuations in equivalent electrical circuits. For the general volume recombination model, a method based on network reduction is presented which allows one to calculate the spectral density of the electron and hole fluctuations without solving for the spectra of the fluctuations in occupancy of the recombination centers and traps. The method is extended to a surface recombination model, thereby avoiding the ambiguities found in previous formal treatments. It is shown that the concept of ambipolar diffusion, the location and spectral density of the random sources, and the spatial correlation of Fourier coefficients of carrier density fluctuations all have simple significance in electrical terms. Using transmission line techniques, the generation-recombination(GR) spectrum is calculated for a two-level semiconductor where recombination occurs at opposite plane surfaces. This new result is examined in detail for the limiting cases approached when the recombination process is 1) volume-limited, surface-limited, and 3) diffusion-limited. It is shown that in the first two cases, the spectrum is identical with that obtained from a zero-dimensional analysis provided the time constant is properly defined. For the diffusion-limited case, however, the spectrum varies as $1/\omega^{3/2}$ at high frequencies, and at low frequencies the noise is 5/6 that predicted by the simple theory. The new result is shown to compare favorably with measurements reported previously by Hill and van Vliet.

Hot Electron Emission from Silicon Junctions - See 6222.

Relation Between Electron Energy Dissipation and Secondary Emission in Solids - See 6055.

6127 ON THE FREQUENCY DEPENDENCE OF THE FIELD EFFECT IN SEMICONDUCTORS. II. by A. E. Yunovich (Moscow State U.); Soviet Phys. - Solid State, Vol. 1, pp. 998-1006, Jan. 1960

Dependence of the field effect in semiconductors on frequency is discussed for the case in which current carriers of both signs are present in the bulk of the semiconductor and on its surface. Assuming that conditions depart only a little from equilibrium, that surface recombination predominates over volume recombination, and that surface states of only one type exist, it is shown that the kinetics of the field effect involves several characteristic times. The conditions under which it is possible to neglect minority carriers are given including those applicable to Garrett's treatment [see 1180].

6128 ON THE NATURE OF RELAXATION PROCESSES IN THE FIELD EFFECT by V. I. Lyashenko and N. S. Chernaya (Kiev Inst. Phys.); Soviet Phys. - Solid State, Vol. 1, pp. 921-929, Jan. 1960

OTHER ELECTRICAL PROPERTIES (Cont'd)

Long-term relaxation processes in the field effect in germanium are reported. It is shown that these processes depend on the adsorption of ions from the surrounding space. The hypothesis that the ions arise as a result of emission under the action of the field is introduced.

6129 A.C. AND D.C. FIELD EFFECTS ON CLEANED GERMANIUM SURFACES by S. Kawaji (Gakushuin U., Tokyo); J. Phys. Soc. Japan, Vol. 15, pp. 95-99, Jan. 1960

Measurements of the a-c and d-c field effects on the conductance of germanium surfaces cleaned by Joule heating up to about 800°C in ultra-high vacuum are discussed. In the measurements of the a-c field effect on the cleaned surface, the minimum of conductance indicating that the surface was slightly n-type was observed and the density of fast states was estimated at $1.7 \times 10^{13}/cm^2$ volt. When the surface was exposed to oxygen, the fast state density decreased to $2.4 \times 10^{12}/cm^2$ volt and the surface potential decreased by 0.03 volts. These results suggest that the fast states are dangling bonds at the surface. In the measurements of the d-c field effect on the cleaned surface, the slow decay of the changes in conductance was not observed. The slow decay appeared when the surface was exposed to air. These results show that the slow states are due to adsorbed gases on the outer surface of the oxide layer of germanium.

6130 MAGNETOPLASMA REFLECTION IN SOLIDS by B. Lax and G. B. Wright (Lincoln Lab.); Phys. Rev. Lett., Vol. 4, pp. 16-19 (L), Jan. 1, 1960

The reflection edge at the plasma frequency ω_p due to the dispersive properties of charge carriers in solids is split and shifted in a magnetic field. The use of this phenomena to measure directly the effective mass m* of electrons in n-type InSb and in n-type Hg Se is reported. For InSb with a carrier concentration 1.8×10^{18} cm^{-3}, $m^*m_o = 0.041 \pm 0.002$ and for HgSe with a carrier concentration 2.45×10^{18} cm^{-3}, $m^*m_o = 0.045 \pm 0.003$. The value for InSb agrees within experimental error with values measured by the zero-field technique of Spitzer and Fan. The dielectric constant of HgSe has been determined to be 14.0 at 16.3 microns.

Theory of Plasma Recombination - See 6092.

6131 ZENER TUNNELING IN SEMICONDUCTORS by E. O. Kane (GE Res. Lab.); J. Phys. Chem. Solids, Vol. 12, pp. 181-188, Jan. 1960

The Zener current in a constant field is calculated both with and without Wannier-Adams reduction of the interband-coupling terms. The Zener current is only slightly different for the two cases, as already noted by Wannier. The apparent reduction of interband coupling is interpreted as a polarization correction. A detailed calculation of the Zener current is made for a simple two-band model which is applicable to InSb. The evaluation of the tunneling integral follows closely a calculation due to Keldysh.

ELECTRICAL PROPERTIES OF SPECIFIC MATERIALS

6132 THE ELECTRICAL AND OPTICAL PROPERTIES OF THE SEMICONDUCTOR TIN SELENIDE by D. L. Mitchell (Syracuse U.); Diss. Abstr., Vol. 20, pp. 2857-2858 (A), Jan. 1960

The preparation and properties of SnSe are discussed. Of the several crystal growing techniques investigated, the vapor technique provided crystals with the highest degree of crystal perfection together with a very low concentration of excess charge carriers. All crystals exhibited p-type conduction, no way having been found to prepare n-type crystals. The structure of SnSe is orthorhombic and is a slight distortion of the face-centered-cubic lattice characteristic of the other group IV-group VI compounds. The anisotropy is evident in the measurements of the index of refraction and the intrinsic optical absorption but has no effect on electrical conductivity and Hall constant. From measured values of mobility μ_h (100 $cm^2/volt\text{-}sec$) and relaxation time τ_h (1×10^{-14} sec) the effective mass for holes, m_h^*, has been found to be $0.2\ m_e$. It has not been determined whether the absence of n-type conduction is due to trapping of electrons or to the absence of a true conduction band. In general the properties of SnSe seem to relate more to the valence type crystals such as Si than to the ionic salts PbSe and PbTe.

6133 ELECTRICAL PROPERTIES OF N-TYPE CADMIUM SULFIDE by W. W. Piper and R. E. Halsted (GE Res. Lab.); Bull. Am. Phys. Soc., Ser. II, Vol. 5, p. 63 (A), Jan. 27, 1960

Measurements between 20°K and 350°K of the conductivity and Hall coefficient of single-crystal samples of hexagonal CdS:Ga grown from the vapor phase were presented. Initial measurements were performed on bars, 2 x 2 x 10 mm, cut with the long dimension perpendicular to the c-axis. The Hall voltage was measured both parallel to and perpendicular to the c-axis. Gallium was incorporated in the crystals as they were grown. A gallium concentration greater than 5×10^{16} cm^{-3} yields samples with low resistivity due to the presence of uncompensated donors. Above a concentration of Ga of 10^{18} cm^{-3} the Hall coefficient R_H is almost independent of temperature, in agreement with earlier work. At lower concentrations R_H increases exponentially with increasing reciprocal temperature. At low temperatures, behavior consistent with competition from impurity band conduction is encountered. The Hall coefficient has been observed to be anisotropic and is larger when the Hall voltage is measured parallel to the c-axis.

Electrical Properties of Gallium Antimonide - See 6060.

Electrical Properties of Bi_2Te_3 and Sb_2Te_3 containing Group III Atoms - See 6003.

Electrical Properties of $CdSnAs_2$ - See 6108.

FERROMAGNETISM AND FERRITES

6134 DETERMINATION OF THE MAGNETIC PROPERTIES OF SOLIDS USING CONFIGURATION INTERACTION by D. I. Paul (UCLA); Bull. Am. Phys. Soc., Ser. II, Vol. 5, p. 59 (A), Jan. 27, 1960

An investigation of the theory of strong magnetic effects from the point of view of orthogonal atomic functions for the case of one dimension was described. Thus the exchange integral is considered positive and the interaction between the polar and nonpolar states for all possible arrangements of electron spin is included in this formulation of the problem. The resulting secular equations have been solved for both large and small interaction between states for the case of only one electron spin oriented in a direction opposite to all other electron spins, and they have been solved for small interactions between states for the more general case of any number of electron spins in a given direction. Inclusion of the polar states can yield either a ferromagnetic or an antiferromagnetic ground state depending on the differences in absolute magnitude among (1) the exchange integral, (2) the extra Coulomb energy of the polar states, and (3) integrals representing electron-nuclei interactions and thus the splitting of the energy bands.

6135 EXPLANATION FOR THE LOW-TEMPERATURE BEHAVIOR OF THE ANISOTROPY OF IRON by W. J. Carr, Jr. (Westinghouse); J. Appl. Phys., Vol. 31, p. 69, Jan. 1960

The seemingly anomalous results obtained by Graham for the temperature dependence of magnetic anistoropy in iron are interpreted on the basis of Zener's theory. The effect of thermal expansion is included.

6136 THEORY OF SPIN-WAVE INTERACTIONS IN FERRO- AND ANTIFERROMAGNETISM by T. Oguchi (U. Pittsburgh); Phys. Rev., Vol. 117, pp. 117-123, Jan. 1, 1960

The spin-wave theory in an ideal Heisenberg model of a ferromagnet is studied using Holstein and Primakoff's method including the spin-wave interactions. The result is in agreement with Dyson's to the order which has been considered. This method can easily be applied to antiferromagnetism. The correction arising from interactions between spin waves has been obtained. The correction term is quite small which means that the simple theory neglecting the spin-wave interactions is sufficient for practical purposes.

6137 MAGNETIC COUPLING IN CRYSTALLINE COMPOUNDS. A PHENOMENOLOGICAL THEORY OF MAGNETISM IN 3d METALS by E. O. Wollan (Oak Ridge Natl. Lab.); Phys. Rev., Vol. 117, pp. 387-401, Jan. 15, 1960

Magnetic coupling processes are considered in terms of the orbitals which result from the splitting of the d levels by the crystalline field. It is shown that the antiferromagnetic and ferromagnetic structure properties of many crystalline compounds can be qualitatively accounted for on the basis of indirect coupling processes which depend on the overlap of magnetic cation d orbitals of intervening anions and on the electron spin occupation appropriate to the particular cations involved. The orbital approach has also been used in considering the magnetic properties of the 3d metals and a coupling mechanism which is consistent with much of the magnetic data relating to the iron group metals and their alloys has been proposed.

6138 POSSIBLE EXPLANATION OF THE "COEXISTENCE" OF FERROMAGNETISM AND SUPERCONDUCTIVITY by B. T. Matthias and H. Suhl (Bell Labs); Phys. Rev. Lett., Vol. 4, pp. 51-52 (L), Jan. 15, 1960

It is suggested that dilute solutions of rare earths (particularly gadolinium) in host superconductors can be superconductive and ferromagnetic at the same time if the superconducting regions extend only through the thicknesses of the ferromagnetic domain walls. The consistency of this explanation with the Bardeen-Cooper-Schrieffer theory of superconductivity is pointed out.

6139 X-RAY STUDY OF FERROMAGNETIC DOMAINS IN COBALT ZINC FERRITE by K. M. Merz (Rutgers U.); J. Appl. Phys., Vol. 31, pp. 147-154, Jan. 1960

A study of ferromagnetic domains in cobalt zinc ferrite single crystals by double crystal diffractometer and x-ray micrograph techniques is discussed. Diffraction curves of the (400) reflection were observed to broaden when a magnetic field was applied to the crystal. Berg-Barrett x-ray micrographs showed there was a "d" spacing shift in the crystal during the magnetization process.

6140 DETERMINATION OF MOLECULAR FIELD COEFFICIENTS IN FERRIMAGNETS by G. T. Rado and V. J. Folen (U. S. Naval Res. Lab.); J. Appl. Phys., Vol. 31, pp. 62-68, Jan. 1960

An improved method for determining the three molecular field coefficients which yield essentially the best agreement between the Néel theory and the experimental curve of saturation moment per unit mass (σ) versus temperature (T) in a given ferrimagnetic material is presented. This method is analytical, and for a given accuracy it is more rapid than previously used trial-and-error methods. Experimental data on σ vs. T are presented for microcrystals of lithium ferrite and two compositions of magnesium-iron ferrite. One of the latter ferrites was measured in two states of ionic distribution which were obtained by varying the heat treatment. Application of the analytical method to these data shows that the agreement between the Néel theory and experiment is somewhat better than that expected on the basis of previous work. The present method is particularly useful for determining the temperature dependence of the sublattice magnetizations. Accurate values of these magnetizations are required, for example, in calculations of the temperature dependence of magnetocrystalline anisotropy by means of crystalline field theory.

6141 RECTANGULAR HYSTERESIS LOOP FERRITES WITH LARGE BARKHAUSEN STEPS by A. P. Griefer and W. J. Croft (RCA); J. Appl. Phys., Vol. 31, pp. 85-88, Jan. 1960

Observations made at low temperatures of large discontinuities (steps) in the 60-cycle hysteresis loops of polycrystalline ferrites containing copper are reported. At the temperature for step formation, which is a function of copper content, the coercivity decreases and the loop squareness approaches unity. This behavior is attributed to the formation (in the toroidal specimens used) of circular 180° domain walls having different threshold fields. This domain wall configuration is probably brought on at low temperatures by a low effective magnetocrystalline anisotropy provided by the localized distortions exerted by divalent copper in the spinel lattice.

6142 REGARDING THE ARBITRARY REVERSAL OF THE MAGNETIC POLARITY OF Mn-Mg AND Ni-Zn FERRITES by V. V. Kobelev and I. I. Nadashkevich (Inst. of Exact Mech. and Computer Tech.); Soviet Phys. - Solid State, Vol. 1, pp. 1043-1048, Jan. 1960

Certain problems of the reversal of the magnetic polarity of Mn-Mg and Ni-Zn ferrites, used in computer technology, are considered. The effect of the past history on the change of the magnetic state of toroidal ferrite cores is investigated.

6143 LINE WIDTH NARROWING IN GALLIUM SUBSTITUTED YTTRIUM IRON GARNET by E. G. Spencer and R. C. LeCraw (Bell Labs.); Bull. Am. Phys. Soc., Ser. II, Vol. 5, p. 58 (A), Jan. 27, 1960

Measurements of ferromagnetic resonance line widths in single-crystal yttrium iron garnet (YIG) in which some of the ferric ions had been replaced by non-magnetic gallium ions were discussed. There is an almost complete preference of the gallium ions for the tetrahedral sites. In spherical samples of YIG grown using the highly purified yttrium oxide, the (full) line width at 6000 mc and 300°K was $\Delta H = 0.375$ oe when $4\pi M = 1750$ gauss. For YIG-Ga of various concentrations of gallium $\Delta H = 0.62$ oe when $4\pi M = 1050$ gauss and $\Delta H = 1.2$ oe when $4\pi M = 400$ gauss. The continued narrowness of these lines in the presence of large inhomogeneous fields due to missing ferric ions in the ordered sites is evidence for the effectiveness of exchange or dipolar narrowing. Although the temperature dependence is similar to previous data on YIG, there is a stronger frequency dependence.

6144 HIGH POWER FERROMAGNETIC RESONANCE AT X-BAND IN POLYCRYSTALLINE GARNETS AND FERRITES by J. J. Green (Harvard U.) and E. Schlomann (Raytheon) IRE Trans., Vol. MTT-8, pp. 100-103, Jan. 1960

Resonance experiments performed at X-band on spherical samples of polycrystalline yttrium garnet, yttrium-gadolinium garnet, yttrium-holmium garnet, and nickel-cobalt ferrite are discussed. The r-f field strength extended up to 60 oe. In the case of yttrium garnet the samples differed considerably in density and hence in linewidth. At fairly low power levels the susceptibility at resonance varies linearly with the square of the r-f magnetic field strength. At high power levels the susceptibility is inversely proportional to the amplitude of the microwave magnetic field. The "spin-wave linewidth" ΔH_k is inferred by extrapolation from the behavior at very high powers. It is found that ΔH_k is, to a large extent, independent of the linewidth ΔH observed by the usual low power experiments. In particular ΔH_k was found to be essentially the same (approximately 4 oe) for all yttrium iron garnets (single crystals and polycrystals with linewidth varying between 1.8 oe and 450 oe). On the other hand, ΔH_k increases very rapidly if the yttrium is partially substituted by holmium ($\Delta H_k \sim 11$ oe for 1 per cent substitution.)

6145 L-BAND FERROMAGNETIC RESONANCE EXPERIMENTS AT HIGH PEAK POWER LEVELS by E. Schlomann, J. H. Saunders, and M. H. Sirvetz (Raytheon); IRE Trans., Vol. MTT-8, pp. 96-100, Jan. 1960

The observation of ferromagnetic resonance absorption at high peak power levels at 1300 mc in yttrium-gadolinium garnets and in a nickel ferrite-aluminate is reported. In agreement with theoretical predictions, the critical field characterizing the onset of nonlinear effects, in a series of yttrium-gadolinium garnet disks of a given shape, was found to be very sensitively dependent on the gadolinium content. Similarly, for samples of a given composition, the critical field strength was sensitively dependent on the shape of the sample in agreement with theoretical predictions. At moderate power levels the susceptibility varies linearly with the square of the r-f magnetic field strength over an appreciable range. This result can be understood in terms of an extension of Suhl's theory. The results can be used to predict the high power performance of these materials when used in isolators.

6146 NUCLEAR MAGNETIC RESONANCE IN MULTIDOMAIN FERROMAGNETIC COBALT PARTICLES by A. C. Gossard and A. M. Portis (U. Calif.); Bull. Am. Phys. Soc., Ser. II, Vol. 5 p. 74 (A), Jan. 27, 1960

The effect of domain wall motion on the nuclear magnetic resonance of Co^{59} in 5 to 10μ multidomain metallic cobalt particles was discussed. It was shown that the bulk of the resonance absorption arises from nuclei within the domain walls. From the extraordinary intensity of the initially observed cobalt resonance absorption, it was inferred that the rf magnetic field of the cobalt nuclei is much stronger than the applied rf field. Saturation measurements now show directly the value of the rf field at the participating nuclei to be 1300 times the applied rf field. Domain rotation can produce an rf field enhancement to greater than 100. Domain wall motion, however, produces a larger enhancement than domain rotation by a factor of the ratio of domain diameter to domain wall thickness and satisfactorily accounts for the observed enhancement. Spin-spin and spin-lattice relaxation processes have been interpreted with the wall motion mechanism and a nuclear spin interaction through spin waves as proposed by Suhl.

6147 SPIN-PHONON INTERACTION IN YTTRIUM IRON GARNET by H. Bömmel and K. Dransfeld (Bell Labs.); Bull. Am. Phys. Soc., Ser. II, Vol. 5, p. 58 (A), Jan. 27, 1960

Measurements of the acoustic absorption in Yttrium Iron Garnet at a frequency of 1000 mc as a function of an applied d-c magnetic field were described. The single-crystalline YIG specimens were round disks 0.120 in. diameter and between 0.005 in. and 0.012 in. thick. Both the end faces were indium bonded onto oriented AC-cut quartz rods for the propagation of transverse hypersonic waves through the disk, in the direction normal to the plane of the disk. The d-c magnetic field, also oriented normal to the disk, was varied up to 7000 gauss. The acoustic transmission through the disks showed an enormous decrease around the field for ferrimagnetic resonance corresponding to an additional acoustic resonance absorption of several hundred db/cm. This absorption is temperature independent between 20° and 2°K, and does not occur for longitudinal sound waves or if the magnetic field is misaligned by more than 10° from its direction normal to the disk. Further experiments are being performed to determine whether the absorption arises from the acoustic excitation of spinwaves having the same energy and momentum as the incident phonon.

6148 SPECIFIC HEATS OF $NiCl_2 \cdot 6H_2O$ and $CoCl_2 \cdot 6H_2O$ BETWEEN 1.4° and 20°K by W. K. Robinson and S. A. Friedberg (Carnegie Inst. Tech.); Phys. Rev., Vol. 117, pp. 402-408, Jan. 15, 1960

Measurements of the specific heats of $NiCl_2 \cdot 6H_2O$ and $CoCl_2 \cdot 6H_2O$ in the temperature range from 1.4° to 20°K are reported. Lambda-type anomalies were observed at 5.34°K and 2.29°K and $NiCl_2 \cdot 6H_2O$ and $CoCl_2 \cdot 6H_2O$, respectively, associated presumably with antiferromagnetic-paramagnetic transitions. It has been possible in each case to separate out the magnetic contribution to the specific heat and thus to compute the total magnetic entropy gained in the transition from the fully ordered to completely disordered condition. This quantity was found to be given accurately by $R\ln(2S + 1)$ with $S = 1/2$ for Co^{++} and $S = 1$ for Ni^{++}. Short range order is particularly pronounced in these substances, the fraction of the total magnetic entropy gained above the Neel point being 0.52 for $CoCl_2 \cdot 6H_2O$ and for 0.40 for $NiCl_2 \cdot 6H_2O$. Other features of the anomalies are discussed.

6149 GAS ABSORPTION BY VACUUM EVAPORATED MAGNETIC FILMS by F. R. Gleason, J. H. Greiner, and L. R. Yetter (IBM); Vacuum, Vol. 9, p. 301 (A), Nov. 1959/Jan. 1960

Mass spectrometric determinations of the types and amounts of gases absorbed during the deposition of vacuum evaporated magnetic thin films were reported. The films were evaporated under varying conditions. Gas samples collected by outgassing the source material, outgassing evaporated films, and by sampling the bell jar atmosphere during the evaporation have been analyzed. It was shown that the gas absorbed in the films is much greater than that present in the starting charges and is due to dissociation of vapor backstreaming from the oil diffusion pump. The gas molecules absorbed per metal atom degassed are independent of the film thickness, indicating that the gas is trapped in the film structure as well as on the surface.

6150 LOW-TEMPERATURE MAGNETIC REMANENCE, MOLECULAR FIELD, AND APPROACH TO SATURATION OF HOLMIUM METAL by W. E. Henry (U. S. Naval Res. Lab.); Phys. Rev., Vol. 117, pp. 89-92, Jan. 1, 1960

The achievement of magnetization approaching absolute magnetic saturation for polycrystalline holmium is described. At 1.3°K and 70 000 gauss, the magnetic moment approaches 4.0 Bohr magnetons per atom of holmium in contrast to the 10 Bohr magnetons per atom expected on the basis of the spectroscopically determined quantum numbers. The actual results are explained on the basis of crystalline electric field splitting of the ground term of holmium and application of the Pauli exclusion

principle. In the liquid helium range, there is a pronounced hysteresis; i.e., the moment at 10000 gauss is 50% higher in decreasing fields than in increasing fields. The remanence is 9.22 Bohr magneton per atom of holmium at 4.2°K and 0.42 Bohr magneton per atom at 1.3°K. A sample motion technique was used to measure the magnetic moment of the 5-gram sample. The equipment was calibrated with iron and nickel.

6151 MAGNETIC AND ELECTRICAL RESISTIVITY PROPERTIES OF ERBIUM SINGLE CRYSTALS by R. W. Green, S. Legvold, and F. H. Spedding (Iowa State U.); Bull. Am. Phys. Soc., Ser. II, Vol. 5, p. 59 (A), Jan. 27, 1960

Measurements of magnetic properties and resistivity of erbium single crystals grown by the Bridgman method were discussed. The magnetic properties were determined in fields up to 18 kilooersteds with the field applied parallel to and perpendicular to the c axis at 4.2°K and between 20.4°K and 300°K. The c axis was found to be the direction of easy magnetization and a Neel point was observed at 84°K. The ferromagnetic-antiferromagnetic transition temperature inferred from the magnetic data is 19.6°K. The saturation moment $\sigma_{\infty,0}$ obtained by an extrapolation of the data is 268.7 cgs units/g. Between 1.3°K and 300°K the resistivity was determined with the current parallel to the c axis and also with the current parallel to the a axis. With the current parallel to the c axis a decided increase in resistivity was observed at 20.4°K, the ferromagnetic-antiferromagnetic transition temperature, a large peak occurred at 53.5°K, and a minimum occurred at the Neel point. These features were not observed with the current parallel to the a axis.

6152 MAGNETIZATION OF THE COMPOUND TiFe by M. V. Nevitt (Argonne Natl. Lab.); J. Appl. Phys., Vol. 31, pp. 155-157, Jan. 1960

Magnetization curves determined for the CsCl-type compound TiFe at six temperatures ranging from 9°K to 110°K are discussed. The curves show a saturation effect at high field strength but they are of a form that is not characteristic of ferromagnetism. A saturation magnetization of 3.30 ± 0.07 cgs units per gram was derived from the high field data. This moment is tentatively interpreted as resulting from a small concentration of uncompensated spins produced by disorder in the CsCl-type lattice. The electrical resistance of samples of TiFe was measured over the temperature range from 10°K to room temperature. Magnetization measurements were attempted on the CsCl-type compounds TiCo and TiNi, but their magnetizations were too small to be detected.

6153 NEUTRON DIFFRACTION STUDY OF THE MAGNETIC STRUCTURE OF $(Mn, Co)_4C$ by S. S. Sidhu, F. P. Campos, and D. D. Zauberis (Argonne Natl. Lab.); Bull. Am. Phys. Soc., Ser. II, Vol. 5, pp. 58-59 (A), Jan. 27, 1960

Preparation of a ternary alloy $Mn_{1.75}Co_{2.25}C$, with a structure similar to the compound Mn_2Co_2C, by alloying carbon with a binary alloy $Mn_{2.19}Co_{2.81}$ was described. An x-ray diffraction pattern of the binary alloy shows that it is face-centered-cubic with $a_0 = 3.618$ A, but its neutron pattern gives no Bragg peaks since the Mn atoms scatter thermal neutrons 180° out of phase with those of Co atoms. Therefore, there is no ordering of the metal atoms in this alloy. A neutron diffraction study of $Mn_{1.75}Co_{2.25}C$ then determines uniquely (1) order-disorder of metal atoms, (2) positions of C atoms, and (3) magnetic moment alignments in its unit cell.

6154 MAGNETIC STRUCTURE OF Mn CO_3 by S. J. Pickart (U. S. Naval Ord. Lab. and Brookhaven Natl. Lab.); Bull. Am. Phys. Soc., Ser. II, Vol. 5, p. 59 (A), Jan. 27, 1960

A low temperature powder neutron diffraction study undertaken in order to investigate the parasitic ferromagnetism observed in rhombohedral manganous carbonate (Rhodochrosite) below 31.7°K was discussed. The neutron pattern at 4.2°K shows coherent reflections which are traceable to a magnetic ordering, since they follow a Brillouin temperature dependence; these peaks disappear at about 32°K. The occurrence of these reflections at positions forbidden by the space group can be explained if the alignment of the Mn^{2+} spins is anti-ferromagnetic, the spin sign alternating around the rhombohedral axis. The observed magnetic intensities are not satisfied if the moments are aligned either parallel or perpendicular to the [111] axis, but a good fit is obtained by taking the spin direction as [100], although this is by no means a unique solution. The data were discussed in relation to the "canted spin" model predicted from thermodynamic consideration, as well as to other plausible origins of the parasitic moment.

6155 MAGNETIC CERAMICS: VII, EFFECT OF IRON OXIDE PARTICLE SIZE ON NICKEL FERRITE FORMATION by G. Economos and T. R. Clevenger, Jr. (MIT); J. Am. Ceram. Soc., Vol. 43, pp. 48-52, Jan. 1960

The results of heating five iron oxides of increasing particle-size distribution, mixed with nickel oxide of a constant-size range, at various temperatures and time intervals are reported. The extent of nickel ferrite formation, as influenced by particle-size distribution of the iron oxide constituent, was measured with a compensating-coil magnetometer. Using the Jander relation for this type of reaction, activation energies ranging from 54 to 70 kcal were computed for increasing particle size. These results are examined and compared with current procedures for the production of ferrite powders.

6156 THE THERMOMAGNETIC BEHAVIOR OF PURE NICKEL FERRITE by L. F. Bates and H. Clow (U. Nottingham); Proc. Phys. Soc., Vol. 75, pp. 17-23, Jan. 1960

Measurements of the small heat changes which accompany the magnetization of pure nickel ferrite, made on a rod specimen at -10 and 18°C are reported. The results have been analyzed using a theory for thermal changes which accompany the magnetization of ferromagnetic substances in high fields. Some support for the Lilley disperse field theory has been found.

6157 MAGNETIC PROPERTIES OF THE MANGANESE CHROMITE-ALUMINATES by P. L. Edwards (U. S. Naval Ord. Lab.); U. S. Gov. Res. Rep., Vol. 33, p. 88 (A), Jan. 15, 1960

An experimental study of the magnetic properties of the spinel series $MnCr_2O_4$ - $MnAl_2O_4$ is discussed. This series was chosen for study because $MnCr_2O_4$ has a saturation moment at absolute zero which is inconsistent with the Neel theory and which has been attributed to the existence of Yafet and Kittel angles on the B sites by both Gorter and Lotgering. The $MnCr_2O_4$ - $MnAl_2O_4$ series is particularly useful for such a study because there is only one type (approximately) of magnetic ion on each sub-lattice. The Neel theory of ferrimagnetism, the crystal preparation, the experimental apparatus and data are discussed.

6158 ANTIFERROMAGNETISM IN $CoBr_2 \cdot 6H_2O$ by H. Forstat, M. Garber, and R. D. Spence (Mich. State U.); Bull. Am. Phys. Soc., Ser. II, Vol. 5, p. 59 (A), Jan. 27, 1960

Measurements of the magnetic susceptibility, specific heat, and proton resonance of single crystals of $CoBr_2 \cdot 6H_2O$ in the

liquid helium temperature range were discussed. The susceptibility measurements show a Neel temperature of 3.2°K with spin alignment direction normal to the monoclinic b axis. If the a axis represents spin direction, then $\chi_a = 0.60$, $\chi_b = 0.68$, and $\chi_c = 0.18 \times 10^{-3}$ emu/g at 4.2°K. A λ-type anomaly is observed in the specific heat measurements at 3.07°K. The entropy change associated with the magnetic ordering, calculated from the specific heat curves, is 1.42 cal/deg mole. The value of R ln (2S + 1) is 1.38 cal/deg mole where S = 1/2 for Co^{++}. Short-range ordering is indicated by a 38 percent contribution to the total magnetic entropy above the Neel point, and by a constant susceptibility from 3.2° to 4.2°K. The proton resonance data indicate an antiferromagnetic state below 3.08°K. The resonance pattern shows symmetry about a frequency on the high-frequency side of the free proton resonance and a periodicity of 360° in the angular variation of the individual components.

6159 CRYSTAL CHEMICAL AND MAGNETIC STUDIES OF GARNET SYSTEMS $M_3^{2+}Fe_2Sn_3O_{12}$-$Y_3Fe_2Fe_3O_{12}$ by S. Geller, R. M. Bozorth, M. A. Gilleo, and C. E. Miller (Bell Labs.); J. Phys. Chem. Solids, Vol. 12, pp. 111-118, Jan. 1960

A complete solid-solution range exists in the system $Ca_3Fe_2Sn_3O_{12}$ (CIS)-$Y_3Fe_2Fe_3O_{12}$(YIG). Because of its large size, the Sn^{4+} ion prefers the octahedral positions; thus for dilute solutions of CIS in YIG the saturation magnetization of 0°K increases. A maximum of 7.3μ_B per formula unit is reached at about 20 mol. per cent CIS solid solution. However, the plot of n_B (∞,0) vs. composition deviates markedly from that which depends only on a simple interaction model. At 33 mol. per cent CIS, n_B = 5.2μ_B, and at 50 mol. per cent n_B = 1.2μ_B, even though the Sn^{4+} ions are very nearly all in the octahedral sites. At 67 mol. per cent CIS, 90 per cent of the octahedral sites are filled with Sn^{4+} ions, as determined by x-ray diffraction and $n_B \approx 0.25\mu_B$. The magnetic behavior of this system may be explained on the basis of the reduction of the number of octahedral-tetrahedral magnetic-ion interactions with increasing concentration of CIS and, at the higher concentrations, the establishment of two magnetic sublattices among the tetrahedral ions. No other end-members $M_3^{2+}Fe_2Sn_3O_{12}$ were obtained, but with M = Sr the extent of solubility in YIG is ~33 mol. per cent, and when M = Ba, <5 mol. per cent. Some inconclusive experiments also indicated some solution when M = Cd, Zn, Mn, Ni and Mg.

6160 SYSTEM $(Ba_{6-2x}R_{2x})(Nb_{9-}Fe_{1-})O_{30}$. II. FERRIMAGNETIC PROPERTIES by P. M. Pan (Westinghouse) and P. H. Fang and R. S. Roth (NBS); Bull. Am. Phys. Soc., Ser. II, Vol. 5 p. 57 (A), Jan. 27 1960

Observation of ferrimagnetic properties in the system $(Ba_{6-2x}R_{2x})(Nb_{9-x}Fe_{1-x})O_{30}$ where R is one of the trivalent rare earth ions was reported. The Curie temperatures of these materials, which increase with the decrease of the ionic radius, are -30°C for Nd, 35°C for Sm, 60°C for Eu, and 90°C for Gd. At room temperature, frequency dispersions of these materials in the ferrimagnetic state are in the region of 15 to 25 mc. A dielectric dispersion is also found in the same frequency region at room temperature. For Sm, Eu, and Gd the coercive field is about 900 oe measured at 455 kc. The intrinsic magnetic permeability is about 35 to 50 for R = Nd, Sm, Eu and 120 for R = Gd. These compositions seem to represent a new ferrimagnetic structure.

Ferrimagnetic Properties of the System $(Ba_{6-2x}R_{2x}{}^{+3})(Nb_{9-x}M_{1-x}{}^{+3})O_{30}$ - See 6082.

6161 PARAMAGNETIC RESONANCE IN SOLIDS by W. Low (Hebrew U.); Solid State Physics (Academic Press) suppl. 2, 212 pages, 1960

The theory of the crystalline field, paramagnetic resonance spectra of the transition elements in single crystals, relaxation times and line width, paramagnetic resonance of color centers and defects in crystals, and paramagnetic resonance spectrometers are discussed. Both theory and experiment are considered. In a brief discussion of masers, three methods for inverting the spin population are reviewed. [280 references]

6162 "SPIN-FLIP NARROWING" OF PARAMAGNETIC RESONANCE LINES by J. M. Daniels and H. A. Farach (U. Brit. Columbia); Can. J. Phys., Vol. 38, pp. 151-152 (L), Jan. 1

The paramagnetic resonance spectrum of copper measured at 3 cm wavelength at room temperature and at 77°K in (5% Cu 95% Zn) $K_2(SO_4)_2 \cdot 6H_2O$ and in (5% Cu 95% Co) $K_2(SO_4)_2 \cdot 6H_2$ is discussed. In the Cu-Zn specimen a broad line, 300 gauss wide, appears at room temperature and narrows at 77°K so that the four hyperfine components start to be resolved. In the Cu specimen, a line 300 gauss wide also appears at room temperature. This line almost disappears, becoming very feeble and at least 2000 gauss wide at 77°K. It is suggested that in the Cu-Zn case the line broadens at room temperature because of the shorter spin-lattice relaxation time of the Cu ions and that in the Cu-Co case the Cu line is broadened at 77°K by the spin-spin interaction between the Cu and Co ions. It is pointed out that in compounds which have paramagnetic ions with very different values of spin-lattice relaxation time, the variation of the line width of one component as a function of temperature can be studied to determine the spin-lattice relaxation time of the other component.

6163 MICROWAVE PARAMAGNETIC RESONANCE SPECTRUM OF THE FOUR NONEQUIVALENT Cr^{+++} SITES IN DOPED $K_3Co(CN)_6$ by J. O. Artman and J. C. Murphy (Johns Hopk. U.); Bull. Am. Phys. Soc., Ser. II. Vol. 5, pp. 73-74 (A), Jan. 27, 1960

Investigations on the microwave resonance of Cr^{+++} in single crystals of doped $K_3Co(CN)_6$ which indicate the existence of four nonequivalent magnetic sites rather than the two customarily described were reported. The effect is seen dramatically in the b-c crystal plane as a periodic splitting of supposedly single resonance lines into sets of three. The symmetry of the two additional resonances precludes their generation by simple crystal twinning. The microwave spectrum seems to be associated with the "polytypism" recently found in this crystal by Kohn and Townes, which would predict four molecules per unit cell rather than two. Further details and implications on maser performance were presented.

6164 SPIN RESONANCE OF TRANSITION METALS IN SILICON by H. H. Woodbury and G. W. Ludwig (GE Res. Lab.); Phys. Rev., Vol. 117, pp. 102-108, Jan. 1, 1960

Spin resonance measurements for various charge states of four transition metals in silicon, namely for V^{++}, Cr^{+}, Mn^{-}, Mn^{++} and Fe^{0}, are reported. In each case the g tensor and the hyperfine interaction with the impurity nucleus are isotropic. Thus each element exists in an isolated form in silicon and undergoes no distortion from the site of maximum symmetry. The site may be either the substitutional position or the interstitial position of maximum symmetry in the silicon lattice. For

$(Cr^{51})^{++}$, S = $\frac{3}{2}$, A = -42.10; for $(Cr^{53})^{+}$, S = $\frac{5}{2}$, a = +30.16, A = +10.67; for $(Mn^{55})^{-}$, S = 1, A = -71.28; for $(Mn^{55})^{++}$, S = $\frac{5}{2}$, a = +19.88, A = -53.47; for $(Fe^{57})^{0}$, S = 1 A = 6.98, where a is the cubic field splitting parameter, A is the hyperfine interaction of the isotope noted, and both are expressed in units of 10^{-4} cm^{-1}. Electron-nuclear double resonance was used for accurate measurement of A and for the determination of S. In the case of Fe^{0}, the electron spin was checked by noting that the iron line splits into two fine structure components under uniaxial stress. Association of Cr, Mn, and Fe with acceptors in silicon has been observed, as well as another charge state of isolated Fe.

6165 PARAMAGNETIC RESONANCE OF Fe^{3+} IN RUTILE by T. Okaya, D. Carter, and F. Nash (Columbia U.); Bull. Am. Phys. Soc., Ser. II, Vol. 5, p. 73 (A), Jan. 27, 1960

An experimental investigation of the electron spin resonance of the $^6S_{5/2}$, $3d^5$ ground state of Fe^{3+} in TiO_2 (rutile) was reported. The local crystalline field is orthorhombic. The spectrum has been observed from 2 kmc to 120 kmc by a simple video type spectrometer using dielectric microwave resonators. The directly measured zero field splittings are 43.3 ± 0.1 kmc for the Ms = 3/2 → 1/2 transition and 81.3 ± 0.1 kmc for the Ms = -3/2 → 3/2 transition. The spectrum has been well explained by the constants:

= +20.35 ± 0.2 kmc	E = +2.14 ± 0.06 kmc
= + 0.8 ± 0.4 kmc	g = 2.00 ± 0.02 kmc

T_1 at 1.4°K was about 4 msec at X-band frequencies and less than 1 msec at K band. The saturation of 10^{19} spins was observed at 78°K, X-band frequency with only 0.1 mw power input. This was caused by the high Q and high dielectric constant of the dielectric resonator. The line breadth varies between 3.5 to 15 gauss at X band depending upon the transition.

6166 PARAMAGNETIC RESONANCE OF X-IRRADIATED ROCHELLE SALT by G. C. Moulton, W. G. Moulton, and W. B. Ard, Jr. (U. Alabama); Bull. Am. Phys. Soc., Ser. II, Vol. 5, p. 73 (A), Jan. 27, 1960

An investigation of the paramagnetic resonance spectrum of rochelle salt irradiated with 50 kv x-rays at 9000 Mc was reported. The spectrum consists of at least 10 lines. The total width about the C axis is invariant and is 46 gauss with the center of the spectrum corresponding to a g value near 2. There is small orientation dependence and data have been taken about all three crystalline axes. At least two sets of lines are present as indicated by the orientation dependence and the unequal decay rates of the components with time; one is a strong short-lived set, the other a weak long-lived set. The crystal becomes bright yellow after irradiation and the color and the anomalous hysteresis effects remain after the strong set of paramagnetic lines has decayed. The spectrum is the same whether observed above the ferroelectric Curie points or in the ferroelectric temperature range. It is concluded that the anomalous ferroelectric hysteresis effects found after irradiation are not due to the short lived paramagnetic centers.

6167 RESONANCE SPECTRUM OF A PARAMAGNETIC FERROELECTRIC: Cr^{+++}IN GUANIDINE ALUM by E. G. Brock, E. Hormats, and F. C. Unterleitner (Stromberg-Carlson); Bull. Am. Phys. Soc., Ser. II, Vol. 5, p. 58 (A), Jan. 27, 1960

The observation of electron paramagnetic resonance for low concentrations of guanidine chromium sulfate hexahydrate in isomorphous guanidine aluminum sulfate hexahydrate was reported. Both materials are ferroelectric. The single crystals used in the resonance measurements were prepared by crystallization from a saturated aqueous solution. The crystals grew in the form of hexagonal plates with the trigonal crystalline symmetry axis as the normal. Results obtained at room temperature using a TM_{010} mode reflection cavity at 9540 mc on single crystals of $(CN_3H_6)\,Al_{0.99}Cr_{0.01}(SO_4)_2\cdot 6H_2O$ suggest an effective 3/2 spin for the chromium ion. The principal magnetic axis coincides with the crystalline trigonal axis. No off-axis splitting is indicated. However, a distinctive pairing of all transitions suggests that the chromium ions occupy two magnetically dissimilar lattice sites, I and II. In terms of the usual spin Hamiltonian, $\mathcal{H} = \beta H\cdot g\cdot S + D[S_z^2 - 1/3\ S\ (S+1)]$, $g = g_{\parallel} = g_{11} = 1.98$ and is almost isotropic; while $D_1 = 0.0575\ cm^{-1}$. The crystal structure suggests that Type I chromium is in a special position on the mirror plane and that Type II chromium is in a general position. On this basis relative chromium populations should be I:II = 1:2, in agreement with the observed resonance amplitude ratios.

6168 SPIN-LATTICE INTERACTION FOR DONOR ELECTRONS IN Ge and Si by L. M. Roth (Lincoln Lab.); Bull. Am. Phys. Soc., Ser. II, Vol. 5 p. 60 (A) Jan. 27, 1960

The effect of spin-orbit interaction on the g factors of electrons in Ge and Si was analyzed. Calculations indicate strongly that the effect is quite anisotropic, with $g_{\parallel}$ (i.e., parallel to the axis of the electron's ellipsoids) differing from 2 by considerably more than $g_{\perp}$. For donor electrons in either material the ground electronic state is split, due to interactions between the ellipsoids, into excited states (a doublet and triplet for Si and a triplet for Ge) and a singlet state whose wave function involves a symmetric combination of wave functions from the various ellipsoids, and which is generally lowest. The effective g factor depends on which state the system is in, and for the singlet state g is a scalar. One consequence of the anisotropic g tensor is a strong interaction between the spin and shear waves, which modulate the g tensor for the singlet. This interaction can account in order of magnitude for the observed spin-lattice time τ_s in Si for low temperatures, including both a one-phonon process and a two-phonon Raman-type process. The temperature and magnetic field dependence of the two processes are predicted to be $\tau_s^{-1} \propto TH^4$ and $\tau_s^{-1} \propto T^7H^2$, respectively.

6169 SPIN - LATTICE RELAXATION TIMES IN RUBY AT 34.6 KMC/SEC by J. H. Pace, D. F. Sampson, and J. S. Thorp (RRE); Phys. Rev. Lett., Vol. 4, pp. 18-19 (L), Jan. 1, 1960

Measurements of the spin-lattice relaxation time in ruby containing 0.1% Cr performed at 34.6 kmc between 1.4°K and 90°K are reported. A pulse saturation method was used and the polar angle was 90°. The relaxation times for the Δ1 transitions are of the same order of magnitude as previously reported at 7.2 kmc, 9.3 kmc, and 24.2 kmc. At 1.4°K the relaxation times are appreciably different for the Δ2 and Δ3 transitions. Initial measurements indicate that the relaxation time for all these levels approaches a common value at about 77°K. The results indicate that ruby is suitable for use in masers which operate in the millimeter region.

6170 ELECTRON-SPIN RESONANCE IN SEMICONDUCTING RUTILE by P. F. Chester (Westinghouse Res. Labs.); Bull. Am. Phys. Soc., Ser. II, Vol. 5, p. 73 (A), Jan. 27, 1960

Observation of electron spin resonance in single crystals of oxygen deficient TiO_2 at liquid helium temperatures was reported. The spectrum is described by four magnetic sites with S = 1/2, $g_z = 1.930$, $g_x = 1.972$, and $g_y = 1.975$. The four z axes coincide and lie along the crystal c axis, while the four x (or y) axes make angles of approximately ±25° with the crystal a axes. The single line observed with H ∥ c axis has a

full width of ~0.7 oe and is accompanied by a pattern of very weak satellites extending for 10 oe on either side. The spin lattice relaxation time at 2.16°K is 0.012 sec. No resonance could be seen at 77°K or at room temperature because of microwave losses which were observed to increase exponentially in the range 8°K to 12°K, with an activation energy of ~0.01 ev. D-C resistivity measurements on the same sample (10 ohm cm at 300°K) yielded the same activation energy over the range from 5°K to 40°K by which temperature the resistivity had fallen to 0.1 ohm cm. An explanation of the paramagnetic center, in terms of Ti^{3+} associated with certain oxygen vacancies, was discussed. No resonance was observed in oxygen deficient $SrTiO_3$ at liquid helium temperatures.

6171 ELECTRON SPIN-LATTICE RELAXATION IN PHOSPHORUS-DOPED SILICON by A. Honig and E. Stupp (Syracuse U.); Phys. Rev., Vol. 117, pp. 69-89, Jan. 1, 1960

An investigation of electron spin-lattice relaxation in phosphorus-doped silicon over a magnetic field range of 0 to 11000 oersteds, a temperature range of 1.25 to 4.2°K, and a concentration range of 10^{14} P/cc to 3×10^{16} P/cc is presented. Three distinct τ_S ($\Delta m_S = \pm 1$, $\Delta m_I = 0$) relaxation mechanisms have been identified, and their functional dependences on magnetic field, temperature, and concentration have been determined. In addition to these three τ_S mechanisms, the horizontal relaxation modes ($\Delta m_I = \pm 1$, $\Delta m_S = 0, \pm 1, \mp 1$) have been investigated. A theory is proposed to explain a concentration dependent τ_S mechanism, according to which rapidly relaxing close pairs of phosphorus atoms, which are few in number, relax the spins of the large number of isolated phosphorus atoms via a spin diffusion process. Experiments supporting this hypothesis are presented.

6172 INFLUENCE OF EXCHANGE INTERACTION ON PARAMAGNETIC RELAXATION TIMES by J. P. Goldsborough, M. Mandel, and G. E. Pake (Stanford U.); Phys. Rev. Lett., Vol. 4, pp. 13-15 (L), Jan. 1, 1960

Measurements of the spin-lattice relaxation time T_1 and the spin-lattice relaxation time T_2 in several free radicals in the temperature range 1.5°K to room temperature are reported. The solid free radicals α_1, α-diphenyl β-picryl hydrazyl (DPPH), α, γ-bisdiphenylene β-phenyl allyl (BDPA), Wurster's blue perchlorate, and some solid solutions of DPPH in polystyrene were investigated. In DPPH, BDPA, and Wurster's blue T_1 is approximately equal to T_2 at 77°K and room temperature. In those substances with higher exchange frequency, T_1 is more nearly equal to T_2 and temperature independent. In the most concentrated solid solution of DPPH in polystyrene T_1 was found equal to T_2 and temperature independent. As the concentration is reduced, T_1 becomes temperature dependent and longer than T_2. Eventually T_1 becomes independent of concentration. At a sufficiently low concentration, exchange interaction diminishes and the hyperfine structure characteristic of DPPH appears. The experimental results are interpreted by the three-level reservoir model of Bloembergen and Wang.

6173 SPIN COUPLING IN CRYSTALS WITH TWO PARAMAGNETIC SPECIES by A. Kiel (Johns Hopkins U.) Bull. Am. Phys. Soc., Ser. II, Vol. 5, p. 73 (A), Jan. 27, 1960

In some recent work, it has been shown that terms in the spin-spin interaction may lead to a diffusion of spins in frequency space. The reality of these effects is now well established in multi-level systems. By applying the appropriate rate equatio modified by a cross-coupling term, the effects of (nearly) ove lapping resonance lines of different paramagnetic ions may be investigated. A formula for an effective relaxation time, observed in saturation experiments when only species α interacts with the rf field, was given. More general saturation expressions were derived and the pulse case was considered in detai Estimates of the magnitude of the T_{21} based on lattice sum computations were presented for the cases $T_{21} << T_1^{\alpha}, T_1^{\beta}$ and $T_1^{\beta} < T_{21}^{\alpha} < T_1^{\alpha}$.

6174 ON THE ORIGIN OF DISTORTIONS PRODUCED BY Ni^{2+} ON TETRAHEDRAL LATTICE SITES by P. K. Baltzer (RCA Labs.); Bull. Am. Phys. Soc., Ser. II, Vol. 5, p. 49 (A), Jan. 27, 1960

All the 3d-electronic states of Ni^{2+} have been calculated, including L-S coupling, for the case in which this ion is subject to the crystalline fields of tetrahedral and octahedral lattice sites which have cubic, tetragonal or trigonal symmetry. The origin of the low-symmetry distortion that Ni^{2+} induces on tetrahedral lattice sites, a point of considerable interest and debat has been resolved. A general criterion for predicting the occurrence of induced spontaneous distortions is that the distortion perturbation lowers the energy of at least one component of the electronic ground state. The Jahn-Teller theorem is applicable only for the special case when the trace of the distortion perturbation over all the components of the electronic ground stat is zero, and then only a degenerate ground state will induce distortions. When this trace is nonzero, spontaneous distortion may or may not be induced for either degenerate or non-degenerate ground states. The L-S interaction (1000 cm^{-1} for Ni^{2+}) in general makes the trace over any state nonzero for a perturbation acting only on the spatial part of the wave functions. It is calculated that the singlet ground state of Ni^{2+} in tetrahedral lattice sites in oxides is lowered in energy 1000 cm^{-1} by a 10 percent tetragonal distortion.

6175 NUCLEAR RELAXATION VIA QUADRUPOLE COUPLI by R. L. Mieher (U. Illinois); Phys. Rev. Lett., Vol. 4, pp. 57-59 (L), Jan. 15, 1960

The angular and temperature dependences of the quadrupolar nuclear spin-lattice relaxation time T_1 in cubic crystals with r static quadrupole interactions are discussed and an expression for T_1 in terms of the predicted transition probabilities is derived. It is found theoretically that T_1 is isotropic because th angular dependences of the transition probabilities exactly can cel. T_1 measurements on In^{115} in a single crystal of InSb at 77 give an isotropic T_1 of 0.80 ± 0.05 sec. Measurements of thee temperature dependence of I^{127} in KI between 77°K and 800° showed a $T_1 \propto T^{-2}$ relationship. T_1 measurements on In^{115} in In were found to agree with Van Kranendonk's E(T*) function at temperatures less than the Debye temperature.

OPTICAL PROPERTIES

6176 THE THEORY OF OPTICAL PROPERTIES OF ELECTRON SEMICONDUCTORS IN THE INFRARED REGION OF THE SPECTRUM by V. I. Cherepanov (Ural State U.); Soviet Phys Solid State, Vol. 1, pp. 947-955, Jan. 1960

An investigation of the interaction between electromagnetic waves in the infrared region of the spectrum and the conductio electrons in an electron semiconductor on the basis of the clas sical free-electron model is discussed. The basic differential equation for the electrical intensity of the electromagnetic wave for normal spin-effect conditions is derived and solved, and the surface impedance is determined. The general dis-

OPTICAL PROPERTIES (Cont'd)

ersion formulas for the optical constants of the nondegenerate ectron semiconductor with arbitrary dependence of the elec- nic relaxation time τ on the electron velocity v are obtained. e explicit form of these formulas is determined for homopolar miconductors for which $\tau = lv^{-1}$. The results are compared th the classical Drude-Zener-Kronig theory of metals.

otoelectric Properties of Grain Boundary Layers - See 6072.

177 CHARACTERISTIC ENERGY LOSSES AND OPTICAL TRANSMISSIVITY by H. Mendlowitz (NBS); Bull. Am. Phys. oc., Ser. II, Vol. 5, p. 68 (A), Jan. 27, 1960

orrelation of the reflectivities and transmissivities of a number f materials as a function of wavelength through the vacuum ltraviolet in terms of the complex dielectric constant as a func- ion of frequency was presented. In general, the onset of trans- ission in metal films occurs at a photon energy which is slightly ss than the energy loss suffered by the electron in the major haracteristic loss. Also, the general form of the transmissivity urves was interpreted in terms of the dielectric constant.

frared Studies of Electron Irradiated Silicon - See 6050, 6051.

178 OPTICAL ABSORPTION IN TELLURIUM by K. C. No- ura and J. S. Blakemore (Honeywell Res. Ctr.); Bull. Am. hys. Soc., Ser. II, Vol. 5, p. 62 (A), Jan. 27, 1960

easurements of the optical absorption coefficient in Te single rystals as a function of polarization from 1000 cm^{-1} to 0.2 m^{-1} by use of transmission techniques at 300°K and 110°K were resented. Previous theories that the conduction and valence and extrema occur at the same point in the Brillouin zone were uestioned, since the present results can be interpreted most eadily in terms of indirect (phonon-aided) transitions for both olarizations. The absorption edge shifts by -2×10^{-5} ev/°K or radiation polarized parallel to the c axis and at a rate of 3.5×10^{-5} ev/°K for the perpendicular polarization.

179 ELECTRICAL AND OPTICAL EFFECTS OF OXYGEN IN GERMANIUM by W. Kaiser, H. J. Hrostowski, and C. D. hurmond (Bell Labs.); Bull. Am. Phys. Soc., Ser. II, Vol. 5, p. 61-62 (A), Jan. 27, 1960

he electrical and optical effects of doping germanium single rystals with oxygen via the ambient were discussed. The in- ensity of the absorption band at 11.69μ has been quantitatively orrelated with the oxygen content determined by vacuum fusion as analysis. During heat treatment at several hundred degrees entrigrade donor states appear quite rapidly (within minutes) and ne amount of dissolved oxygen decreases. At 470°C the ratio f loss of dissolved oxygen atoms to the number of donors formed approximately 4, indicating that the donors result from aggre- ates of oxygen atoms similar to those found in silicon. A eries of small absorption bands at 7.95μ, 10.81μ, 12.3μ and 2.8μ appears during the heat treatment of germanium (similar ands occur at 9.5μ and 9.75μ in silicon). They are attributed o vibrations of various germanium-oxygen (silicon-oxygen) ag- regates. The band at 12.8μ is proportional to the donor con- entration (formed at 470°C) and is tentatively believed caused y a GeO_4 vibration. Precipitation of oxygen is observed after ong annealing (65 hr) at high temperature (e.g., 650°C).

180 OPTICAL ABSORPTION IN GERMANIUM by J. C. hillips (U. Calif.); J. Phys. Chem. Solids, Vol. 12, pp. 08-209 (L), Jan. 1960

Measurements of the spectral dependence of the absorption coef- cient of germanium from 1 to 10 ev are analyzed. It is shown hat the edge measured at 2.1 ev is due to the transition $L3' \rightarrow L_1$ and it is suggested that the strong peak near 4.5 ev is due to the transition $X_4 \rightarrow X_1$. The analysis indicates that the quantum ef- ficiency of electron-hole pair production is quite different from that proposed by Antoncik (Abstr. 3440).

6181 INFLUENCE OF DEGENERACY ON RECOMBINATION RADIATION IN GERMANIUM by J. I. Pankove (RCA Labs); Phys. Rev. Lett., Vol. 4, pp. 20-21, Jan. 1, 1960

An emission spectrum measured at 77°K on a germanium tunnel diode biased in the injection mode is discussed. In the spectrum there is a low-energy peak which moves to higher energies as the current increases and a rapidly growing peak at 0.71 ev. It is suggested that the spectrum can be explained by consider- ing the occupancy of the degenerate conduction band.

Electroenhancement and Electroquenching of X-Ray Excited Luminescence - See 6191.

6182 MICROSCOPIC OBSERVATIONS ON ELECTROLUMIN- ESCENT PHOSPHORS by A. Kremheller (Sylvania Res. Labs.); J. Electrochem. Soc., Vol. 107, pp. 8-12, Jan. 1960

Microscopic observations of the electroluminescent brightness of single phosphor particles in liquid dielectric cells are dis- cussed. A simple visual technique in conjunction with a mi- croscope permits one to analyze the brightness distribution within and among electroluminescent particles. Some experi- mental results on the nonuniformity of the emission, the influ- ence of ball milling and acid etching on the brightness, the improvement of brightness by particle separation, the analysis of the integrated light output as a function of the processing temperature, and the brightness changes due to particle orien- tation, contact, and irradiation are presented.

6183 VOLTAGE DEPENDENCE AND PARTICLE SIZE DISTRI- BUTION OF ELECTROLUMINESCENT PHOSPHORS by W. Lehmann (Westinghouse); J. Electrochem. Soc., Vol. 107, pp. 20-26, Jan. 1960

The particle sizes of electroluminescent zinc sulfide phosphors prepared by common firing techniques usually range over broad distributions which always have the same shape. Every phos- phor of this "normal" particle size distribution shows a voltage (V) dependence of electroluminescent brightness (L) which, over many decades of L, can closely be described by $L = Lo \exp[-(V_o/V)^{0.5}]$. Every deviation of the particle size dis- tribution from the "normal" form also causes a deviation of the measurable L(V) dependence from this expression. Measure- ments on phosphor particles and on uniform phosphor films in- dicate that the basic excitation mechanism of electrolumines- cence follows the voltage dependence $L = L_o \exp[-(V_o/V)]$ and that the square root in the exponent of the usual equation is due mainly to the broad particle size distribution of regular phosphors. This view is supported also by a mathematical a- nalysis.

6184 ELECTROLUMINESCENCE UNDER PULSED SQUARE- WAVE EXCITATION by R. Zallen, W. T. Eriksen, and H. Ahlburg (Raytheon); Bull. Am. Phys. Soc., Ser. II, Vol. 5, pp. 69-70 (A), Jan. 27, 1960

The slow return of an electroluminescent cell to its equilibrium state following a field excitation has been studied for a blue- green emitting Zn(S,O): Cu, Cl phosphor and for a yellow- emitting ZnS:Mn, Cu phosphor. The light pulse emitted upon the rise of a square-voltage pulse was measured as a function of repetition rate and of temperature between -130°C and 150°C. Relaxation times encountered varied from 10^{-2} sec to more than 10^5 sec. The temperature dependence of the relaxa- tion rate exhibits effective activation energies of about 0.4,

0.7, and 0.6 ev, respectively, for the blue, green, and yellow emission bands. The results do not seem to favor the mechanism of delayed recombination. An alternative mechanism was suggested whereby the number of filled deep donors is assumed to control the electroluminescence emission via the number of field-ionizable electrons available for collision-excitation of centers. Observations were also made on some other effects associated with square-wave excitation.

6185 IRREVERSIBLE THERMODYNAMICS OF INJECTION ELECTROLUMINESCENCE by F. E. Williams (GE Res. Lab.); Bull. Am. Phys. Soc., Ser. II, Vol. 5, p. 70 (A), Jan. 27, 1960

The possible generation by minority carrier injection of electroluminescent emission exceeding the electrical input was discussed. The additional energy would be taken as heat from the lattice and the system would thereby cool. Equilibrium thermodynamics has been applied to the problem and tends to support the possibility. Injection electroluminescence can readily be shown to be irreversible. The application of irreversible thermodynamics provides more severe limitations on the efficiency of injection electroluminescence. Because the second law must be satisfied locally for irreversible processes the entropy increase associated with the radiation must at least balance the entropy decrease accompanying electron-hole pair annihilation. This requirement precludes quite generally realistic electroluminescent emission intensities in excess of the electrical input. Radiative recombination at impurities introduces additional limitations. The thermodynamic limitations which are common to both electro- and photoluminescence were discussed.

6186 FATIGUE IN ELECTROLUMINESCENT PHOSPHORS by S. Nudelman and J. Mudar (U. Mich.); Bull. Am. Phys. Soc., Ser. II, Vol. 5, p. 70 (A), Jan. 27, 1960

Observations of fatigue in electroluminescent phosphor panels (decrease of electroluminescence under constant operating conditions) at frequencies up to 6 mc, with applied voltages up to 1500 v across a 4-mil thick cell, were reported. Fatigue is accelerated with increasing frequency, so that at 2 mc, electroluminescence diminishes from 10 to 25 percent of initial values within 30 minutes. Fatigued phosphors show a decrease in time average light output at the higher frequencies. Mechanically shaking a phosphor-air electroluminescent cell after fatigue causes a partial restimulation of electroluminescence, followed by fatigue. Successive shakes show a decreasing effect, corresponding to all sides of the phosphor particle being fatigued. This indicates a uniform filling of deep surface traps, or a uniform degradation in electroluminescent centers. Tests for deep traps using high voltage, low frequency fields simultaneously with photo-stimulation were negative. Measurements on phosphor in air and in various dielectrics indicate with Roberts that fatigue is characteristic of the phosphor although his law has not been confirmed. Appreciable fatigue occurs for cells operated down to liquid nitrogen temperatures.

Ionic Properties of Electroluminescent Zinc Sulfide - See 6080.

6187 THERMOLUMINESCENCE OF ZnS SINGLE CRYSTALS by H. Arbell and A. Halperin (Hebrew U., Jerusalem); Phys. Rev., Vol. 117, pp. 45-52, Jan. 1, 1960

The blue and green components of the glow of ZnS:Cu:Cl crystals have been recorded separately. Thermoluminescence-excitation spectra taken for each of the components were found to be identical with the excitation spectra for the blue and green luminescence at steady excitation. Other measurements included the spectral distribution of the glow, saturation effects, effects of infrared radiation, and computation of activation energies. The activation energy for the blue peak was found to be about 0.14 ev, and that for the green about 0.20 ev. From the shape of the peaks it was concluded that the recombination process is bimolecular in character. Electrical glow curves were also recorded and were found to be similar to the green glow curves. The results are discussed and an energy model is proposed.

6188 WAVE-LENGTH DEPENDENCE OF THE QUANTUM EFFICIENCY AND ABSORPTION OF POWDER PHOSPHORS by Y. Uehara, I. Masuda, and Y. Kobuke (Tokyo Shibaura Electric); J. Electrochem. Soc., Vol. 107, pp. 1-8, Jan. 1960

Measurements of the properties of a number of powder phosphors made by a direct optical method are reported and the results are compared with other published values. Although slight discrepancies are found for magnesium and calcium tungstate at the 2537A position, the maximum quantum efficiency for magnesium tungstate is in good agreement with the published values. Good agreement is also found for impurity-activated phosphors. New data are presented for a number of ortho-phosphates. The quantum efficiency curves decrease more rapidly than the absorption curves toward both longer and shorter wavelengths from the peak position. The peaks of the quantum efficiency curves lie at longer wave lengths than those of the absorption curves. Reasons for these differences are discussed.

6189 TIN-ACTIVATED ALKALINE-EARTH PYROPHOSPHATE PHOSPHORS by R. C. Ropp and R. W. Mooney (Sylvania); J. Electrochem. Soc., Vol. 107, pp. 15-26, Jan. 1960

The preparation and properties of the Group II metal pyrophosphates activated by tin are described. It is shown that the fluorescent emission is strongly dependent on the matrix, shifting toward higher wave lengths with increasing size of the catio of the pyrophosphate. Excitation and emission spectra of many of the phosphors are given. The most useful of these phosphors is $Sr_2P_2O_7$:Sn, a very efficient blue phosphor emitting at 452 mμ.

6190 THEORY AND APPLICATION OF THERMALLY STIMULATED CURRENTS IN PHOTOCONDUCTORS by R. R. Haering and E. N. Adams (IBM); Phys. Rev., Vol. 117, pp. 451-454, Jan. 15, 1960

The theory of thermally stimulated currents is investigated in the limits of slow and fast retrapping. A method of obtaining the ionization energy E of the relevant traps is discussed. This method depends on the shift of the conductivity maxima with heating rate and does not involve prior knowledge of the trapping cross sections or the heating rate.

6191 X-RAY CONDUCTIVITY OF SOME SULFIDE PHOSPHORS by G. Déjardin and J. Janin (U. Lyon); Bull. Am. Phys Soc., Ser. II, Vol. 5, pp. 47-48 (A), Jan. 27, 1960

X-ray photoconductivity in a common electroluminescent product, two sulfides showing different increases of their x-ray excited luminescence under the action of an electric field (electro-enhancement effect), and a sulfide exhibiting the opposite effect of electroquenching was discussed. A layer (0.5 mm) of each powder, deposited between electrodes consisting of a plate and a fine grid was subjected, in a good vacuum, to an electric field. Measurements of the dark current and of the photocurrent have been made and several factors (field strength, amount, and penetrating power of the exciting radiation) have been investigated. The photocurrent varies approximately as powers of the grid voltage (up to 250 v), of the electron current through the x-ray tube, and of the high voltage applied to it. For each phosphor the exponent depends on the values of the two factors which remain unchanged. The experimental results show that the behaviors of the four sulfides are not very

different and they support the belief that the electroenhancement effect cannot be explained by a classical mechanism of electron acceleration.

6192 FLUCTUATIONS, NEUTRAL TRANSPORT, AND THE PHOTOCONDUCTIVE PROCESS IN CdS by R. J. Robinson and J. J. Brophy (Armour Res. Found.); Bull. Am. Phys. Soc., Ser. II, Vol. 5, p. 63 (A), Jan. 27, 1960

New evidence for neutral energy transport in CdS obtained from electrical noise measurements was reported. In addition, evidence from the magnitude of the noise intensity, response times and conduction band lifetimes suggests that the dynamics of the photoconductive process are different for photodiffusion and for uniform illumination-induced photoconductivity, currently used jointly to determine neutral energy transport. The noise spectra of a lightly CuCl-doped single crystal of CdS which showed long-range photodiffusion was studied under both uniform and masked (photodiffusion) illumination using 5200 A radiation. In the photodiffusion curves a new generation or relaxation (GR) process is evident which is present at all radiation levels, and which does not appear with uniform illumination. This additional GR process has a 500 micro-second time constant.

Photoconductivity in Rhombic Sulfur - See 6113.

6193 FIELD DEPENDENCE OF PHOTOELECTRIC EMISSION FROM TANTALUM by J. L. Gumnick and D. W. Juenker (U. Notre Dame); J. Appl. Phys., Vol. 31 pp. 102-108, Jan. 1960

An experimental study of the dependence of the photoelectric emission from tantalum on accelerating electric field is discussed. Observations cover a range of fields from 0 to 90 kv/cm and illumination wave-lengths from 248 to 300 mμ. The results are in agreement with the Fowler photoelectric theory modified by a Schottky lowering of the surface barrier. No evidence is found for a periodic deviation from this regular behavior such as exists in its thermionic counterpart, but experimental conditions may have been inadequate for the observation of such a deviation. A new method of threshold measurement at high fields is described and applied to drawn tantalum filaments of circular cross section. The resulting value is 4.16 ev for freshly flashed specimens and it is suggested that this is slightly greater than the lowest work function present in the surface. A Fowler determination in the same field range yields 4.13 ev. The influence of nonuniformity of the surface work function on the field dependence of photoemission and on threshold measurements is discussed.

Electromagnetic Properties of Insulators - See 6074.

6194 STUDY OF THE WURTZITE-TYPE BINARY COMPOUNDS. V. THEORY OF DOUBLE REFRACTION by F. Keffer (U. Pittsburgh); J. Chem. Phys., Vol. 32, pp. 62-66, Jan. 1960

The Ewald-Born theory of double refraction is applied to wurtzite-type compounds. Except for the small distortion and polarization, these compounds have identical near-neighbor symmetry to zinc blende (cubic) structures, and hence the double refraction is caused primarily by the distant-neighbor interactions. The effects of anisotropy of the Lorentz-Lorenz force and of the Coulomb force are calculated. In the (ionic) approximation of zero cation polarizability the theory predicts a double refraction larger than the measured one by a factor ~2 for all six compounds that have been measured. In the covalent) approximation of zero effective ionic charge the theory underestimates the double refraction of AlN, but may be made to agree with the measured values of the other compounds by a suitable choice of atomic polarizabilities. In both approximations the theory predicts $n_o < n_e$, in agreement with long-wavelength observations. Anisotropic interaction of polarized light with the solid as a whole, as in exciton transitions, seems to account for the inversion to $n_o > n_e$ near the absorption edge of CdS.

6195 HALL EFFECT DEVICE FOR ELECTROMAGNETIC WAVES by H. Suhl (Bell Labs.); U. S. Pat. 2,922, 129, Issued Jan. 19, 1960

The use of the Faraday effect in high mobility materials such as indium antimonide to rotate the plane of polarization of microwaves and to generate microwaves of any desired frequency is described. To rotate the plane of polarization, the microwaves are introduced into a circular waveguide constructed of the semi-conductor or into a circular waveguide the interior of which is coated with a semiconductor film. A magnetic film is applied along the semiconductor in the direction of the signal propagation. To generate microwaves of a desired frequency, polarized microwaves are converted to positive circularly polarized waves and the latter are introduced into a cavity constructed from the previously described cylindrical waveguides of length $l = \lambda/2$ where λ is the wavelength at which the cavity is to resonate. A magnetic field is applied along the cavity. Any desired frequency can be generated since the propagation velocity of the waves increases with the applied magnetic field and the wavelength is fixed by the length of the cavity.

6196 OPTICAL STUDIES OF IMPURITIES IN GERMANIUM by L. F. Johnson (Syracuse U.); Diss. Abstr. Vol. 20, p. 2862 (A), Jan. 1960

An investigation of the fundamental parameters of gold in germanium between 60-300°K by absorption, photoconductivity, and recombination radiation studies is reported. Photoconductivity measurements reveal the following capture cross sections for electrons and holes at 80°K (subscript refers to carrier being captured; superscript to charge state of gold center): $\sigma_h^- \simeq 1 \times 10^{-13} cm^2$, $\sigma_e^o \simeq 6 \times 10^{-14} cm^2$, $\sigma_e^- \sim 10^{-17} cm^2$. Lifetime studies on n-type samples show the existence of a 0.018 ev Coulomb barrier at singly-charged gold sites and an indication that a thermal (phonon) mechanism is involved in the electron capture process. The lifetime also manifests itself in the noise spectrum. The photoconductive absorption cross section at 80°K of p-type gold-doped germanium (0.15 ev level) is found to be $2 \times 10^{-16} cm^{-2}$ at 1.8 microns. It is suggested that differences between the absorption and photoconductive spectra are due to departure from spherical symmetry of valence band contours away from $\underline{k} = 0$. Recombination radiation which cannot be identified with any intentionally introduced impurity (Au, Zn, or Sb) has been observed. Emission at 0.5 ev is correlated with the presence of edge dislocations, and observations suggest a model in which a dislocation produces a deformation of the energy bands, resulting in intrinsic recombination across a reduced band gap. The origin of emission between 4 and 20 microns is unknown. Indications are that it arises from recombination at point imperfections (vacancies and/or interstitial germanium atoms).

6197 RESEARCH ON OPTICAL AND ELECTRICAL PROPERTIES OF SOLIDS by D. Dutton (U. Rochester); U. S. Gov. Res. Rep., Vol. 33, pp. 91-92 (A), Jan. 15, 1960 PB 138 653

Abstracts of 16 reports which have been published on experimental studies of photoconductivity, luminescence, and optical absorption in various materials including the alkali and silver halides, the thallous halides, cadmium sulfide, lead sulfide, and lead selenide are presented.

6198 OPTICAL PROPERTIES OF THE SEMICONDUCTING COMPOUND $CdIn_2Te_4$ by D. F. Edwards (Willow Run Labs) and D. O'Kane (U. of Mich.); Bull. Am. Phys. Soc., Ser. II, Vol. 5, p. 78 (A), Jan. 27, 1960

An investigation of the optical properties of n-type $CdIn_2Te_4$ at room temperature for wavelengths between 1 and 37μ was reported. Values of the absorption coefficient and index of refraction have been obtained for samples having different carrier concentrations. From a plot of $\alpha^{1/2}$ and α^2 vs. energy, there is evidence of direct and indirect transitions. Details of this analysis and the values of the direct and indirect transition band gaps were given. Values for the electron effective mass and the relaxation time have been estimated from a study of the free carrier susceptibility and the Hall coefficient.

Optical Properties of Some II-VI Compound Solid Solutions - See 6030.

Optical Properties of Tin Selenide - See 6132.

THERMAL PROPERTIES

Temperature Dependence of the Thermal Properties of Lead Telluride - See 6238.

6199 SPECIFIC HEAT OF HIGH PURITY IRON BY A PULSE HEATING METHOD by D. C. Wallace, P. H. Sidles, and G. C. Danielson (Iowa State U. of Sci. and Tech.); J. Appl. Phys., Vol. 31, pp. 168-176, Jan. 1960

A dynamic pulse-heating method for measuring with an error of less than 2 percent the specific heats of metal wires from room temperature to 1000°C is described. The method consists essentially of recording the resistance of the sample wire while it is being heated by a pulse of large current and short time duration; then obtaining the temperature of the wire throughout the pulse with the aid of the measured resistance as a function of temperature; and finally computing the specific heat of the sample from the temperature as a function of time during the pulse, the measured power input to the wire, and the theoretically computed heat loss corrections. Results are given for high-purity iron over the temperature range 25° to 1050°C. Variations of the specific heat near the phase transitions are shown in detail.

Specific Heats of $NiCl_2 \cdot 6H_2O$ and $CoCl_2 \cdot 6H_2O$ at Low Temperatures - See 6148.

Specific Heat of $CoBr_2 \cdot 6H_2O$ at Low Temperatures - See 6158.

6200 LOW-TEMPERATURE THERMAL RESISTIVITY OF POINT DEFECTS by P. Carruthers (Cornell U.); Bull. Am. Phys. Soc., Ser. II, Vol. 5, p. 48 (A), Jan. 27, 1960

A calculation of the scattering of phonons by a displacement field varying as $1/r^2$, appropriate to vacancies and interstitials, was presented. It has been found that for small wave vector q (corresponding to temperatures below the low temperature maximum in the conductivity), the relaxation time varies as q^{-4}, and is much larger than expected from "Rayleigh" scattering. For larger q the specific strain field scattering vanishes. The experimental observation that the depression in the conductivity caused by isotopes (with $\tau^{-1} \propto \omega^4$) is comparable both above and below the peak, while that due to strain field scattering by point defects is large below, but small above the peak was discussed as a striking example. The recent experiments of Pohl on the influence of F-centers on the thermal conductivity of LiF were analyzed and the reasons for the disagreement of the present result with that of Klemens, who obtained no scattering, were explained.

6201 LATTICE THERMAL CONDUCTIVITY AND F-CENTERS by R. O. Pohl (Cornell U.); Bull. Am. Phys. Soc., Ser. II, Vol. 5, p. 49 (A), Jan. 27, 1960

An investigation of the influence of point defects on the lattic thermal conductivity by measurements made on LiF containing photochemically produced F centers was described. The concentration of F centers was determined by measuring the optical absorption and using Smakula's formula. Successive irradiations of the same specimen provide good experimental accura (background imperfections, geometry). Irradiation causes the thermal conductivity to decrease strongly on the low-tempera ture side of the maximum, whereas on the high-temperature sid the decrease is quite small. The results are in fair agreement with Slack's investigations of the thermal conductivity of calcium-doped KCl, but cannot be explained by Klemens' theory for phonon scattering by point defects. An attempt has been made to explain the results assuming the F centers to be randomly distributed and using a different cutoff mechanism for the long wavelength phonons, as suggested by Callaway.

6202 THE THERMAL CONDUCTIVITY OF GERMANIUM, SILICON AND INDIUM ARSENIDE FROM 40°C TO 425°C by A. D. Stuckes (Metropolitan-Vickers Electrical); Phil. Mag., Vol. 5, pp. 84-99, Jan. 1960

Measurements of the thermal conductivity of germanium, sili con, pure ($n = 3 \times 10^{16}$) indium arsenide and impure ($n = 10^{19}$) indium arsenide are reported. In each case the electronic con tribution κ_e to thermal conductivity has been calculated and the phonon contribution κ_p has been estimated by subtraction of κ_e from experimental values. The thermal resistance of the lattice has not generally been found to be proportional to the absolute temperature as expected for three-phonon processes but the trend is towards a higher power relationship. The lattice resistance of heavily doped indium arsenide has been found to be greater than that of the pure material.

6203 MEASUREMENT OF PRESSURE EFFECT ON THE SEEBE COEFFICIENT OF POWDER COMPACTS by A. P. Young, B. B. Robbins, W. B. Wilson, and C. M. Schwartz (Battelle Me Inst.); Rev. Sci. Instr., Vol. 31, pp. 70-71, Jan. 1960

An apparatus for measuring the effect of pressure on the See beck coefficients of metal oxide powder compacts is describe and some observations made while using the apparatus are briefly discussed. To date measurements have been made onl on samples with resistance between 50 and 50,000 ohms at pressures from 10,000 to 80,000 atmospheres. Temperature gradients and thermoelectric voltages cannot be measured across lower resistance samples but they can be measured in higher resistance samples when the apparatus is modified.

6204 THERMO-EMF OF CUPROUS OXIDE AT HIGH TEMP ERATURES (1000° to 1250°C). IV by K. P. Zuev (Semicon. Inst. Leningrad); Soviet Phys.-Solid State, Vol. 1, pp. 1007 1015, Jan. 1960

An investigation of the thermo-emf of Cu_2O in the temperatu interval from 1000° to 1250°C, and as a function of changes in the oxygen pressure of the surrounding medium over a wide interval (P_{O_2} = 1 to 760 mm Hg) is discussed. The absolute value of the thermo-emf in Cu_2O increases continuously with heating and achieves its maximum at the temperature corres ponding to the transition of the sample through the boundary of the stability of Cu_2O-CuO; then it falls rapidly, reaching 250 μv/deg at the melting temperature of Cu_2O (1235°C). In study of the transformation of Cu_2O from the solid to the liq uid phase, the decisive role of short range order is confirmed

THERMAL PROPERTIES (Cont'd)

definite relation between the curves of the dependence of e thermo-emf of Cu_2O on composition near the boundary of e stability region of Cu_2O and CuO is shown to exist, and a orrelation between the temperature dependence of the thermo-nf and of the electrical conductivity at high temperatures 000° to 1250°C) is established.

'05 THERMOELECTRIC EFFECTS IN COPPER-GOLD ALLOYS y M. D. Blue (Honeywell Res. Ctr.); Phys. Rev., Vol. 117, . 134-138, Jan. 1, 1960

easurements of the resistivity and thermoelectric power of the inary alloy CuAu and of CuAu alloys containing dilute amounts Ni are analyzed using the thermoelectric power formula of ott. At the transition temperature, anomalies in the thermo-ectric power have been observed. The scattering cross section nd its derivative with respect to energy for Ni in CuAu are de-ermined. The results are similar in value to these same param-ers measured for dilute amounts of Ni in Cu.

ermoelectric Properties of: $CdSnAs_2$ - See 6108
P-N Junctions - See 6218

206 CONCERNING METHODS OF MEASURING THE ERNST EFFECT by I. V. Mochan and T. V. Smirnova (Semi-on. Inst. Leningrad); Soviet Phys.-Solid State, Vol. 1, pp. 016-1018, Jan. 1960

easurements of the Nernst effect in p-type germanium samples hich give the dependence of the observed change of $1/H_0$ where H_0 is the intensity of the magnetic field for which the Nernst constant $Q = 0$) on the nature of the contact between the Ge and the measuring electrodes are reported. Not only does he magnitude of H_0 fail to satisfy at all times the previously roved equation $1/H_0 \sim \mu \sim T^{-2 \cdot 3}$ where μ is the mobility and T s the temperature, but in some cases it falls as the temperature ncreases. This is explained by the Hall effect which arises from he appearance of circulating currents in the vicinity of the lectrodes and causes an additional positive potential when the Nernst potential difference is measured. When these systematic rrors are eliminated, the equation is shown to be valid. The Hall effect decreases rapidly as the dimensions of the tin dots y which the electrodes are soldered to the Ge samples are in-reased. The method of displaying the apparent additional Nernst effect and an equation to express it in terms of the addi-onal Hall potential difference are given.

Oscillations in the Thermomagnetic Effects in Tin at Low Temp-ratures - See 6120

207 THERMAL EXPANSION OF SILICON by L. Maissel Philco); J. Appl. Phys., Vol. 31, p. 211 (L), Jan. 1960

Measurement of the coefficient of thermal expansion of silicon t various temperatures between 50 and 850°C is reported. An ptical method employed to measure the changes in sample ength is described. Measurements made on samples with (111) nd (110) orientations did not differ significantly within the es-mated experimental error. The (110) values were, however, onsistently lower.

208 EVALUATION OF THERMAL ACTIVATION ENERGIES ROM GLOW CURVES by A. Halperin and A. A. Braner Hebrew U.); Phys. Rev., Vol. 117, pp. 408-415, Jan. 15, 1960

new method for the evaluation of thermal activation energies om glow curves of excited crystals is described. Use is made f the symmetry of the glow peak, from which the activation energy is calculated by a simple formula: $E = (q/\delta)kT_g^2$ where T_g is the peak temperature, k is Boltzmann's constant, δ is the half-width towards the falloff of the glow peak, and q is a factor which can be computed from the shape of the glow peak. Values of $q \leq 1$ were found for monomolecular processes, while $1 \leq q \leq 2$ correspond to bimolecular processes. The method thus enables one to determine the type of kinetics.

6209 THERMAL ACTIVATION ENERGIES IN NaCl AND KCl CRYSTALS by A. Halperin, A. A. Braner, A. Ben-Zvi, and N. Kristianpoller (Hebrew U.); Phys. Rev., Vol. 117, pp. 416-422, Jan. 15, 1960

Thermal activation energies computed from various glow peaks of NaCl and KCl single crystals are presented. The method developed in another paper [see 6208] has been used successfully in these calculations. Good agreement was obtained with the results calculated from the initial rise of the glow peaks. Activation energies varied from 0.3 to 1.5 ev for various peaks in the glow curve of NaCl between 150 and 500°K. Similar results were obtained for KCl crystals. The kinetics of the processes was found to be nearly of first order.

MECHANICAL PROPERTIES

Effect of Dislocations on the Strength of Sodium Chloride Whiskers - See 6009

6210 ELASTIC CONSTANTS OF SINGLE CRYSTAL BERYLLIUM by J. F. Smith and C. L. Arbogast (Iowa State U. Science and Tech.); J. Appl. Phys., Vol. 31, pp. 99-102, Jan. 1960

Determination of the five independent elastic constants of beryllium with the pulse echo technique at a frequency of 10 mc is reported. The values extrapolated to 0°K are $C_{11} = 29.94 \pm 0.06$, $C_{33} = 34.22 \pm 0.12$, $C_{44} = 16.61 \pm 0.05$, $C_{12} = 2.76 \pm 0.08$, $C_{13} = 1.1 \pm 0.5$ in units of 10^{11} dyne/cm^2. Voigt averaging and Reuss averaging of the single crystal elastic constants give excellent agreement because of the small magnitude of the nondiagonal elements, C_{12} and C_{13}. The averaged values compare favorably with previous data from polycrystalline Be.

Elastic Constants of Triglycine Sulfate - See 6043

6211 ULTRASONIC ATTENUATION AND DISPERSION IN METALS AT LOW TEMPERATURES by A. B. Bhatia and R. A. Moore (U. Alberta); Bull. Am. Phys. Soc., Vol. 5, Ser. II, p. 14(A), Jan. 27, 1960

The mechanism for the attenuation and dispersion of ultrasonic waves in metals at low temperatures was discussed. When a sound wave passes through a metal, an electric field is set up in the metal. This electric field exerts a force on the ions. In addition ions experience a force due to the transfer of momentum to the ions in electron-ion collisions. Because of the finite relaxation time τ for the electrons, the resultant of these two forces is out of phase with the displacements of the ions, and hence leads to the attenuation and dispersion of sound. This approach, which seems to be somewhat more physical, gives substantially the same results as obtained by Pippard and Steinberg by other methods. The significance of the relaxation time τ was also discussed. In particular, it is found that when the sound wave-length is large compared with the mean free path of the electrons, τ may be written as $(\tau)^{-1} = a(\tau_\sigma)^{-1} + (\tau_e)^{-1}$. Here, a is of the order of magnitude unity, τ_σ is the relaxation time for the electrical conductivity, and τ_e is a relaxation time describing the inter-electron collisions. Thus, where electron-electron collisions are not unimportant, information regarding their relaxation time τ_e may be deduced from the measurements of attenuation and electrical conductivity.

6212 ACOUSTIC ABSORPTION BY PHONON-PHONON INTERACTION by W. P. Raney, H. E. Bommel, and K. Dransfeld (Bell Labs.); Bull. Am. Phys. Soc., Ser. II, Vol. 5, p. 39 (A), Jan. 27, 1960

A mechanism for the interaction of sound waves with the thermal phonons proposed to explain the observed hypersonic absorption in crystalline quartz was discussed. The coefficient of absorption depends on specific heat, temperature, a properly defined average Grüneisen constant, density, sound velocity, angular frequency and a phonon-phonon relaxation time. Evidence that the same mechanism is also present in germanium was presented. The observed fact that in Ge shear waves are much less attenuated than longitudinal waves is in agreement with values of the average Grüneisen constant data on the second order elastic constants in Ge.

6213 MECHANICAL DAMPING OF GERMANIUM AND SILICON CONTAINING IMPURITY OXYGEN by P. D. Southgate (Mullard Res. Labs.); Solid State Phys. Electronics and Telecommun., Vol. 1, pp. 240-250, 1960

Measurement of the variation of mechanical damping of single crystals of Ge and Si at 100 kc/s over the range 100-1300°C is discussed. Two peaks occur in the damping vs temperature curves of the specimens measured: the low-temperature peak appears in both Ge and Si at about two-thirds of the melting point, i.e., 410°C and 660°C respectively, and the high-temperature peak in Si appears at 1025°C. The former is a relaxation peak with activation energies of about 1.0 ev for Ge and 1.5 ev for Si; the latter is attributed to movement of dissolved oxygen atoms, which is confirmed by the annealing behavior of the Si. The activation energy in this case is about 2.6 ev. A small high-temperature peak appears in some Ge specimens at 770°C which may also be attributed to small quantities of dissolved oxygen, although there is no direct evidence to support this hypothesis.

SOLID STATE DEVICES—DIODES

DIODE FUNCTIONS

Microwave Switching with Computer Diodes - See 6265.

Tunnel Diodes - See 6219.

Gallium Arsenide Varactor Diodes - See 6226, 6308.

Semiconductor Varactors Using Space Charge Layers - See 6251.

POINT CONTACT DIODES

6214 DIPOLE MODE OF MINORITY CARRIER DIFFUSION WITH REFERENCE TO POINT CONTACT RECTIFICATION by B. R. Gossick (Arizona State U.); J. Appl. Phys., Vol. 31, pp. 29-35, Jan. 1960.

The dipole mode of minority carrier diffusion about a spherical emitter is presented and the current-voltage relationship and frequency characteristics of this mode are determined. Compared with the unipole mode, which has been treated extensively, the dipole mode offers superior high-frequency performance, which is partially offset by an inferior d-c characteristic curve. A representative numerical example gives 40 μsec mean response time with the unipole mode and 0.5 μsec with the dipole mode. It is proposed that the reproducibility of special diode characteristics might be improved by designing diodes to suppress either the unipole or dipole mode. Methods for the suppression of either mode are suggested.

6215 MICROPHONISM IN MICROWAVE CRYSTAL MIXERS by W.K. Saunders (Diamond Ord. Fuze Labs.); U.S. Gov. Res. Rep., Vol. 33, p. 46 (A), Jan. 15, 1960 PB 127 980

The microphonic effects noted in a microwave crystal mixer subjected to vibration are discussed and the experimental procedures and results are presented in detail. It is concluded that the catwhisker of the type 1N23 crystal is mechanically resonant at some frequencies of vibration. Another type of crystal is found to perform satisfactorily under the same conditions.

6216 THEORY OF THE GERMANIUM DIODE MICROWAVE SWITCH by R.V. Garver, J.A. Rosado, and E.F. Turner (Diamond Ord. Fuze Labs.); IRE Trans., Vol. MTT-8, pp.108-111, Jan. 1960

The application of a generally neglected theory of microwave detection to the poorly understood problem of metal-to-semiconductor junction behavior at microwave frequencies is discussed. Experimental results which support the theory and appear to be the first experimental verification of it are disclosed. It is shown how the theory predicts that germanium microwave diodes should exercise direct switching action upon microwaves while silicon microwave diodes should not, as had been observed in the past but with no explanation.

6217 MICROWAVE DIODE CARTRIDGE IMPEDANCE by R.V. Garver and J.A. Rosado (Diamond Ord. Fuze Labs.); IRE Trans., Vol. MTT-8, pp. 104-107, Jan. 1960

In any application of a semiconductor microwave diode, the impedance of the diode cartridge plays a very important role. Two commonly made assumptions, which are quite erroneous, are that 1) the impedance of the diode cartridge consists simply of a shunt capacitance and whisker inductance, and 2) the metal-to-semiconductor junction behaves at microwave frequencies approximately as it does at 10 mc. It is shown that the impedance of the diode cartridge at microwave frequencies can be measured accurately by substituting a carbon die for the semiconductor.

JUNCTION DIODES

6218 THERMIONIC BEHAVIOR OF P-N JUNCTIONS by M. Cutler (Gen. Atomic); Bull. Am. Phys. Soc., Ser. II, Vol. 5, p. 78 (A), Jan. 27, 1960

Equations for the flow of carriers and electronically transported heat across a P-N junction were derived using emission theory. In contrast to the usual equations, these apply if there is an appreciable temperature drop in the barrier region. When expressed in terms of external potentials, they show that the usual junction equation is modified simply by having in the exponential a thermoelectric voltage in addition to the applied voltage. The thermoelectric voltage depends on the carrier concentration on the low concentration side of the barrier. The P-N junction equations bear a close relation to those for a thermionic diode. As expected, the P-N junction equations obey Onsager's relations for small signals, but not for large signals. By reducing the barrier to zero, a rough derivation is obtained for equations for

flow in a nearly homogeneous semiconductor which agree with those appearing in the literature. It is possible to show in a simple manner that in the small signal case a junction provides no advantage over homogeneous semiconductors as a thermoelectric device.

6219 TUNNEL DIODES by R. N. Hall (GE Res. Lab.); IRE Trans., Vol. ED-7, pp. 1-9, Jan. 1960

The properties, principle of operation, and implications of the tunnel diode are reviewed. Following a brief description of the unusual characteristics of this device, the mechanism which leads to the negative resistance is discussed. Experiments showing the transition from the tunnel diode characteristic to that of a high-voltage avalanche diode are exhibited. The electrical characteristics of tunnel diodes are outlined making use of the small-signal equivalent circuit which represents the behavior in the negative resistance region. Diodes designed for high-frequency operation are described and examples of circuits which demonstrate their behavior as switches, radio receivers, and microwave oscillators are given. In connection with a discussion of the temperature dependence of these devices, experiments which demonstrate the importance of phonons in determining their characteristics at the temperature of liquid helium are described.

6220 PRESSURE DEPENDENCE OF THE CURRENT-VOLTAGE CHARACTERISTICS OF ESAKI DIODES by S.L. Miller and M.I. Nathan (IBM); and A.C. Smith (MIT); Phys. Rev. Lett., Vol. 4, pp. 60-62 (L) Jan. 15, 1960

Measurements performed at room temperature on the effect of hydrostatic pressure on tunneling in germanium Esaki diodes are reported. It was found that the peak current J_p decreases with pressure and that this variation divides the diodes into three distinct groups. In each group phonon-assisted tunneling is either present or absent at 4°K. The valley current, J_v, is larger than predicted by simple tunneling theory and ordinary diode theory and it decreases with pressure. The over-all change of J_v is smaller than the change in J_p for the same unit. It was found that the variation of E_g with pressure up to 30 000 kg/cm^2 is the same to within 15% for the heavily doped materials in the diodes as in intrinsic Ge. Agreement between some experimental data and the tunneling theories of Price and Radcliffe and of Keldysh is noted. Measurements made on two diodes at liquid nitrogen temperature indicate that the pressure dependence of $\ln J_p$ is about 25% larger at the low temperature than at room temperature. The reason for this is not understood and it is pointed out that more careful measurements are necessary.

Optimum Noise Performance of Tunnel Diode Amplifiers - See 6261.

Emission Spectrum of a Tunnel Diode - See 6181.

6221 AVALANCHE BREAKDOWN STUDIES OF SILICON JUNCTIONS by P.H. Smith (Motorola) and C.J. Kevane (Ariz. State U.); Bull. Am. Phys. Soc., Ser. II, Vol. 5, p. 78 (A), Jan. 27, 1960

Experimental studies of breakdown in silicon junctions which show microplasma current pulses extending well into the low impedance avalanche region were reported. As many as thirteen distinct sets of current pulses were observed in the breakdown of one junction. The occurrence of large numbers of distinct pulse sets is associated with the distribution of microplasma breakdown voltages over a significant range. Junctions in some unusual silicon show this range to be so large that the characteristics of a single microplasma can be studied. There appears to be no spatial correlation between microplasmas having nearly the same breakdown voltage, and it is possible by sectioning to increase the voltage isolation of a low-voltage microplasma. Studies of these isolated microplasmas reveal that many types exist and permit a negative resistance model to be used which is in essential agreement with that of Rose. Direct measurement of the transition probabilities to and from the conducting state have been made for one of these isolated microplasmas.

6222 HOT ELECTRON EMISSION FROM SILICON by W. E. Spicer (RCA Labs.); Bull. Am. Phys. Soc., Ser. II, Vol. 5, p. 69 (A), Jan. 27, 1960

Reported "hot electron emission" (HEE) from a back-biased p-n junction in silicon which has received a Cs surface treatment has been corroborated in experiments using a somewhat different Cs surface treatment. The Si surface is degassed by heating to 775°C and then exposed to Cs vapor while the tube is held at about 110°C. There are indications that the optimum surface coverage approaches a monolayer. The photoemissive quantum efficiency from these Cs-treated Si surfaces is about 10^{-8} electron/photon at 1.5 ev and sometimes rises to 6×10^{-3} electron/photon at about 3.6 ev. The threshold of photoemission is fairly insensitive to surface coverage, but the peak response increases with increasing surface coverage. The plots of HEE current versus applied voltage are similar to those obtained previously. However, peak currents in excess of 1.0 ma have been obtained in comparison to Burton's values < 0.1 ma. The apparent saturation of emission current with voltages greater than about 70v is shown to be due to the IR drop of the Si in series with the junction. This apparent saturation disappears if corrections are made for this effect, and it can be shown that emission currents greater than 1.0 ma are actually obtained for junction voltages of less than 40 v.

6223 TRANSIENT BEHAVIOR OF SEMICONDUCTOR JUNCTION DIODES-THEORY AND APPLICATIONS by W-H Ko (Case Inst. Tech.); Diss. Abstr. Vol. 20, p. 2863 (A), Jan. 1960

The forward and reverse transient behavior of junction diodes are analyzed and the theoretical results are verified experimentally. The forward transient behavior is resolved into junction voltage and diode resistance transient components. The theory yields satisfactory explanation of all the observed phenomena. The diode reverse transient behavior after a forward current pulse is also analyzed approximately. Equations for determining quantitatively the reverse recovery current and voltage as functions of carrier lifetime and circuit parameters are obtained. The relation between the charge stored by forward current and the charge recovered by reverse current is then derived. These equations are confirmed with an accuracy of five percent or better by experimental data from germanium and silicon alloyed diodes. The effect of temperature on the diode transient behavior is demonstrated to be dependent only on the change of carrier lifetime with temperature. Based on the understanding obtained, several applications are briefly investigated. These are: (1)Measurements of carrier lifetime, surface recombination velocity, injection ratio, base resistance, and junction temperature. (2) Diode pulse repeaters and diode amplifiers. (3) Diode amplitude modulator, sampler, pulse duration modu-

lator, and pulse position modulator. A number of other possible applications are also suggested.

6224 CONDUCTANCE AND THE VOLTAGE TRANSMISSION COEFFICIENT OF A SEMICONDUCTOR DIODE IN THE TRANSIENT STATE by E.I. Adirovich (P.N. Lebedev Phys. Inst.); Soviet Phys. - Solid State, Vol. 1, pp. 1019-1028, Jan. 1960

The frequency-phase and transient characteristics of a circuit with a p-n junction and a series ohmic resistance are calculated for the case in which the diffusion capacity plays a predominant role. The critical frequencies and characteristic time constants are determined. A new method of determining the characteristics of a diode, suitable in particular for measuring small values of minority carrier lifetime is described.

6225 ELECTRICAL PROPERTIES OF GOLD-DOPED DIFFUSED SILICON COMPUTER DIODES by A. E. Bakanowski and J. H. Forster (Bell Labs.); Bell Sys. Tech. J., Vol. 39, pp. 87-104, Jan. 1960

Planar diffused silicon junctions with storage times of one millimicrosecond or less are readily obtained by gold doping. The introduction of uniform gold concentrations (in the range from 1.2×10^{15} cm^{-3} to 8×10^{16} cm^{-3}) is conveniently done using solid state diffusion techniques. The gold diffusion technique allows relatively precise control of recombination center density, and, although applicable to almost any diffused silicon device, is particularly useful in control of storage time in small-area diffused silicon computer diodes. In this application, reverse recovery time of about one millimicrosecond may be obtained without substantial degradation of other electrical parameters. The process of gold doping by diffusion and its effect on the electrical characteristics of diffused silicon computer diodes are discussed. Comparisons of first-order calculations and experimental results for variations of reverse recovery time, reverse current and forward current with gold atom density are included.

6226 GALLIUM-ARSENIDE DIFFUSED DIODES by J. Lowen and R.H. Rediker (Lincoln Lab.); J. Electrochem. Soc., Vol. 107, pp. 26-29, Jan. 1960

Gallium arsenide variable reactance and computer diodes which compare favorably with the best commercially available germanium and silicon diodes are discussed. The diodes are fabricated by the diffusion of zinc into n-type gallium arsenide. Ohmic contact is made to the n-type material with an antimony-gold alloy and to the p-type side with indium. Etching is used to remove the p-type diffused skin from everywhere but under the indium contact, thereby forming the mesa and defining the p-n junction area. Rectification ratios (at 2 v) as high as 10^{10} have been achieved. The diodes have been operated successfully in a variable reactance amplifier at S-band (2800 mcps) and in μsec switching computer circuits.

Fabrication of Silicon Carbide Rectifiers - See 6037.

SOLID STATE DEVICES—TRANSISTORS

JUNCTION TRANSISTORS

6227 COMPARISON OF N-P-N TRANSISTORS AND N-P-N-P DEVICES AS TWENTY-AMPERE SWITCHES by H. W. Henkels (Westinghouse) and F. S. Stein (Genl. Instr.); IRE Trans., Vol. ED-7, pp. 39-45, Jan. 1960

The characteristics of a series of 20-ampere silicon n-p-n transistors and three-terminal n-p-n-p switches are compared with respect to high-current switching applications. At the present time, collector-emitter voltages of the transistors are generally lower than those of the switches, which may exceed 400 volts. The n-p-n transistors are somewhat simpler to produce than the n-p-n-p structures. However, the ultimate current-handling capacity of the latter type of device is greater because of the uniform current density. The saturation voltage drops at 20 amperes are comparable, being in the order of one to two volts. The switch has a distinct advantage in the turn-on speed, while the transistor has the equally important advantage that the base retains control for turn-off.

Theory of a Drift Transistor - See 6102.

6228 ON THE VARIATION OF THE TRANSPORT FACTOR OF A JUNCTION TRANSISTOR WITH INJECTED CARRIER CONCENTRATION by A.N. Daw (Calcutta U.); Indian J. Phys. Vol. 34, pp 20-35, Jan. 1960

An attempt is made to set up a general equation governing the distribution of injected carriers in the base region of a p-n-p junction transistor and thereby to obtain an expression for the transport factor β. Subject to certain approximations, a relation giving the emitter current density as a function of the concentration of injected carriers is derived and the transport factor is expressed explicitly in terms of the latter. The expression is critically examined in the light of surface and volume recombination processes and the results are compared with those of other workers. The possible effect of the presence of a significant electronic component of current across the emitter-base junction on the transport factor expression is also considered. It is shown that the effect, if any, would be very small. An electronic component of current, however, affects the value of the current amplification factor, α , and a categorical experimental verdict in favor of one or the other of the different possible modes of recombination is not possible unless the so-called emitter efficiency term can be determined by independent experimental measurement.

Frequency Dependence of the Current Amplification Factor - See 6231 .

6229 NEW THEORY OF TRANSISTORS UNDER SATURATED CONDITIONS: SWITCHING PROBLEMS [in French] by M. Carbonel (Cie. Generale de T.S.F.); Ann. Radioelect. No. 59, pp. 78-89, Jan. 1960

A theory of junction transistors in the saturated condition which employs a two-dimensional model of a transistor is discussed. The model treats the transistor as a central part which behaves as an ideal transistor without base current and another part which forms the edges of the transistor and supplies the base current. Static operation is examined and equations connecting the base current, the collector current, and the collector-emitter voltage are derived. An equivalent circuit diagram is presented and the charge stored in a transistor, the "transient β" coefficient used in switching applications, and various switching times are calculated. These calculations agree well with measurements.

Prediction of Storage Time in Junction Transistors - See 6253 .

6230 TRANSIENT JUNCTION TEMPERATURES IN POWER TRANSISTORS by W.W. Grannemann and J.D. Reese (U. New Mexico); Electrical Engrg., Vol. 79, pp. 53-57, Jun. 1960

The heat flow in an alloyed junction power transistor under pulsed input conditions is analyzed by means of a simple one-dimensional heat-flow model. Fourier's equation for heat flow is solved for the crystal temperatures by the use of Laplace transforms. First an expression is obtained for the crystal temperature in the transform domain for any input waveform for which the transform exists. Then an expression for the junction temperature is obtained as a time function for the repetitive rectangular pulsed input. An approximate expression for the maximum instantaneous junction temperature is then derived from this expression. Experimental and theoretical values for ΔT_j, the difference between the temperature at any time during the cooling cycle and the minimum temperature (the temperature at the end of cooling cycle), are compared. The results are in good agreement over most of the cycle, although no reliable experimental data is available for the period immediately following the pulse.

6231 FREQUENCY DEPENDENCE OF THE NOISE AND THE CURRENT AMPLIFICATION FACTOR OF SILICON TRANSISTORS by E. R. Chenette (U. Minn.); Proc. IRE, Vol. 48, pp. 111-112 (L), Jan. 1960

The shot noise in a junction transistor can be represented by an equivalent noise EMF e_e in series with the emitter junction and an equivalent noise current generator i in parallel with the collector junction. Measurements of I_{eq}, the equivalent saturated diode current of the generator i, as a function of emitter current (with frequency as a parameter) in several n-p-n grown junction silicon transistors are reported and compared with theory. It is concluded that transistor noise theory can explain the observed data if the current dependence of the high frequency behavior of α, the ac current amplification factor, is taken into account and if a relatively small correction is made to account for the difference between α_{dc} and α_o, the low frequency value of α. The present theory of noise in junction transistors is correct only for low current levels. It is shown that the high frequency behavior of α is strongly current dependent.

6232 SHOT NOISE IN TRANSISTORS by A. van der Ziel (U. Minn.); Proc. IRE, Vol. 48, pp. 114-115 (L), Jan. 1960

A modification to an earlier theory of shot noise in junction transistors [see abstract 3523] to account for trapping effects in the emitter space-charge region is discussed.

6233 BASE CONNECTION FOR N-P-N JUNCTION TRANSISTOR by R.N. Hall (GE); U.S. Pat. 2,922,934, Issued Jan. 26, 1960

A process for electroplating a metallic contact on only the thin p-type base region of an n-p-n junction transistor when the latter is entirely immersed in an electrolyte is described. The selective plating is accomplished by maintaining the p-type region at a negative potential with respect to both n-type regions and by maintaining the electroplating solution at a positive potential with respect to the p-type region but negative with respect to each n-type region. In the device, this potential distribution can be achieved either by applying an alternating voltage between the n-type regions or by applying a d-c voltage between the p-type region and each n-type region. In the latter case permanent or temporary electrodes are attached to the p-type region. The thickness of the deposited metal is controlled by the time of electroplating and any excess metal is removed by electrolytically etching the junction.

PHOTO DEVICES

6234 OPERATING CHARACTERISTICS OF A LEAD SULFIDE CELL WITH VARYING BACKGROUND BRIGHTNESS by P. Brannon (U.S. Navy Underwater Sound Lab.); U.S.Gov. Res. Rep., Vol. 33, pp 90-91(A), Jan. 15, 1960 PB 143 425

A study of the operating characteristics of an Eastman Kodak "Ektron" 2 mm x 2 mm lead sulfide photo-conductive detector against varying background brightness is discussed. The signal from a tungsten lamp, chopped at 1000 cps, was reflected by means of a small plane mirror into a receiver pointed either at the sky or at an artificial background. Measurements of signal-to-noise ratio; detector resistance, voltage, and current; and brightness of the background were made for varying background and load resistance. The effect of placing an infrared filter in front of the receiver was also determined. It was found that a cell load resistance of about 1 megohm and a cell current of 20 microamperes gave the best operating signal-to-noise ratio over a sky background which varied from 0 to 10,000 foot-lamberts. When an infrared filter was placed in front of the receiver, the ratio was increased for background brightness above 30 foot-lamberts and decreased for brightness below this value.

6235 ELECTROLUMINESCENT DEVICES by S. Larach and R.E. Shrader (RCA); U.S. Pat. 2,921,218, Issued Jan. 12,1960

Devices which utilize the electroluminescence of boron nitride to produce ultraviolet radiation and several colors in the visible spectrum are described. The ultraviolet radiation is produced by applying an alternating voltage across a cell consisting of finely divided boron nitride dispersed in a light transmitting dielectric medium between a metallic electrode and a transparent, electrically conductive electrode. Several colors are produced by applying an alternating voltage across a similar device which has either an additional layer consisting of an ultraviolet-excitable phosphor or one layer in which the phosphor and the boron nitride are both mixed together and dispersed in the dielectric medium. Phosphors which can be utilized to produce white, red, blue, green, or yellow light are listed.

6236 DEVICE COMPRISING A PHOTO-CONDUCTIVE PART AND AN ELECTRO-LUMINESCENT PART by G. Diemer and H.A. Klasens (N.A. Philips); U.S. Pat. 2,922,892, Issued Jan. 26, 1960

A technique for improving the contrast in images produced in a light amplifier consisting of an electroluminescent panel in series with a photoconductor is described. The proper contrast is achieved by successively applying to the device two or more alternating voltages, each of which has a different frequency, or by applying an alternating voltage which continuously varies between two frequencies.

6237 INFRARED QUANTUM CONVERTER by W.A. Robinson (Space Tech. Labs.); Bull. Am. Phys. Soc., Vol. 5, Ser. II, p. 15 (A), Jan. 27, 1960

A method of converting infrared quanta into quanta of visible or ultraviolet wavelengths by using the Raman effect was described. The intensity of an anti-Stokes Raman line is a measure of the population of the excited state corresponding to that Raman transition. If infrared radiation of wavelength corresponding to an absorption line strikes a material, the population of the excited state may be increased. If this absorption line is also Raman active, the intensity of the anti-Stokes line will be increased. The efficiency of such a converter depends mostly upon the chance that an excited state will decay by thermal interactions before a Raman transition can take place. Spontaneous transitions are probably unimportant since most of such radiation will be recaptured.

THERMAL DEVICES

6238 DESIGN PARAMETERS FOR OPTIMIZING THE EFFICIENCY OF THERMOELECTRIC GENERATORS UTILIZING P-TYPE AND N-TYPE LEAD TELLURIDE by R. W. Fritts (Minn. Mining and Mfg.); Commun. and Electronics, No. 46, pp. 817-820, Jan. 1960

The temperature dependences of the Seebeck coefficient, electrical resistivity, thermal conductivity and, therefore, the figure of merit of several p- and n-type PbTe alloys are discussed and it is shown how this data can be utilized to fabricate thermoelectric generators which are highly efficient in a particular temperature range.

6239 CALCULATION OF EFFICIENCY OF THERMOELECIRIC DEVICES by B. Sherman, R.R. Heikes, and R.W. Ure, Jr. (Westinghouse Res. Labs); J. Appl. Phys., Vol. 31, pp. 1-16, Jan. 1960

A procedure for the exact calculation of the efficiency of thermoelectric generators and cooling devices in which the parameters of the materials have arbitrary temperature dependence is discussed. High speed computer techniques are found necessary. Approximate methods are reviewed and a number of examples are worked out by both the exact and approximate methods. Comparison of these results show that the approximate methods agree with the exact method to about 5 percent in the case of power generation and to about 15 percent in the case of the refrigeration coefficient of performance. However, in the case of the maximum heat pumping rate deviations as large as a factor of 2 are found.

Thermoelectric Behavior of P-N Junctions - See 6218.

Thermoelectric Generators - See 6310(New Product Section).

MAGNETIC DEVICES

6240 NONRECIPROCAL SINGLE CRYSTAL FERRITE DEVICES by H. Suhl (Bell Labs): U.S. Pat. 2,922,125, Issued Jan. 19, 1960

The use of single crystal ferrites in non-reciprocal devices such as gyrators and isolators is discussed. Single crystal ferrites properly oriented with respect to the biasing magnetic field permit operation at resonance frequencies less than 3,000 mc and require a smaller magnetic field than polycrystalline ferrites. The physics underlying this phenomena is discussed.

6241 HIGH POWER EFFECTS IN FERRITE DEVICES by P.E. Seiden and H.J. Shaw (Stanford U.); Proc. IRE, Vol. 48, p. 122(L), Jan. 1960

The large discrepancy between experimentally and theoretically determined values for the threshold of Suhl instability in ferrite devices is discussed. These large differences result from assuming in Suhl's relation for the threshold for instability that ΔH, the profile linewidth of the sample, equals ΔH_k, the linewidth of the spinwave that goes unstable. Better agreement can be obtained by using a measured value of the profile linewidth and a calculated value of the spinwave linewidth in Suhl's relation. Several previously published reports are recalculated using this approach.

Prediction of the High Power Performance of Ferrites in Isolators - See 6145.

6242 CIRCULATORS AT 70 AND 140 KMC by J.B. Thaxter and G.S. Heller (Lincoln Lab.); Proc. IRE, Vol. 48, pp.110-111 (L), Jan. 1960

The design and characteristics of 70 kmc and 140 kmc ferrite circulators are discussed. In each a ferrite (Ferramic R-1) cylinder is inserted into a copper sleeve and the sleeve (with the ferrite slightly protruding from its end) is inserted into a hole carefully centered in the Y junction. The length of the sleeve inserted in the junction and the magnetic field applied perpendicular to the plane of the junction are then simultaneously adjusted for minimum insertion loss. The copper sleeve matches the junction symmetrically. The circulator characteristics are not very sensitive to magnetic field variations. Both circulators require an applied magnetic field of about 200 gauss and the fringing field of a small alnico magnet is sufficiently homogeneous to operate them.

6243 A STRIP-LINE L-BAND COMPACT CIRCULATOR by L. Davis, Jr., U. Milano, and J. Saunders (Raytheon); Proc. IRE, Vol. 48, pp. 115-116 (L), Jan. 1960

An L-band circulator which utilizes a symmetrical Y-type junction of three flat strip transmission lines using air dielectric and containing two disks of polycrystalline YIG located at the center of the junction is described. The magnetostatic polarizing field H_o can be supplied by a small permanent magnet in such a way that the total volume does not exceed 3-1/2 x 6 x 7-1/2 inches. Measurements made of the performance of the circulator vs the magnetostatic field at 975 mc and of the performance vs frequency with a fixed polarizing field are discussed. The results indicate that the circulator configuration is quite suitable for use in the low frequency region of the microwave spectrum.

6244 MINIATURE HIGH-FREQUENCY MAGNETIC AMPLIFIERS FOR MAGNETIC MEMORY SENSING by G. R. Briggs and K. C. Hu (RCA); Commun. and Electronics, No. 46, pp. 863-872, Jan. 1960

The results of investigations into the usefulness of magnetic amplifiers at relatively high excitation frequencies (100 kc to 4 mc) are described. Response times of less than 10 microseconds with a signal power sensitivity of 10^{-10} watts and an equivalent input noise voltage of less than 0.1 microvolts

MAGNETIC DEVICES (Cont'd)

have been obtained. Both ferrite and metal tape cores were used. A magnetic-memory sensing amplifier having adequate sensitivity, gain, and response and recovery times has been built. Zero drift, due to excitation heating of the cores, and the need for core matching to obtain good zero balance are mentioned as difficulties still to be overcome.

245 THEORETICAL LIMITATIONS TO FERROMAGNETIC PARAMETRIC AMPLIFIER PERFORMANCE by R.W. Damon and J. R. Eshbach (GE Res. Lab.); IRE Trans., Vol. MTT-8, pp. 4-9, Jan. 1960

It has been commonly expected that improved operation of the ferrite parametric amplifier could be obtained by use of materials of narrower resonance linewidth, ΔH. This parameter is critical in determining the pumping power (P_p) required for operation of the device. Also of importance, however, is the limitation of device properties determined by the dependence on ΔH of the instability threshold of the spin-wave system. Considering this limitation, the maximum voltage gain-fractional bandwidth product ($g_v \Delta\omega/\omega_1$) has been determined as a function of other device parameters, and typical values have been calculated for several modes of operation. For the electromagnetic mode, for example, there is an optimum ΔH which yields maximum $g_v \Delta\omega/\omega_1$ at a given pumping power. It is also shown that a minimum filling factor, also a function of ΔH for some types of operation, is required to reach the oscillation threshold even in the unloaded device.

246 THE FERREED - A NEW SWITCHING DEVICE by H. Feiner, C.A. Lovell, T.N. Lowry, and P.G. Ridinger (Bell Labs.); Bell Sys. Tech. J., Vol. 39, pp. 1-30, Jan. 1960

An experimental switching device - the ferreed (ferrite and magnetic reed) - which has sealed metallic contacts, control times in the microsecond range, coincident selection, memory without holding power, and small size is described. The device may be used as a memory for display, buffer, and input-output functions in digital systems. The development of the ferreed is traced from a conceptual model, through realization of a practical model, to possible applications in switching networks. Two methods of coincident control are discussed and three devices related to the conceptual ferreed are briefly described.

247 SOME CHARACTERISTICS OF A MASER AT 1420 MHz by B. Bolger, B. J. Robinson, and J. Ubbink (Kamerlingh Onnes Lab.); Physica, Vol. 26, pp. 1-18, Jan. 1960

A regenerative solid-state maser constructed for 1420 mc using 0.05% Cr^{+++} in $K_3Co(CN)_6$ and a pump frequency of 850 mc is discussed. With a magnetic field of 480 oe at 1° to the crystalline a-axis in the ac-plane, the 1-2 transition was used for the signal-frequency and the 1-3 transition for the pump frequency, numbering the levels in order of increasing energy. The product of voltage gain and bandwidth was 1.7 mc. Weaker emission was observed for several other transitions. For ruby (Cr^{+++} in Al_2O_3) emission could be produced for the 2-3 transition at 1420 mc with the 1-3 transition pumped at 9500 mc. The emission for Cr^{+++} in $K_3Co(CN)_6$ was found to be much higher when the pump field extended throughout the crystal than when it had a node within the crystal. The observation suggests that in $K_3Cr(CN)_6/K_3Co(CN)_6$ the phonon saturation mechanism proposed by Strandberg does not take place.

6248 MASER BEHAVIOR: TEMPERATURE AND CONCENTRATION EFFECTS by T.H. Maiman (Hughes); J. Appl. Phys., Vol. 31, pp. 222-223 (L), Jan. 1960

Ruby maser operation at temperatures above the liquid-helium range is discussed. It is reported that a maser has been operated at 195°K with dry ice used as the coolant. A ruby crystal containing 0.20 percent Cr_2O_3 by weight has been operated with a gain bandwidth product of about 14 mc and an effective noise temperature of approximately 100°K (excluding input losses) at 77.4°K. The noise temperature agrees with the 95°K value calculated by taking into account cavity losses and the spin temperature of the ruby. It has been found that ruby crystals having a chromium concentration larger than approximately 0.1 percent exhibit a poorer performance (gain-bandwidth product) at 4.2°K than more dilute crystals at the same temperature. An explanation for this phenomenon based on cross-relaxation effects and experimental results which support the theory are given.

Duplexing a Ruby Maser - See 6273.

6249 ON THE TE_{n0} MODES OF A FERRITE SLAB LOADED RECTANGULAR WAVEGUIDE AND THE ASSOCIATED THERMODYNAMIC PARADOX by A. D. Bresler (Polytech. Inst. Brooklyn); IRE Trans., Vol. MTT-8, pp. 81-95, Jan. 1960

It has been known for some time that the secular equation for the TE_{n0} modes of a perfectly conducting rectangular waveguide loaded with a transversely magnetized dissipationless full height ferrite slab located against one of the narrow walls of the waveguide admits the possibility of the existence of only a single propagating mode (transporting energy in one direction only). It is shown that the existence of a passive dissipationless uniform waveguide supporting only a single propagating mode leads to a thermodynamic paradox. A uniqueness theorem which establishes that, for the waveguide described above, the paradox is associated with the TE_{n0} mode set alone is cited. This conclusion has led to a thorough study of the secular equation for the TE_{n0} modes of this waveguide.

6250 PARTICLE INTERACTION IN MAGNETIC RECORDING TAPES by J. G. Woodward and E. Della Torre (RCA Labs.); J. Appl. Phys., Vol. 31, pp. 56-62, Jan. 1960

The magnetic coating of recording tape is assumed to be composed of an assemblage of small, single-domain particles. Each particle is assumed to have a symmetrical, square hysteresis loop when the reversible component of magnetization is neglected and when the particle is not influenced by the fields of neighboring particles. When influenced by the fields of its neighbors, the particle may exhibit an asymmetrical loop when the loop is plotted relative to an external applied field. In this case the positive and negative switching fields for the particle are not equal, and their difference gives an indication of the particle interaction. While it is not possible to measure the switching fields of a single particle on the recording tape, the distribution of switching fields in the assemblage of particles and the associated magnetic moment can be measured. The two switching fields and the magnetic moment define a 3-dimensional distribution function which describes the magnetic properties of the tape, and in terms of which both d-c and anhysteretic magnetization processes may be described. The distribution functions have been measured for two recording tapes. While the functions for the two tapes are markedly different in detail, both show that particle interaction is very appreciable in recording tapes and that it is a significant

factor in determining the bulk magnetic properties and the recording performance of tapes.

OTHER SOLID STATE DEVICES

FUNCTIONAL UNITS

Binary Multivibrators - See 6309 (New Product Section).

HALL EFFECT DEVICES

Hall Generators - See 6298.

DIELECTRIC DEVICES

Method of Forming Thin Films of $BaTiO_3$ for Use in Various Devices - See 6042.

Barium Titanate Piezoelectric Crystals - See 6307 (New Product Section).

Solid State Transducers - See 6311 (New Product Section).

6251 SEMICONDUCTOR VARACTORS USING SURFACE SPACE-CHARGE LAYERS by W. G. Pfann and C.G.B. Garrett (Bell Labs.) Proc. IRE, Vol. 47, pp. 2011-2012 (L), Nov. 1959

Semiconductor varactors which utilize the voltage-sensitive capacitance that exists in the space-charge region at the surface of a semiconductor bounded by an insulating layer are discussed. The discussion centers on two structures, the ON varactor and the ONO varactor. The ON structure is fabricated by applying an ohmic contact to one surface of a semiconductor, an insulating dielectric (e.g. SiO_2) to the other surface, and a metallic film to the dielectric. In the ONO structure, the dielectric film is applied to both surfaces of the semiconductor. The physical phenomena involved in the operation of the devices are discussed. They are suitable for use in parametric amplification and have certain advantages over p-n diodes. A feature of the ONO structure is that there is no metal-semiconductor contact, and therefore none of the contact resistance problems found in p-n diodes. It is suggested that microwave devices whose active regions are not small in comparison with a wavelength can be fabricated by ONONO.....structures. Such structures simplify construction, increase power handling ability, and permit extended structures with distributed gain properties. The carrier generation effect employed in the devices can also be used for the study of trapping in semiconductors and for devices which depend on conductivity modulation.

SUPERCONDUCTING DEVICES

Crowe Cells - See 6289.

CATHODES

6252 MOBILE ACCEPTOR MODEL FOR OXIDE-COATED CATHODES by E. B. Hensley and K. Okumura (U. Missouri); Bull. Am. Phys. Soc., Ser. II, Vol. 5, p. 69 (A), Jan. 27, 1960

Measurement of the diffusion of the activation in oxide-coated cathodes by observing the profile of the thermionic emission along a cathode coated on a ribbon of pure platinum was described. A peaked initial distribution is obtained by inserting a small tab of active cathode nickel at the center of the ribbon. The diffusion coefficient at 1000°K is 3×10^{-7} cm^2 sec^{-1} with an activation energy of 0.4 ev. This diffusion is consistent with the diffusion of barium ion vacancies assuming that the ratio of these vacancies to the barium ion lattice sites is of the order of 10^{-5}. A mobile acceptor model for oxide-coated cathodes in which the principal donors are oxygen ion vacancies was proposed. Since these have a very low-diffusion coefficient, their number will remain relatively unchanged during normal activation or deactivation processes. Activation of an oxide-coated cathode is achieved not by increasing the density of donors but by decreasing the density of acceptors, the barium ion vacancies. This process is governed by the rate at which these barium ion ion vacancies diffuse to a source of excess barium. The familiar m-decay phenomenon is accounted for by drift of the positively charged acceptors.

SOLID STATE DEVICE MEASUREMENTS

Tunnel Diode Curve Tracer - See 6312 (New Product Section).

Measurement of Transistor Parameters - See 6258.

6253 PREDICTION OF STORAGE TIME IN JUNCTION TRANSISTORS by R. P. Nanavati (Syracuse U.); IRE Trans., Vol. ED-7, pp. 9-15, Jan. 1960

It is pointed out that in the prediction of storage time only a single fundamental device parameter, the storage time constant T_s, must be known. Several methods of measuring T_s are considered and compared both theoretically and experimentally. A single nonoscilloscopic method of measuring T_s is discussed and its theory is presented. This method holds out the best promise for the ability to predict the storage time of very fast transistors. It is therefore now possible to predict large signal transient response of transistors on the basis of small signal nonoscilloscopic measurements.

SOLID STATE DEVICE CIRCUITS

GENERAL

6254 EQUIVALENT CIRCUIT DIAGRAMS FOR THE TRANSISTOR DRIVEN AS LINEAR AMPLIFIER [In German] by W. Benz (Telefunken); Elektron. Rundschau, Vol. 14, pp. 5-9, Jan. 1960

The different transistor equivalent circuit diagrams are surveyed, their properties are described, and schematic diagrams and four-pole evaluations are demonstrated. The physical equivalent circuit diagram of an idealized transistor and the movements of the charge carriers within the semiconductor material

at the barrier layers are considered in detail. The terms internal transistor path resistance and barrier layer capacince are explained.

5 TRANSISTOR BEHAVIOR AT HIGH FREQUENCIES by P. Abraham (Bell Labs.); IRE Trans., Vol. ED-7, pp. 59-69, n. 1960

e tee equivalent circuit for junction transistors is modified to account of the electric field in the base region which reits from a graded impurity density. It is shown that a graded ise improves the high-frequency performances of the common stage; however, the improvement in common emitter perance is considerably less because of the increased "excess" se which accompanies the improved high-frequency perform-. The complex hybrid parameters are calculated for the mon base and common emitter configurations; these calculas take into account the parasitic interterminal capacities of transistor. The common emitter calculations are compared easured data, and substantial agreement is obtained.

nsistor Equivalent Circuits - See 6258.

56 TRANSISTOR MATCHING IMPEDANCES by A. G. Bogle; ctronic Tech., Vol. 37, pp. 28-30, Jan. 1960

ee techniques - variation of operating point, negative feedck from collector to base (shunt feedback), and negative dback caused by an unbypassed resistor (series feedback) - varying the input impedance, output impedance, and gain a transistor in the grounded emitter configuration are desbed.

nsistor Mounting Washers - See 6313 (New Product Section).

57 MICROELECTRONICS: AN INTRODUCTION AND A ATUS REPORT by T. A. Prugh (Diamond Ord. Fuze Labs.); S. Gov. Res. Rep., Vol. 33, p. 46 (A), Jan. 15, 1960 143 566

o techniques developed for constructing small transistorized dules are described. The first uses etched wiring boards and ndard subminiature components. The second technique gives reater than ten to one volume reduction over the first by orporating an uncased transistor directly into a printed cirt ceramic plate. The degree of reduction is such that optiaids must be used in constructing and inspecting the cirtry. The term microelectronics has been selected to desige the latter technique and related efforts.

AMPLIFIERS

C Amplifier Using a Thermistor Chopper - See 6295.

plexing a Ruby Maser - See 6273.

58 TRANSISTOR VIDEO AMPLIFIERS by C. R. Zimmer racuse U.); U. S. Gov. Res. Rep., Vol. 33, p. 57 (A), 1. 15, 1960 PB 143 495

e following topics are discussed. Basic low pass amplifier ory: Vacuum tube amplifiers, and 2- and 4- terminal interge networks. Theoretical equivalent circuits: Fused-junction nsistor, effect of the base spreading resistance, transistor parameters in the grounded-emitter connection, approximations for transistor parameters, relations among design and circuit parameters, fabrication of fused- and grown-junction transistors, and modified junction transistor designs. Measurement of transistor parameters: Simplified equipment for h-parameter measurements, measurement of transistor parameters using bridge techniques, and experimental results for the fused- and grown-junction transistors. Single stage amplifier: Simplified equivalent circuit, amplifier stage with resistive terminations, input circuit compensation (series peaking), effect of load capacitance, output circuit equalization, and compensation using local RC feedback. Multistage amplifiers: Shunt resistance interstage, shunt peaking (simple RL network), 4-terminal networks and all-pole transfer functions, and ultimate limitations of interstage compensating network. Large signal operation: Effect of the transistor output impedance, output circuit equalization, addition of feedback equalization, and experimental results using feedback equalization.

6259 AN EXTENSION OF THE MODE THEORY TO PERIODICALLY DISTRIBUTED PARAMETRIC AMPLIFIERS WITH LOSSES by K. Kurokawa and J. Hamasaki (U. Tokyo); IRE Trans., Vol. MTT-8 pp. 10-18, Jan. 1960

For the extension of the mode theory of the lossless periodically distributed parametric amplifier to the lossy case, a "conjugate circuit" is introduced. The conjugate circuit is an imaginary circuit which is obtained in the pass band by replacing each resistance in the original circuit with the negative resistance of the same magnitude. The orthogonality properties between the modes of the original circuit and those of the conjugate circuit are derived. The power gain and the noise figure of the amplifier are calculated, showing the usefulness of this mode theory in accounting for the spreading resistance of the semiconductor diode.

Parametric Amplification Using Surface Space Charge Layer Varactors - See 6251.

S-Band Variable Reactance Amplifier Using Gallium Arsenide Diodes - See 6226.

6260 ANALYSIS OF THE TRANSISTOR CASCODE CONFIGURATION by J. R. James (Semicon.); Electronic Engrg., Vol. 32, pp. 44-48, Jan. 1960

The Y matrix of the transistor cascode amplifier is derived and used to investigate the stability and gain of the amplifier. The results of the analysis are then compared with experimental results.

Diode Amplifiers - See 6223.

6261 THE OPTIMUM NOISE PERFORMANCE OF TUNNEL-DIODE AMPLIFIERS by K. K. K. N. Chang (RCA Labs.); Proc. IRE, Vol. 48, pp. 107-108 (L), Jan. 1960

It is shown analytically that with a given I-V characteristic of a tunnel diode, a minimum value of A (F-1), the product of the excess noise and a constant depending on gain, exists at a unique point on the characteristic. A small value of A (F-1) means small noise factor and/or large power gain. An ideal I-V characteristic which can be used as a guide for the design of tunnel diode amplifiers with low values of A (F-1) is suggested.

AMPLIFIERS (Cont'd)

6262 SELF-REGULATION IN MAGNETIC-TRANSISTOR AMPLIFIERS by C. E. Hardies and R. L. Van Allen (Magnetics); Commun. and Electronics, No. 46, pp. 905-909, Jan. 1960

A magnetic amplifier incorporating a transistor as a switching element and featuring self-regulation with variation in supply voltage is described. Gain, temperature stability, and frequency stability remain high and stabilization with load is very good. The self-regulating feature results from the principle of having output occur during prefiring, rather than postfiring, intervals. The design procedure is simple, since the magnetic amplifier portion of the circuit is a conventional self-saturating design. Circuit examples include d-c, a-c, and push-pull (reversible polarity) d-c amplifiers. Operation from higher supply frequencies is possible because of the greater switching speed of the transistor, as compared with the magnetic circuitry.

6263 TRANSISTOR AC AMPLIFIERS WITH HIGH INPUT IMPEDANCE: A SURVEY by J. A. Ekiss (Philco); J. Audio Engrg. Soc., Vol. 8, pp. 18-22, Jan. 1960

Various high input impedance transistor a-c amplifier circuits are presented and their level of performance is indicated. The two important design criteria for these amplifiers, bias point stability and low noise figure, are discussed.

OSCILLATORS

6264 DESIGNING HIGH-POWER TRANSISTOR OSCILLATORS by W. E. Roach (Pacific Semicon.); Electronics, Vol. 33, pp. 52-55, Jan. 8, 1960

A design procedure for high-power, high frequency transistor oscillators is presented. Outputs of the order of tenths of a watt at several hundred megacycles are available with present units. The procedure involves design of an amplifier for the frequency and power levels desired, addition of a separate feedback network and consolidation and simplification of the result. All needed formulae are included, as well as a résumé of experimental results.

Multifrequency Oscillator-Generator - See 6272.

Solid Circuit Binary Multivibrators - See 6309 (New Product Section).

Multivibrator with Linear Control of Output Pulse Duration - See 6268.

Blocking Oscillator for Driving Counter Tubes - See 6304.

SWITCHING CIRCUITS

6265 MICROWAVE SWITCHING WITH COMPUTER DIODES by M. Bloom (Sylvania); Electronics, Vol. 33, pp. 85-87, Jan. 15, 1960

The use of computer diodes for microwave switching is discussed. Small area junction diodes have been used at 1 to 10 kmc, switching up to 4 watts at X-band. Both spst and spdt switching can be achieved by proper biasing controls and switch placement. The crystal diode creates a very small mismatch in the waveguide or coax when biased in the forward direction, but makes a strong mismatch under reverse bias. The switching effect is essentially a result of reflection rather than absorption, so that little power is needed for switching or is dissipated in the diode.

6266 TRANSISTOR BIAS METHOD RAISES BREAKDOWN POINT by A. Somlyody (Burroughs); Electronics, Vol. 33, pp. 48-49, Jan. 8, 1960

The operation of reverse-biased transistors with switching voltages greater than their collector-to-emitter breakdown is described. In practice, units rated at 25 volts are found to be reliable for switching 40 volts if the base is reverse-biased whenever the collector voltage rises above its breakdown rating. The technique, which is used in production modular drive units for Nixie tubes, operates adequately from -30 to 55°C.

SIGNAL CONVERTERS

Diode Modulators - See 6223.

6267 IMPROVEMENT IN THE SQUARE LAW OPERATION OF 1N23B CRYSTALS FROM 2 to 11 KMC by A. Staniforth and J. H. Craven (Natl. Res. Council, Ottowa); IRE Trans., Vol. MTT-8, pp. 111-115, Jan. 1960

The conditions required to increase the dynamic range over which square law response may be achieved for crystal rectifiers used as video detectors in microwave measurements have been investigated experimentally. Results indicate that a forward bias current of 100 μa or more with a low video load resistance makes the operation of the crystal closer to the ideal square law over a larger dynamic range.

WAVE GENERATORS

Generation of Microwaves Using the Faraday Effect - See 6195.

PULSE CIRCUITS

6268 A STUDY OF TRANSISTOR LINEAR TIME DELAY by R. P. Nanavati (Syracuse U.); U. S. Gov. Res. Rep., Vol. 33, p. 57 (A), Jan. 15, 1960 PB 143 526

A transistor emitter-coupled monostable multivibrator in which the duration of the output pulse can be controlled linearly by the setting of a potentiometer at the input is described. This circuit can be used as a linear delay circuit or as a gate. It can also serve as an important "building block" for linear time base circuits.

FILTERS

6269 LOW-PASS FILTER FOR SUBAUDIO FREQUENCIES by R. C. Onstad (Convair-Astronautics); Electronics, Vol. 33, pp. 88-90, Jan. 15, 1960

An active filter with very flat response to the one cps cutoff, designed for use in missiles, is described. Required to remove unnecessary higher frequency components from telemetered multiplexed data, the filter uses active elements to provide

e feedback necessary for an overall circuit damping coeffi-ient less than one, as is needed to provide the very sharp ...ner desired at the cutoff. The side-benefit of zero insertion ...ss is also possible. Matched silicon transistors and a thermis-...r-regulated input improve the temperature stability.

270 TRANSISTORIZED MATCHED FILTER FOR PULSED SINU-OIDS by P. L. Fleck Jr. (Lincoln Lab.); U. S. Gov. Res. Rep., ...l. 33, p. 51 (A), Jan. 15, 1960 PB 138 607

. matched filter for pulsed sinusoids which utilizes transistors ... the active elements is described. The filter has a gain varia-...n of less than one db due to variation of component param-... rs, temperature, age, and supply voltages, and it has a use-...l dynamic range of at least 80 db.

SOLID STATE DEVICE APPLICATIONS

COMMUNICATIONS, ETC.

...nsistorized Low-Noise Television Tuners - See 6314 (New ...oduct Section).

271 A TELEVISION MASTER SWITCHER by B. Marsden ...ssociated TV); J. Brit. IRE, Vol. 20, pp. 47-54, Jan., 1960

...e standard methods presently used to switch video signals are ...rveyed and a video selection method in which the switch ele-...ents are made up of semiconductor diodes is described. Both ...aster control room and studio type switchers are discussed. ...ference is made to current development work in which tran-...storized pulse generators are being used to achieve vision ...itching between successive frames of the television waveform.

272 TRANSISTORIZED MULTIFREQUENCY RINGING GEN-ATOR by J. F. Kostelich and B. W. Howald (Lorain Products); ...mmun. and Electronics, No. 46, pp. 987-991, Jan. 1960

... sharply tuned transistorized oscillator-generator, capable of ...justment to any of several frequencies for use as a selective ...lephone ringing generator, is described. Good output voltage ...gulation with load and supply variation was required, as well ... low harmonic content. Self-protection, ease of frequency ...justment, reliability, and low noise feedback to the telephone ...ttery power supply are features of the final unit.

273 DUPLEXING A SOLID-STATE RUBY MASER IN AN X-...ND RADAR SYSTEM by F. E. Goodwin (Hughes Aircraft); ...c IRE, Vol. 48, p. 113 (L), Jan. 1960

...e use of a reflective type ferrite switch between the TR tube ...d the maser preamplifier of a conventional X-band pulse ...dar TR circuit to reduce leak-through power and therefore ...mit the use of the maser preamplifier is discussed. The con-...uction and operation of the switch are described. It has an ...sertion loss of 0.25 db and an isolation of more than 30 db ...er a 120 mc band. When the switch was used, the measured ...ise temperature of the maser, circulator, mixer, and IF am-...ifier combined was 65°K and that of the over-all receiver ...as 173°K. This is an excellent value compared with the ...500° to 2500°K noise temperature of a good X-band radar ...ceiver without a maser preamplifier

6274 DATA CONVERSION CIRCUITS FOR EARTH SATELLITE TELEMETRY by D. N. Carson (Bell) and S. K. Dhawan (Columbia U.); Electronics, Vol. 33, pp. 82-84, Jan. 15, 1960

Two types of transistorized pulse-height-to-time converters are described. Designed as part of a complete pulse height analyzer to be included as satellite payload, both circuits maintain a high order of linearity. The first, capable of taking pulses up to 40 volts P-P, and linear within 1% for signals up to thirty volts, uses a transistor constant-current circuit to discharge a capacitor. The capacitor turns on a gate generator as long as it remains charged. The other circuit compares the magnitude of the input pulse with that of a ramp signal, so that ramp length is determined by input amplitude. Linearity is 0.1% for inputs up to seven volts.

Filters for Multiplex Telemetry - See 6269.

6275 A TRANSISTORIZED STEREO PREAMPLIFIER AND TONE CONTROL FOR MAGNETIC CARTRIDGES by A. B. Bereskin (U. Cincinnati); IRE Trans., Vol. AU-8, pp. 17-20, Jan.-Feb. 1960

A transistorized stereo preamplifier developed for use with magnetic cartridges in which RIAA equalization with ±4 db bass control and ±8 db treble control have been achieved together with negligible hum, noise, and distortion is described. Simple circuit modifications adapt this preamplifier for use with most magnetic cartridges.

6276 AUDIO VOLUME COMPRESSOR by E. C. Miller (Inland Broadcasting); Electronics, Vol. 33, p. 62, Jan. 8, 1960

A transistorized automatic gain adjuster, designed to maintain a constant level on tape-recording inputs, is described. The amplifier has essentially unity gain, providing from 3 db of expansion to 12 db of compression in the region around 45 db below one volt at 10,000 ohms. The output of a single-stage amplifier is fed to an L-pad attenuator, one leg of which is a diode whose impedance varies logarithmically in inverse proportion to the d-c voltage across it. Power consumption is about 0.6 ma.

6277 MORE BANDWIDTH FOR MAGNETIC RECORDERS by D. R. Steele (Ampex); Electronics, Vol. 33, pp. 44-47, Jan. 8, 1960

Direct-record and direct reproduce circuits for magnetic recorders, designed to work with newly available tape heads at frequencies from 250 cps up to 250 kc, are described. The record circuit, stable at over 65°C, also provides a monitor output corresponding to the effective record current, with actual head current unaffected by the monitor load. The reproduce system provides separate amplitude equalization circuits for each tape speed, as well as phase equalization circuits providing appreciably improved transient response while maintaining a flat amplitude response throughout the specified bandwidth.

COMPUTERS, ETC.

6278 THE CONSTRUCTION OF A DIGITAL-COMPUTING SYSTEM FROM A BASIC TRANSISTOR CIRCUIT by P. L. Cloot and G. E. Jackson (Met.-Vickers Electrical); Electronic Engrg., Vol. 32, pp. 37-43, Jan. 1960

A special purpose digital computer which utilizes a built in program for binary-decimal conversion and a basic circuit consisting of one transistor, one capacitor, and three resistors is

described. The logical design, circuit design, and the mechanical construction of the machine are discussed. The extremely compact computer uses printed wiring throughout. [See also 2192.]

6279 LEPRECHAUN: A SOLID-STATE DIGITAL COMPUTER by J. A. Githens and M. J. Gilmartin (Bell Labs.); U. S. Gov. Res. Rep., Vol. 33, p. 75 (A), Jan. 15, 1960 PB 143 648S

The TRADIC second feasibility computer, better known as LEPRECHAUN, a high-speed solid-state digital computer capable of solving complex weapons guidance control problems in real-time, is discussed. The computer was built to demonstrate the feasibility of using direct-coupled transistor logic (DCTL) in a system involving thousands of transistors and to test and evaluate a moderately large magnetic-core memory driven by transistors. It serves as a vehicle for the continuing study and evaluation of the operating characteristics and reliability of transistors in these techniques. Complete details of the design and construction of the LEPRECHAUN computer are given.

Computer Switching Circuits Using Gallium Arsenide Diodes - See 6226.

Application of Ferreeds to Switching Circuits - See 6246.

6280 ELECTRONIC COUNTER by H. K. Henisch (Sylvania); U. S. Pat. 2,922,898, Issued Jan. 26, 1960

A counting device which consists essentially of a number of point contact diodes constructed from a single semiconductor rod is described. At any particular instant, by means of a switch, all the odd number diodes and all the even number diodes are either grounded or biased in the reverse direction, respectively. When the switch is reversed the condition of each diode also changes. Carriers are injected by an additional point contact at one end of the rod. If all the odd diodes are reverse-biased, the injected carriers reduce both the spreading resistance (i.e., the resistance of the region near the point contact) and the resistance of the other (base) contact to the first diode. The field at the point contact and its spreading region decreases and the field at the base contact is increased. As a result, the carriers injected by the base contact flow to the collector and the first diode becomes highly conductive. Since most of the injected carriers are collected in the first diode or recombine, not enough reach the third diode to cause conduction. When the switch reverses, only the second diode conducts. At each succeeding reversal of the switch only the next diode can conduct. By noting the diode which is conducting the number of switch reversals can therefore be counted.

6281 STEERING CIRCUITS CONTROL REVERSIBLE COUNTERS by R. D. Carlson (Victor Adding Mach.); Electronics, Vol. 33, pp. 86-88, Jan. 1, 1960

A reversible decade counter using symmetrical n-p-n transistors to determine the direction of count is described. Each decade stage employs four bistable multivibrators to provide the ten signal states and two carry signals required. The steering transistors act as trigger amplifiers as well as controlling the direction of count. A pulse discriminator allows random input of additive or subtractive signals without loss of information. The stored data may be changed to the nines complement of the excess-three code employed by a single control pulse, allowing use of the unit in computer operation. Normal output is to a Nixie lamp; a 20% variation in lamp supply voltage is permissible.

Solid Circuit Binary Multivibrators for use in Counters and Shift Registers - See 6309 (New Product Section).

6282 SONIC DELAY LINES by W. W. Keith (Raytheon); U. S. Pat. 2,920,294, Issued Jan. 5, 1960

A technique for reducing unwanted signals in the output of liquid and solid delay lines is described. The undesired signals are made to arrive at the output of the device out of phase with each other so that they cancel. The latter is accomplished by making the undesired signals travel distances which differ from each other by amounts which depend on the number of undesired paths and on the frequency of the sound. In an illustration, the path lengths in a nine-faced quartz delay line are varied by slightly altering the faces to which the input and output transducers are attached so that the transducers are perpendicular to the desired paths.

6283 FACTORS INFLUENCING THE APPLICATIONS OF MAGNETIC TAPE RECORDING TO DIGITAL COMPUTERS by D. P. Franklin (E.M.I. Electronics); J. Brit. IRE., Vol. 20, pp. 9-21, Jan. 1960

The merit of magnetic tape for storage of digital information and the benefits of two-state operation are briefly discussed. Limitations on the density of recorded information are reviewed to show the extreme precision required in the manufacture of magnetic heads and tape guidance mechanisms. Design features made necessary by high speed and acceleration requirements are considered with reference to a recently developed high performance tape handler.

6284 MAGNETIC FILM FILE FOR COMPUTER STORAGE by A. St. Johnson (Elliot Bros.); J. Brit. IRE., Vol. 20, pp. 25-30, Jan. 1960

A 35-mm oxide-coated film store in which the pick-up head does not contact the oxide is described. The high quality backing medium provided by the film has resulted in complete freedom from drop outs. Interchangeability between all mechanisms has been achieved with available production heads by using special auto-strobing circuits.

Particle Interaction in Magnetic Recording Tapes - See 6250.

6285 A HIGH-DENSITY FILE DRUM AS A COMPUTER STORE by L. Knight and M. P. Circuit (Int. Computers and Tabulators); J. Brit. IRE., Vol. 20, pp. 41-45, Jan. 1960

A large-capacity magnetic drum store having a capacity of ~15,000,000 bits and an average random access time of ~200 ms is described. A packing density of just over 1,000 bits per in has been obtained by floating specially designed heads on a film of oil which automatically maintains a spacing of 0.002 in between the head and the drum surface. Special considerations led to the use of a copper-nickel-iron alloy for the drum surface. A self-clocked reading system is used to obviate the need for high mechanical stability. The reading circuit also has special features which keep it operating under optimum conditions over a range of signal amplitudes.

6286 THE MAGNETIC DRUM STORE OF THE 'MERCURY' COMPUTER by K. I. Turner and J. E. Thompson (Ferranti); Electronic Engrg., Vol. 32, pp. 16-21, Jan. 1960

detailed description of the mechanical and electronic design of the magnetic drum store of the high speed digital computer 'Mercury' is given. The main store consists of up to 8 magnetic drums, each of which can store 64 x 3456 bits of information. Each drum is housed with necessary circuits in a self-contained cabinet measuring approximately 5'6" x 3' x 2'6". Electronic track selection on writing and reading permits switching between tracks in less than 20 μsec. Synchronism between the drum and the computer is achieved by means of an electronic system of speed control.

6287 A MAGNETIC DISK, RANDOM ACCESS MEMORY by A. C. Glover (IBM Brit. Labs.); J. Brit. IRE., Vol. 20, pp. 22-24, Jan. 1960

large capacity, random access storage device which uses rotating magnetic disks is described. Total storage capacity 5×10^5 alphanumeric characters with access time between 0.15 and 0.8 sec.

6288 HIGH-SPEED DIGITAL STORAGE USING CYLINDRICAL MAGNETIC FILMS by G. R. Hoffman, J. A. Turner, and T. Kilburn (U. Manchester); J. Brit. IRE., Vol. 20, pp. 31-36, Jan. 1960

digital stores consisting of closed magnetic circuits deposited on long glass tubes, which promise considerably increased operating speeds compared with present stores and the possibility of producing multi-element systems are described. A set-up designed to produce 30 tubes with 16 elements per tube in a single evaporation is now operating. Selection modes suitable for an array of this type which permit greater tolerances than conventional selection systems have been tested.

6289 LOW TEMPERATURE STORAGE ELEMENTS by E. H. Broderick (SERL); J. Brit. IRE, Vol. 20, pp. 37-40, Jan. 1960

The philosophy underlying the use of low temperature computer elements is discussed and the cryogenic aspect of the problem is briefly reviewed. The most advanced low temperature storage element at the moment is the Crowe cell, in which a persistent current is set up around an aperture in a thin superconducting film, the direction of the current determining whether a 0 to 1 is stored. The switching time of these elements can be as short as 10 μsec and the size is such that between 10^6 and 10^7 can be packed into a cubic foot. The main problem involved in the fabrication of a large memory is that of reproducibility. To exploit the high speed of the Crowe cell it may be necessary to perform the selection and logical operations in the low temperature cryostat. Modifications of Buck's original cryotron or avalanche breakdown in a semiconductor could conceivably be used for this purpose.

Magnetic-Memory Sensing Amplifiers - See 6244.

6290 PULSE-HEIGHT-TO-DIGITAL SIGNAL CONVERTER by J. W. Grannemann, C. D. Longerot, R. D. Jones, D. Ensley, G. Summers, T. Lommasson, A. Pope, and A. D. Smith (U. New Mexico); Electronics, Vol. 33, pp. 58-60, Jan. 8, 1960

A transistorized system which will convert a 0-to-2 volt input pulse into a 7-digit binary output pulse is described. Capable of sampling at rates up to 13,000 pps, the converter changes pulse height into pulse length, then uses the length pulse to gate the output of a continuously-running clock. The clock pulses occurring during the gate are counted by a binary counter, whose output is joined with an 8-pulse train to provide the timed serial binary output.

Transistorized Input Scanner - See 6315 (New Product Section).

6291 ELECTROLUMINESCENT ALPHANUMERIC DISPLAY by T. Hamburger (Westinghouse); Electronics, Vol. 33, pp. 49-51, Jan. 22, 1960

A displaying typewriter is described. Electroluminescent materials are used to form alphanumeric indicators, which are excited by ferroresonant switching circuits. A nonlinear iron-core inductor in series with an ordinary capacitor presents a bistable a-c v-i curve, and can be used for information switching and storage. The alphanumeric indicators consist of segments of dielectric-imbedded phosphors sandwiched in transparent conducting material. Each segment appears as a lossy capacitor, facilitating the use of the display as a portion of the information storage circuit. A typewriter may be connected to supply trigger signals to the proper segments, so that an electroluminescent display of the typed information may be achieved. Erasure may be selective or display-wide.

POWER APPLICATIONS

6292 A MAGNETIC-AMPLIFIER-SILICON-TRANSISTOR POWER SUPPLY FOR MISSILE APPLICATION by B. Mokrytzki and R. A. Stuart (Westinghouse); Commun. and Electronics, No. 46, pp. 835-843, Jan. 1960

A power supply utilizing high-power silicon transistors in combination with magnetic amplifiers is described. Designed for use in missiles, the supply was required to feed several direct and alternating voltages, with 1% regulation, from a d-c supply with a possible 10% variation. A wide operating ambient temperature range, small size limits, and high efficiency and ruggedness requirements further complicated the problem. The design procedure is reviewed and the circuit is described. An RMS sensing circuit using only transformers and rectifiers which was specially designed for this application is also described.

6293 A TRANSISTORIZED CURRENT STABILIZER FOR AN ELECTROMAGNET by J. C. S. Richards (Aberdeen U.); Electronic Engrg., Vol. 32, pp. 22-23, Jan. 1960

An electromagnet current stabilizer which can supply up to 4a, at 200 v with the current stable to ±2 parts in 10^5 over an hour and ±2 parts in 10^4 over ten hours is described. The stabilizer utilizes an auxiliary electromechanical control system on the input to overcome the low maximum voltage rating of presently available power transistors.

6294 ULTRASONIC FREQUENCY POWER GENERATOR USING TRANSISTORS by Y. M. Wei (Westinghouse); Commun. and Electronics, No. 46, pp. 1062-1065, Jan. 1960

A transistorized ultrasonic frequency power generator is described. The transistors are used in the switching mode to decrease power losses, resulting in an over-all d-c to a-c power conversion efficiency around 85%. A push-pull square wave oscillator is used to feed a series-connected double-bridge type

power inverter. A diode shaping circuit is used to provide non-symmetrical drive voltages to each of the bridges, preventing a short-circuit condition across the d-c power supply because of the difference in speed between ON and OFF switching. An r-c circuit in the base connection to each transistor speeds switching and further cuts power losses. Good frequency stability is reported.

6295 USE OF A THERMISTOR AS A DC-AC CONVERTER by N. W. Bell (Consolidated Electrodynamics); Rev. Sci. Instr., Vol. 31, p. 65, Jan. 1960

The use of the variable resistance property of thermistors to convert a small d-c signal to a proportional a-c signal is briefly discussed. Capacitively-coupled r-f energy can change the resistance of a directly heated thermistor without the introduction of spurious d-c or low-frequency signals. The thermistor must have good voltage-current linearity and must be cooled rapidly. A d-c amplifier which utilizes a 30 cps thermistor "chopper" has been constructed.

CONTROL APPLICATIONS

6296 THEATER LIGHTING CONTROL SYSTEM by F. S. Macklem (Kliegl Bros. Universal Electric Stage Lighting); U. S. Pat. 2,920,240, Issued Jan. 5, 1960

The operation of the silicon controlled rectifier is discussed and a circuit which utilizes two of these devices to control the intensity of stage lighting is described. The apparatus weighs about 100 times less than a conventional magnetic amplifier arrangement for controlling stage lighting and occupies less than 27 cubic inches while the conventional apparatus occupies about 1500 cubic inches.

INSTRUMENTATION

6297 MEASUREMENT OF ION BEAM CURRENTS USING A HALL EFFECT MAGNETOMETER by W. S. Whitlock and C. Hilsum (SERL); Nature, Vol. 185, p. 302 (L), Jan. 30, 1960

A device which utilizes an indium antimonide Hall effect magnetometer to measure an ion current of less than 1 ma is described. The beam of ions passes through a "Mumetal" ring about 6 cm in diameter which concentrates the magnetic field of the ions (2×10^{-4} oersteds) onto an InSb crystal 0.025 cm thick placed in a 0.040 cm air gap in the ring. Two current balancing loops around the ring cancel the magnetic field due to the ion beam. The magnetometer indicates the null point, at which the beam current is the same as the current in the balance loops. Measurements were made with a steady beam (with a 1 kc alternating current in the crystal) and with a beam modulated at 1 kc (with a steady direct current in the crystal). The minimum detectable current in the former case was about 10μa and in the latter case slightly less than 10μa. In the former the accuracy of the device was limited by the zero drift caused by small temperature changes in the crystal and in the latter zero drift was negligible.

6298 THE HALL GENERATOR AND ITS USE IN MEASUREMENT TECHNIQUE [in German] by F. Kuhrt; Elektron. Rundschau, Vol. 14, pp. 10-13 Jan., 1960

The electrical properties and some applications of indium antimonide and indium arsenide Hall generators are discussed. Applications such as the measurement of magnetic fields, power measurement, contactless signalling, and static interrogation of magnetic diagrams are covered.

Nuclear Technique for Measuring Magnetic Fields in Super-Conductors - See 6116.

6299 A PIEZOELECTRIC OSCILLATOR MANOMETER by D. J. Pacey (Brunel Coll. Tech.); Vacuum, Vol. 9, pp. 261-263; Nov. 1959/Jan. 1960

A simple manometer for the measurement of gas and vapor pressures in the range 760 torr to 10^{-1} torr with a linear scale is described. The manometer uses the damping effect of the gas or vapor upon the sustained vibrations of a commercially available piezoelectric quartz crystal. The damping effect is examined theoretically and the behavior of the gauge is shown to be generally in agreement with calculation.

6300 HOW RADIATION MONITOR GUARDS NUCLEAR NAV... by H. E. DeBolt (Fairchild); Electronics, Vol. 33, pp. 43-45, Jan. 22, 1960

A transistorized radiation monitor for use on nuclear-powered ships is described. Ambient air is circulated through filter paper, which travels slowly past an anthracene scintillation crystal. A photomultiplier behind the crystal feeds a counting multivibrator circuit. This in turn drives a logarithmic integrating circuit, which provides input to a front-panel meter, as well as to a latching alarm. A Strontium-90 source is used for calibration. Leakage from this source causes a minimum count rate, so that a front-panel indicator may interpret any count cessation as flip-flop failure. Diagrams of the circuits used are included.

6301 RESPONSE OF SURFACE-BARRIER SEMICONDUCTOR COUNTERS TO N^{14} IONS by M. L. Halbert, J. L. Blankenship, and M. V. Goldman (Oak Ridge Natl. Lab.); Bull. Am. Phys. Soc., Ser. II, Vol. 5, p. 38 (A), Jan. 27, 1960

Measurement of the response of a germanium surface-barrier counter at 77°K and of a silicon counter at room temperature for N^{14} ions from the 63-in. cyclotron was reported. For the Si counter, the ratio R of pulse height to particle energy was constant from 15 to 25 Mev within experimental error ($\lesssim 1$ percent). These data were obtained by detecting N^{14} elastically scattered from Al^{27} at various angles. Other data were obtained for both counters by degrading the beam energy with absorbers. Within the accuracy with which the energy loss in the absorbers is known, R = constant from 3 to 24 Mev. The ratio of N^{14} to Po^{210} α-particle pulse height equals their energy ratio for both Ge and Si. Stability is excellent. The N^{14} peak position varied less than 1/2 percent over a 5-day period and no shift with counting rate was observed. The resolution for the scattered N^{14} is ~2 percent. Probably most of this spread is due to target nonuniformity, beam-energy spread, etc., since the resolution for 5.3 Mev particles is considerably better. The energy loss per ion pair is about 25 percent greater in Si than in Ge.

6302 SEMICONDUCTOR SURFACE BARRIER COUNTERS OF IMPROVED ENERGY RESOLUTION by J. L. Blankenship and C. J. Borkowski (Oak Ridge Natl. Lab.); Bull. Am. Phys. Soc., Ser. II, Vol. 5, p. 38 (A), Jan. 27, 1960

INSTRUMENTATION (Cont'd)

Gold silicon surface barrier counters which operate satisfactorily at room temperature have been reported previously. Silicon counters exhibit good energy resolution and pulse height-energy linearity if the alpha range does not exceed the barrier depletion region. Counters made from 50 ohm-cm material require at least 18 v bias for a 5.3 Mev alpha particle, but counters made from 150 ohm-cm material require only 4-1/2 v bias. The energy resolution of a 5 mm x 5 mm counter made from 50 ohm-cm material operating at room temperature was 45-50 kev (0.9 percent) full width at half-height for Po^{210} (5.3 Mev) alpha particles. Germanium surface barrier counters similar to those previously reported except operated at dry-ice temperatures, have given good energy resolution. A 4 mm x 4 mm counter made from 15 ohm-cm germanium gave a resolution of 1.2 percent for U^{233} (4.82 Mev) alphas, using a bias of 6 v.

6303 BEHAVIOR OF SEMICONDUCTOR COUNTERS by F. J. Walter, J. W. T. Dabbs, and L. D. Roberts (Oak Ridge Natl. Lab.); Bull. Am. Phys. Soc., Ser. II, Vol. 5, p. 38 (A); Jan. 1960

The behavior of semiconductor surface barrier counters with fast rise times, good energy resolution, and nearly linear energy response to short-range charged particles was explained by means of a simple model based on a Schottky-type barrier. This model predicts a maximum output voltage pulse corresponding to the charge liberated by ionizing radiation divided by the Schottky capacitance of the barrier. Higher purity of the semiconducting material corresponds to a thicker barrier, and thus to a larger output pulse. Minimum pulse rise time is obtained when the barrier thickness just exceeds the particle range. For n-type germanium counters, measurements of pulse heights, effective capacitances, and pulse rise times as functions of applied bias and sample purity are in agreement with this model, provided the bulk resistivity of the crystal is relatively low. However, at very low temperatures where the resistivity of germanium is large, the experimental evidence indicates that significant potential gradients can exist across the whole crystal rather than only in the narrow barrier region.

Conduction Counting of Alpha Particles Using Rhombic Sulfur - See 6113.

6304 DRIVE OF EZ-10 COUNTER TUBES BY TRANSISTORS [in French] by P. F. Gutmann and D. T. Jovanovic (Centre d'Etudes Nucleaires de Saclay); Nuc. Instr. Methods, Vol. 6, pp. 206-208, Jan. 1960

Two circuits suitable for the operation of the EZ-10 type counting tube are described. One is a monovibrator which is supplied by a high voltage transformer and which utilizes four transistors and operates up to a frequency of 250 cps with small power consumption. The other circuit works on the principle of a blocking oscillator, the transformer of which has an additional high voltage winding. The upper limit of the frequency used is imposed by the maximum power dissipated in the transistor.

Thermoelectric Energy Converters - See 6310 (New Product Section).

NEW PRODUCTS

6305 ELECTRON BEAM ZONE REFINER (MRC Manufacturing Corp., 47 Buena Vista Avenue, Yonkers, New York)

An electron beam floating zone apparatus for purifying, joining, and growing single-crystals of refractory metals such as molybdenum, tungsten, tantalum, vanadium, and columbium is announced. Specimens from 5" to 18" long and up to 3/16" in diameter can be used. The specimen compression and tension is controlled by a pushbutton-operated reversible motor control and the number and speed of passes can be controlled automatically. A specially designed filament control makes it possible to produce smooth, concentric single crystals of high purity.

6306 CRYSTAL WAFER SLICER (Fitchburg Engineering Corp., Fitchburg, Massachusetts)

A machine which can automatically slice a semiconductor ingot up to 4" in length after an operator positions the machine for the first cut is announced. Slices with thicknesses down to 0.007" ± 0.0005" can be cut. If desired for special work such as rate-grown crystals, the machine can be operated by hand. A controlled adjustable speed spindle drive allows for variations in diamond wheel size and quality and for differences in semiconductor materials.

6307 BARIUM TITANATE PIEZOELECTRICS (Erie Technical Ceramics, State College, Pennsylvania)

The barium titanate piezoelectric ceramic PZ 1011 is announced. This material which is available in a number of shapes, has the following characteristics: Young's modulus, 11.2×10^{10} new/m^2; dielectric constant, 700; dissipation factor, 0.65%; k_r, 0.27; k_{31}, 0.16, k_{33}, 0.51; d_{31}, -38×10^{-12} m/v; d_{33}, 120×10^{-12} m/v; g_{31}, -6.1×10^{-3} v-m/new; g_{33}, 19.3×10^{-3} v-m/new; frequency constant (radial), 1540 cyc-m; mechanical Q (24 hr.), 300; Curie temperature, 145°C; and maximum temperature, 125°C.

6308 GALLIUM ARSENIDE VARACTOR DIODE (Texas Instruments Inc., 13500 N. Central Expressway, Dallas, Texas)

A gallium arsenide diffused junction varactor diode designed for low-noise, narrow-band amplifier circuits is announced. The device, which is sealed in a reversible polarity, double ended ceramic microwave package, has a junction capacitance which varies from 0.1 pf minimum to 1.0 pf maximum at zero bias and a Q of 30 at 2 kmc and -2 volts. The device exhibits a cutoff frequency of 60 kmc at -2 volts and has an extremely low inductance with a 0.4 pf package capacitance measured at 100 kc.

6309 SOLID CIRCUIT BINARY MULTIVIBRATOR (Texas Instruments, Inc., 13500 N. Central Expressway, Dallas, Texas)

A microminiaturized binary multivibrator (type 502) constructed by incorporating resistors, capacitors, diodes, and transistors into a single high purity semiconductor wafer is announced. The unit is enclosed in a glass-to-metal hermetically sealed package measuring 0.250" x 0.120" x 0.030" and is suitable for use in binary counter, flip-flop, or shift register applications where miniaturization and reliability are extremely important. The solid circuit represents a 100:1 reduction in size over units containing conventional components.

6310 THERMOELECTRIC GENERATOR (General Instruments Corp., Thermoelectric Division, 245 Passaic Street, Newark, New Jersey)

A thermoelectric generator which utilizes semiconductor thermopiles to convert heat into electrical energy is announced.

The thermopiles are attached to the four sides of a combustion chamber and are heated by burning propane gas. The generator produces 5 watts of power, weighs 10 lbs., and is 12" high and 12" in diameter. It will run continuously for a year on approximately $20 worth of fuel. The many applications for the device include supplying power for radio communications, sea and air navigational aids, and industrial and scientific instrumentation in remote areas.

6311 SOLID STATE TRANSDUCERS (Statham Instruments, Inc., 12401 W. Olympic Blvd., Los Angeles 64, California)

A solid state transducer which has thermal characteristics equivalent to the standard tolerances of strain gage devices is announced. The thermal coefficient of sensitivity is on the order of 0.015 percent per degree Fahrenheit. The devices can be fabricated with a transfer function of 0.2 volt per volt of excitation. The output levels which are therefore possible make the instrument compatible with existing telemetry and industrial receiving instruments.

6312 TUNNEL DIODE CURVE TRACER (Trak Electronics Co., 48 Danbury Rd., Wilton, Conn.)

An instrument which is used with an oscilloscope to present the current-voltage characteristic of tunnel diodes throughout the negative resistance region is announced. A plug-in adapter range switch with a clip that holds all present tunnel diode packages is utilized. Additional plug-in adapters can be provided as new diode packages are developed. The plug-in range switch adjusts the scale factor of the transformation from current to voltage for the vertical deflection signal and simultaneously changes the shunt impedance on the tunnel diode. The accuracy of the conversion from current to voltage is ± 1%. The stray inductances are so small that diodes which can oscillate at 2 kmc are adequately damped. The source impedance is approximately one ohm and the oscilloscope curve is continuous throughout the negative resistance region.

6313 TRANSISTOR MOUNTING WASHERS (Reliance Mica Co., Inc., 341-351 39th St., Brooklyn 32, New York)

A series of mica transistor mounting washers is announced. The washers are available in a number of sizes and shapes (e.g. square, circular, rectangular, and diamond-shaped) with a wide variety of hole configurations and sizes. Microminiature film washers are also available for mesa type transistors.

6314 TV TUNERS (Philco Corp., Landsdale, Pa.)

Television tuners which have a noise figure that varies from a maximum of 4.6 db on the high channels to 3.3 db on the low channels and a power gain that varies from about 32 db on the high channels to about 45 db on the low channels are announced. This noise figure, which is superior to that of presently available tuners, is achieved by using extremely low noise micro-alloy diffused base germanium transistors which have noise figures less than 3.5 db at 200 mc.

6315 TRANSISTORIZED INPUT SCANNER (Non Linear Systems, Inc., Del Mar, California)

Completely transistorized input scanners for use with digital measuring equipment in such applications as a data logging system which automatically samples, digitizes, and records a large number of input signals are announced. The scanners, which are essentially automatic selector switches, can automatically scan 100 or 200 separate inputs, depending on the model. Special scanners which can scan up to 1000 inputs can be supplied. The scanner initiates the system operation at each channel by issuing a "start reading command" to the digital measuring instrument. At the end of each measuring and recording cycle the scanner switches to the next channel. The scanner can be set to scan a number of channels either once or continuously and has a switching time of about 20 ms. The system sampling rate is determined by the speed of the digital instrument and printer used with the scanner.

CONFERENCE PROGRAMS ABSTRACTED IN THIS ISSUE

International Congress on the Physics of the Solid State and Applications to Electronics and Telecommunications, Brussels, June 2-7, 1958 (Solid State Phys. Electronics and Telecommun.) (Academic Press, 1960)

1960 Annual Meeting of the American Physical Society, New York, Jan. 27-30, 1960 (Bull. Am. Phys. Soc., Ser. II, Vol. 5, Jan. 27, 1960)

SUBJECT INDEX

sorption:
by Phonon-Phonon Interaction, Acoustic 6212
in Germanium, Optical 6180
in Tellurium, Optical 6178
in Various Materials, Studies of Optical 6197
of Gases by Vacuum Evaporated Magnetic Films 6149
of Powder Phosphors 6188
oustic Absorption:
by Phonon-Phonon Interaction 6212
in Yttrium Iron Garnet 6147
tivation of Oxide Coated Cathodes 6252
sorbed Gases on Semiconductor Surfaces, Mass-Spectrometric Determination of 6046
sorption:
on Relaxation Processes in Germanium, Effect of Ion 6128
Techniques, Purification of Silicon Tetrachloride by 6017
kali Halides, Optical Absorption in 6197
kaline Earth Pyrophosphate Phosphors, Preparation of 6189
loys, Superconductivity of Dilute Indium-Mercury 6119
umina, Anomalous Dielectric Loss in 6081
uminum, Domain Distribution in Superconducting 6117
uminum:
and Arsenic in Germanium, Interaction Between 6018
Films,
Characteristic Energy Losses of Electrons in 6054
Electron Energy Dissipation in 6055
in Silicon, Solid Solubility of 6002
luminum Nitride Crystals, Synchesis of 6038
mplifiers,
Dielectric: Barium Titanate Thin Film 6042
Diode: 6223
Optimum Noise Performance of Tunnel- 6261
Light: Improved 6236
Magnetic-Transistor: Self Regulation in 6262
Paramagnetic: Ferromagnetic 6245
Parametric:
Periodically Distributed 6259
Using Galium Arsenide Diodes 6226
Thermistor: D-C 6295
Transistor:
Cascode 6260
High Input Impedance 6263
Linear 6254
Stereo 6275
Video 6258
nnealing of Gamma Ray Damage in Germanium 6056
ntiferromagnetism, Theory of Spin-Wave Interactions in 6136
ntiferromagnetic Structure Properties of Crystalline Compounds, Theory of 6137
ntiferromagnetic-Paramagnetic Transitions in Nickel Chloride and Cobalt Chloride 6148
ntiferromagnetism in $CoBr_2 \cdot 6H_2O$ 6158
ntimony, Solubility of Silicon in 6001
ntimony in Silicon, Solid Solubility of 6002
ntimony Telluride, Solid Solubilities of Indium Telluride and Thallium Telluride in 6003
ntimony Telluride Containing Group III Atoms, Electrical Properties of 6003
rc-Image Furnace for Growth of Single Crystals 6044
rsenic, Solubility of Germanium in 6001
rsenic and Aluminum in Germanium, Interaction Between 6018
udio Volume Compressors, Transistor 6276
utomatic Gain Adjustors, Transistor 6276
valanche Breakdown in Silicon Junctions 6221

Barium Complex System,
Ferrimagnetic Properties of a 6160
Ferroelectric Properties of a 6086
Structure of a 6082
Barium Titanate,
Crystal Symmetry of the Low Temperature Phase of 6084
Domain Patterns of 6084
Formation of Thin Films of 6042
Growth of Large Single Crystals of 6041
Piezoelectric Properties of 6307
Barium Titanate:
Crystals, Dynamic Permittivity Spectra of 6076
Piezoelectric Crystals 6307
Barkhausen Steps, Rectangular Hysteresis Loop Ferrites with 6141
Base Connection for Junction Transistors 6233
Beryllium, Elastic Constants of Single Crystals of 6210
Beryllium Oxide Flagpole Whiskers 6045
Biasing Transistors 6266
Bicrystals, Anisotropy of Carrier Transport in Semiconductor 6071
Binary Multivibrator Functional Unit 6305
Bismuth, Solubilify of Germanium in 6001
Bismuth, Solubility of Silicon in 6001
Bismuth Telluride, Solid Solubilities of Indium Telluride and Thallium Telluride in 6003
Bismuth Telluride Containing Group III Atoms, Electrical Properties of 6003
Blocking Oscillators for Driving Counter Tubes 6304
Bombardment Conductivity in Rhombic Sulfur 6113
Boron Content of Silicon 6013
Boron Nitride Electroluminescent Devices 6235
Boron Nitrides, Self-Consistent Calculations of Crystal Potential and Energy Bands of 6066
Breakdown:
in Cadmium Sulfide at Low Temperatures 6112
Point by Bias Methods, Increase of Transistor 6266

Cadmium, Solubility of Germanium in 6001
Cadmium Arsenide, Hall Field in 6121
Cadmium Indium Telluride,
Optical Properties of 6198
Purification and Crystal Growth of 6015
Cadmium Sulfide,
Breakdown in 6112
Electrical Properties of 6133
Evidence for Neutral Energy Transport in 6192
Fluctuations in 6192
Frequency Factor of Shallow Traps in 6095
Optical Absorption in 6197
Photoconductive Process in 6192
Cadmium Sulfide:
at Low Temperatures, Non-Ohmic Conductivity of 6112
Crystals, Dislocations in 6011
Due to Multiple Retrapping, Current Noise in 6095
-Mercury Sulfide, Preparation of Solid Solutions of 6030
Cadmium Tin Arsenide, Properties of 6108
Cadmium Tin Arsenide by Directional Freezing, Preparation of 6108
Carbon Films, Electron Energy Dissipation in 6055
Carrier:
Concentrations in Semiconductors, Transient 6099
Current in a Linearly Graded Drift Field, Minority 6102
Diffusion, Influence of Grain Boundaries on Minority 6073
Lifetime:
in P-Type Silicon 6104
in Semiconductors, Determination of 6093, 6223
Mobility in Silicon and Germanium, Field-Dependence of 6101
Recombination in Homopolar Semiconductors, Plasma Mechanism of 6092
Transport in Semiconductor Bicrystals, Anisotropy of 6071
Carriers,
Effects of Transient Sweep-out on the Decay Rate of Excess 6094
Influence of Grain Boundaries on the Diffusion of Minority 6073
Nonequilibrium Cyclotron Resonance of Negative Effective Mass 6122
Carriers:
in Germanium, Scattering of Hot 6109
in Semiconductors, Microwave Heating of 6090
Cartridge Impedance of Microwave Diodes 6217
Cascode Configuration, Analysis of the Transistor 6260
Cathodes, Mobile Acceptor Model for Oxide Coated 6252
Ceramics,
Ferroelectric Characteristics of Lead Zirconate Titanate 6085
Magnetic 6155
Cesium Antimony Films,
Electrical Resistivity of 6070
Formation of 6070
Cesium Chloride Whiskers from Aqueous Films, Growth of 6034
Characteristic Energy Losses in Metal Films 6177
Chromium Ions in:
Guanidine Alumn, Paramagnetic Resonance Spectrum of 6167
Potassium Cobalticyanide, Microwave Paramagnetic Resonance Spectrum of 6163
Ruby, Spin-Lattice Relaxation Times of 6169
Circulators, Strip Line L Band Compact 6243
Circulators at 70 and 140 KMC 6242
Cleaned Germanium Surfaces, A-C and D-C Field Effects on 6129
$CoBr_2 \cdot 6H_2O$, Antiferromagnetism in 6158
$CoBr_2 \cdot 6H_2O$ at Low Temperatures, Specific Heat of 6158
$CoCl_2 \cdot 6H_2O$, Specific Heat of 6148
Cobalt Particles, Nuclear Magnetic Resonance in Multidomain Ferromagnetic 6146
Cobalt Zinc Ferrite, X-Ray Study of Ferromagnetic Domains in 6139
Colemanite, Model for Switching and Polarization Reversal in 6087
Color Centers in Potassium Chloride, Effects of Plastic Deformation on X-Ray Production of 6005
Compacts, Effect of Pressure on the Seebeck Coefficient of Powder 6203
Compressors, Transistor Audio Volume 6276
Computer:
Diodes,
Gold-Doped Diffused Silicon 6225
Microwave Switching with 6265
Ferrites, Magnetic Polarity Reversal in 6142
Storage,
Magnetic Film Files for 6284
High Density File Drum for 6285
Switching Circuits Using Gallium Arsenide Diodes 6226
Computing System from a Basic Transistor Circuit, Construction of a 6278
Computers,
Applications of Magnetic Tape Recording to Digital 6283
Magnetic Drum Store for 6285, 6286
Solid State: Leprechaun 6279
Condensers, Barium Titanate Thin Film 6042
Conduction:
Band of Gallium Antimonide, Experimental Investigation of the 6060
Counting of Alpha Particles Using Rhombic Sulfur 6113

Conductivity, Theory of Electrical 6110
Conductivity:
in Rhombic Sulfur, Bombardment 6113
of Cadmium Sulfide at Low Temperatures, Non-Ohmic 6112
Configuration Interaction, Determination of Magnetic Properties of Solids Using 6134
Contamination of Silicon by the Crucible 6027
Control Systems, Theater Lighting 6296
Converters,
Infrared Quantum 6237
Pulse Height to Digital Signal 6290
Thermistor: D-C-A-C 6295
Thermoelectric Energy 6310
Transistor Pulse Height to Time 6274
Copper:
Gold Alloys, Thermoelectric Effects in 6205
in Indium Arsenide, Determination of 6014
in Semiconductors, Solubility of Interstitial 6020
Paramagnetic Resonance Spectrum of 6162
Corundum, Growth of Single Crystals of 6041
Counter Tubes, Blocking Oscillators for Driving 6304
Counters,
Solid Circuit Binary Multivibrators for Use in 6309
Surface Barrier 6301, 6302, 6303
Transistor Steering Circuits for Controlling Reversible 6281
Counters Using Multiple Diodes 6280
Counting of Alpha Particles Using Rhombic Sulfur, Conduction 6113
Critical Field of Superconducting Tin Film 6118
Crowe Cells, Superconducting 6289
Crucible, Contamination of Silicon by the 6027
Crucible Technique of Growing Single Crystals, Floating 6024
Crucibles, Growth of Silicon Crystals from Fused Quartz 6028
Crystal:
Imperfections in Silicon and Germanium, Study of 6007
Potential of Semiconductors 6066
Structure of 174 Layered Silicon Carbide 6023
Symmetry of the Low Temperature Phase of Barium Titanate 6084
Wafer Slicer 6306
Crystalline Fields in Solids, Theory of 6161
Crystals,
Houston's Method of Face-Centered Cubic 6004
Observation of Layer Structure in Dislocation Free Silicon 6012
Cuprous:
Halides, Energy Band Structure of the 6067
Oxide at High Temperatures, Thermal Emf of 6204
Current:
Amplification Factor, Frequency Dependence of 6231
Flow in Dielectric Layers Between Cylindrical Electrodes 6079
Flow in Insulators, Theory of 6098
Noise in Cadmium Sulfide Due to Multiple Retrapping 6095
Stabilizer for an Electromagnet, Transistor 6293
Curve Tracers, Tunnel Diode 6312
Cyclotron Resonance:
in Silicon, Millimeter 6123
of Negative Effective Mass Carriers, Nonequilibrium 6122

Damping of Germanium and Silicon Containing Impurity Oxygen, Mechanical 6213
Data Conversion Circuits for Earth Satellite Telemetry 6274
Decay of Excess Carriers in Semiconductors 6094
Defects, Low Temperature Thermal Resistivity of Point 6200
Defects on Lattice Thermal Conductivity, Influence of Point 6201
Degeneracy on Recombination Radiation in Germanium, Influence of 6181
De Haas-van Alphen Oscillations in the Hall Effect, Ettingshausen Effect, and Thermoelectric Power in Tin 6120
Delay Lines, Sonic 6282
Dendrites, Growth of Germanium 6033
Detectors, Microwave Video 6267
Dielectric:
Amplifiers, Barium Titanate Thin Film 6042
Constant:
Measurements in Germanium and Silicon 6075
of Mercury Selenide 6130
of a Mixed Titanate System 6088
Dispersion and Loss in Ferroelectrics, Microwave 6076
Layers Between Cylindrical Electrodes, Space Charge and Current Flow in 6079
Loss in Alumina, Anomalous 6081
Susceptibilities of Triglycine Sulfate 6043
Diffusion,
Dipole Mode of Minority Carrier 6214
Influence of Grain Boundaries on Minority Carrier 6073
Diffusion of:
Impurities in Gallium Antimonide 6069
Minority Carriers, Influence of Grain Boundaries on the 6073
Diode:
Amplifiers 6223
Counters, Multiple 6280
Curve Tracers, Tunnel 6312
Modulators 6223
Diodes,
Computer: Microwave Switching with 6265
Junction:
Computer 6225
Gallium Arsenide 6226
Silicon Carbide 6037
Transient Behavior 6223, 6224
Point Contact:
Dipole Mode of Minority Carrier Diffusion in 6214
Microwave Switches 6216
Tunnel 6181, 6219, 6220
Varactor: Gallium Arsenide 6226, 6308
Dipole Mode of Minority Carrier Diffusion 6214
Directional Freezing, Preparation of Cadmium Tin Arsenide by 6108
Dislocation:
Density in:
Silicon Crystals by an Optical Method, Determination of 6008
Silicon Crystals, Control of 6025
Structure of Sodium Chloride Whiskers 6009
Dislocations:
in Cadmium Sulfide Crystals 6011
in Silicon and Germanium by Infrared Microscopy, Localization of 6007
in Silicon Single Crystals 6010
in Tellurium, Recombination Through 6096
on the Strength of Sodium Chloride Whiskers, Effect of 6009
Displays, Electroluminescent Alphanumeric 6291
Dispersion in Ferroelectrics, Microwave Dielectric 6076
Distortions Produced by Ni^{2+} on Tetrahedral Lattice Sites 6174
Distribution Coefficients of Impurities in Indium Antimonide 6036
Domain:
Distribution in Superconducting Tin and Aluminum 6117
Patterns of Barium Titanate 6084
Double Refraction in Wurtzite-Type Binary Compounds 6194
Drift:
Field, Minority Carrier Current in a Linearly Graded 6102
Mobility as a Function of Concentration of Scattering Centers 6104
Transistors, Theory of 6102
Duplexing a Ruby Maser 6273

Effective Mass:
Carriers, Nonequilibrium Cyclotron Resonance of Negative 6122
of Carriers in:
Cadmium Indium Telluride 6198
Indium Antimonide 6130
Mercury Selenide 6130
Silicon 6065, 6123
Tin Selenide 6132
Efficiency of Thermoelectric Devices 6239
Elastic Constants of:
Single Crystals of Beryllium 6210
Triglycine Sulfate 6043
Electrical:
Conductivity of Gallium Antimonide, Effect of Pressure on 6068
Properties of:
Bismuth Telluride and Antimony Telluride Containing Group III Atoms 6003
Cadmium Sulfide 6133
Cadmium Tin Arsenide 6108
Gallium Antimonide 6060
Grain Boundary Layers in Germanium 6072
Tin Selenide 6132
Resistivity of a Film of Cesium Antimony 6070
Electrification of Sodium Chloride Crystals, Influence of X-Rays on 6078
Electroenhancement of X-Ray Excited Luminescence 6191
Electroluminescence, Irreversible Thermodynamics of Injection 6185
Electroluminescence under Pulsed Square-Wave Excitation 6184
Electroluminescent:
Alphanumeric Displays 6291
Devices, Boron Nitride 6235
Panels in Light Amplifiers, Use of 6236
Phosphors,
Fatigue in 6186
Microscopic Observations on 6182
Voltage Dependence and Particle Size Distribution of 6183
Zinc Sulfide, Ionic Properties of 6080
Electromagnet, Transistor Current Stabilizer for an 6293
Electromagnetic:
Properties of Insulators 6074
Waves, Hall Effect Device for 6195
Electron:
Beam Zone Refiner 6305
Capture by a Lattice Vacancy in Silicon 6097
Emission from Silicon Junctions, Hot 6222
Energy Dissipation and Secondary Emission for Solids, Relation Between 6055
Irradiated Silicon, Infrared Studies of 6050, 6051
Spin-Lattice Relaxation in Phosphorus-Doped Silicon 6171
Spin Resonance:
in Germanium, Effect of Strain on 6062
in Semiconducting Rutile 6170
Electronic Counters Using Multiple Diodes 6280
Electrons in:
an Electric Field, Wave Functions and Effective Hamiltonian for Bloch 6091
Germanium and Silicon, Spin-Lattice Interaction for Donor 6168
Semiconductors, Microwave Heating of 6090
Solids,
Interpretation of Characteristic Energy Losses of 6054
Range of 6053
Electroplated Base Connections for Junction Transistors 6233
Electroquenching of X-Ray Excited Luminescence 6191

ission:
from Silicon Junctions, Hot Electron 6222
from Tantalum, Field Dependence of Photoelectric 6193
Spectrum of a Germanium Tunnel Diode 6181
nergy:
Band Structure of:
Cuprous Halides 6067
Gallium Antimonide, Effect of Pressure on 6068
Indium Phosphide 6111
Semiconductors, Theory of 6066
Tellurium 6178
III-V Compounds, Theory of 6058
Band Theory to Include Self-Energy Corrections, Generalization of 6059
Converters, Thermoelectric 6310
Gap in Lead 6061
Levels in Gold-Doped Germanium 6064
Losses of Electrons in Solids, Interpretation of 6054
Transport in Cadmium Sulfide, Neutral 6192
ivalent:
Circuit Analysis of Generation-Recombination Noise in Semiconductors 6126
Circuits of Junction Transistors 6254, 6255, 6258
ium Single Crystals, Magnetic and Resistivity Properties of 6151
aki Diodes - See Tunnel Diodes
ch Rates, Correlation of Shape of Etch Hillock and Pits with 6047
rching of:
Silicon and Germanium, Ion Bombardment 6049
Silicon Carbide Surfaces, Differential 6048
Tellurium 6096
tingshausen-Nernst Effect in Tin, Oscillations in the 6120
vaporation of Antimony during Heat Treatment of Indium Antimonide, Preferential 6021
change Interaction on Paramagnetic Relaxation Times, Influence of 6172
pansion of Silicon, Thermal 6207

-Centers:
in Lithium Fluoride, Concentration of 6201
in Potassium Chloride, Growth of 6006
on Lattice Thermal Conductivity in Lithium Fluoride, Influence of 6201
raday Effect, Generation of Microwaves Using the 6195
tigue in Electroluminescent Phosphors 6186
rreeds to Switching Circuits, Application of 6246
rrimagnetic Properties of a Barium Complex System 6160
rrimagnets, Determination of Molecular Field Coefficients in 6140
rrite, X-Ray Study of Ferromagnetic Domains in Cobalt Zinc 6139
rrite:
Circulators at 70 and 140 KMC, Design and Characteristics of 6242
Devices,
High Power Effects in 6241
Non Reciprocal Single Crystal 6240
Slab Loaded Rectangular Waveguide, Modes of a 6249
rrites, High Power Ferromagnetic Resonance at X-Band in Polycrystalline 6144
rrites:
in Isolators, Prediction of High Power Performance of 6145
with Large Barkhausen Steps, Rectangular Hysteresis Loop 6141
rroelectric, Resonance Spectrum of a Paramagnetic 6167
rroelectric:
Characteristics of Lead Zirconate Titanate Ceramics 6085
Colemanite Crystals During Polarization Reversal, Displacement Current Transients Obtained from 6087
Materials, Paramagnetic Resonance in 6166, 6167
Monocrystals by Zone Recrystallization, Preparation of 6041
Properties of:
a Complex Barium System 6086
Triglycine Sulfate and Selenate, Effect of Hydrostatic Pressure on 6083
Properties, Structure of a System Having 6082
Rochelle Salt, Paramagnetic Resonance Spectrum of 6166
Triglycine Sulfate, Preparation of Large Single Crystals of 6043
Ferroelectrics,
Microwave Dielectric Dispersion and Loss in High-Permittivity 6076
Theory of the Electric Field Variation of Incremental Permittivity in Perovskite-Type 6077
Ferromagnetic:
Cobalt Particles, Nuclear Magnetic Resonance in Multidomain 6146
Domains in Cobalt Zinc Ferrite, X-Ray Study of 6139
Parametric Amplifier Performance, Theoretical Limitations to 6245
Properties, Structure of a System Having 6082
Resonance:
at X-Band in Polycrystalline Garnets and Ferrites, High Power 6144
Experiments at High Peak Power Levels, L-Band 6145
Line Widths in Gallium Substituted Yttrium Iron Garnet 6143
Structure Properties of Crystalline Compounds, Theory of 6137
Ferromagnetism, Theory of Spin-Wave Interactions in 6136
Ferromagnetism and Superconductivity, Coexistence of 6138
Field:
Dependence of Photoelectric Emission from Tantalum 6193
Effect, Relaxation Processes in the 6128
Effect:
in Germanium, Effect of Ion Adsorption on Relaxation Processes in the 6128
in Semiconductors, Frequency Dependence of the 6127
on Cleaned Germanium Surfaces, A-C and D-C 6129
Film Drum as a Computer Storage, High Density 6285
Films,
Characteristic Energy Losses in Metal 6177
Critical Fields of Thin Superconducting Tin 6118
Gas Absorption by Vacuum Evaporated Magnetic 6149
of Barium Titanate, Formation of Thin 6042
Filters for:
Pulsed Sinusoids, Transistorized Matched 6270
Multiplexed Telemetry 6269
Subaudio Frequencies, Transistor-Thermistor Low Pass 6269
Flagpole Whiskers, Beryllium Oxide 6045
Flame Fusion Process of Growing Single Crystals of Yttrium Iron Garnet 6040
Floating Crucible Technique of Growing Single Crystals 6024
Fluctuations:
from the Nonequilibrium Steady State 6125
in Cadmium Sulfide 6192
Free Radicals, Spin-Lattice Relaxation in 6172
Frequency:
Dependence of the Field Effect in Semiconductors 6127
Factor of Shallow Traps in Cadmium Sulfide 6095
Functional Unit, Binary Multivibrator 6309
Furnace for Growth of Single Crystals, Arc-Image 6044
Gallium, Solubility of Germanium in 6001
Gallium in Silicon, Solid Solubility of 6002
Gallium Antimonide,
Diffusion of Impurities in 6069
Effect of Impurities on the Electrical Properties of 6069
Effect of Pressure on the Electrical Properties of 6068
Electrical Properties of 6060
Energy Band Structure of 6068
Experimental Investigation of the Conduction Band of 6060
Gallium Arsenide,
Calculation of Mobility in N-Type 6107
Evidence for a Mobility Killer in 6105
Gallium Arsenide Varactor Diodes 6226, 6308
Galvanomagnetic Effects in Tin at Low Temperatures, Oscillations in 6120
Gamma Ray Damage in Germanium, Annealing of 6056
Garnet System, Magnetic Properties of a 6159
Garnets, High Power Ferromagnetic Resonance at X-Band in Polycrystalline 6144
Gas Absorption by Vacuum Evaporated Magnetic Films 6149
Gases Adsorbed on Semiconductor Surfaces, Mass-Spectrometric Determination of 6046
Generation of Microwaves Using the Faraday Effect 6195
Generation-Recombination Noise in Semiconductors 6126
Generators,
Hall 6298
Thermoelectric 6310
Transistor Ultrasonic-Frequency Power 6294
Germanium,
Acoustic Absorption by Phonon-Phonon Interaction in 6212
Annealing of Gamma Ray Damage in 6056
Cyclotron Resonance of Optically-Excited Holes in 6122
Dielectric Constant Measurements in 6075
Effect of Ion Adsorption on Relaxation Processes in 6128
Electrical and Optical Effects of Oxygen in 6179
Electrical and Photoelectrical Properties of Grain Boundary Layers in 6072
Energy Levels in Gold-Doped 6064
Field Dependence of Carrier Mobility in 6101
Influence of:
Degeneracy on Recombination Radiation in 6181
Grain Boundaries on the Diffusion of Minority Carriers in 6073
Interaction between Arsenic and Aluminum in 6018
Ion Bombardment Etching of 6049
Long Term Relaxation Processes in the Field Effect in 6128
Nernst Effect in 6206
Optical Absorption in 6180
Optical Studies of Impurities in 6196
Plasma Mechanism of Carrier Recombination in 6092
Recombination Centers in 6196
Scattering of Hot Carriers in 6109
Solid Solubilities of Impurity Elements in 6002
Spin-Lattice Interaction for Donor Electrons in 6168
Surface States on 6129
Thermal Conductivity of 6202
Germanium:
by Infrared Microscopy, Localization of Dislocations in 6007
by the Disproportionation of Germanium Di-iodide, Formation of Thin Films of 6032
Containing Impurity Oxygen, Mechanical Damping of 6213

Crystals with Constant Resistivity, Growth of 6024
Dendrites, Growth of 6033
from Effect of Strain on Electron Spin Resonance, Valley-Orbit Splitting in 6062
in Various Elements, Solubility of 6001
Liquidus Curves 6001
Surfaces, A-C and D-C Field Effect on Cleaned 6129
Surfaces, Mass-Spectrometric Determination of Gases Adsorbed on 6046
Glow Curves, Evaluation of Thermal Activation Energies from 6208
Gold-Doped Germanium, Energy Levels in 6064
Gold in Germanium, Optical Studies of 6196
Grain Boundaries on Minority Carrier Diffusion, Influence of 6073
Grain Boundary Layers in Germanium, Electrical and Photoelectrical Properties of 6072
Growth of:
Germanium Dendrites 6033
Hexagonal Zinc Sulfide Crystals by Controlled Cooling 6039
Indium Antimonide Crystals 6026, 6036
Indium Arsenide Crystals 6036
Semiconductor Crystals, Compensation Method for the 6029
Silicon Crystals, 6013
Contamination During 6027
Effects of Seed Rotation on the 6025
from Fused Quartz Crucibles 6028
Single Crystals, Arc-Image Furnace for 6044
Single Crystals with Constant Resistivity 6024
Yttrium Iron Garnet Single Crystals by the Flame Fusion Process 6040
Guanidine Alum, Paramagnetic Resonance Spectrum of Cr^{+++} in 6167
Gyrators, Single Crystal Ferrite 6240

Hall:
Coefficient of Cadmium Sulfide 6133
Constants of Gallium Antimonide, Effect of Pressure on 6068
Effect:
Device for Electromagnetic Waves 6195
in P-Type Silicon 6104
in Tin, Oscillations in the 6120
Magnetometer for Measuring Ion Beam Currents 6297
Microwave Mixer for Measuring Carrier Mobility 6100
Field in Cadmium Arsenide 6121
Generators, Indium Antimonide and Indium Arsenide 6298
Mobility of Holes in Silver Bromide 6106
Hamiltonian for Bloch Electrons in an Electric Field 6091
Hardware, Transistor 6313
Heat:
of Sublimation, Correlation of Solid Solubility with 6002
Treatment, Behavior of Indium Antimonide Surfaces during 6021
Heating of Carriers in Semiconductors, Microwave 6090
High Frequency Equivalent Circuits for Junction Transistors 6255
Holmium Metal, Low-Temperature Magnetic Remanence, Molecular Field, and Approach to Saturation of 6150
Hot:
Carriers in Germanium, Scattering of 6109
Electron Emission from Silicon Junctions 6222
Hydrogen in Semiconductors, Solubility of Interstitial 6020
Hydrothermal Preparation of Solid Solutions from II-VI Compounds 6030

Impedance of Microwave Diodes, Cartridge 6217
Impedances, Transistor Matching 6256
Impurities in:
Gallium Antimonide, Diffusion of 6069
Germanium, Optical Studies of 6196
Indium Arsenide, Determination of 6014
Semiconductors, Theory of Solubility of Interstitial 6020
Impurity:
Effects on Mobility in Silicon 6103
Ions in Silicon, Spin Resonance of 6164
Levels in P-Type Silicon, Internal 6065
Indium, Solubility of Silicon in 6001
Indium in Germanium, Solid Solubility of 6002
Indium Antimonide,
Distribution Coefficients of Impurities in 6036
Effective Mass of Electrons in 6130
Magnetoplasma Reflection in 6130
Spin-Resonance of Conduction Electrons in 6124
Zener Tunneling in 6131
Indium Antimonide:
Crystals, Growth of 6026, 6036
Devices Using the Faraday Effect 6195
Hall Effect Magnetometer 6297
Hall Generators 6298
Surfaces during Heat Treatment, Behavior of 6021
Indium Arsenide,
Determination of Copper and Lead in 6014
Evidence for a Mobility Killer in 6105
Thermal Conductivity of 6202
Indium Arsenide:
Crystals, Growth of Large 6036
Hall Generators 6298
Indium-Mercury Alloys, Superconductivity of Dilute 6119
Indium Phosphide,
Energy Band Structure of 6111
Evidence for a Mobility Killer in 6105
Piezoresistance in N-Type 6111
Indium Telluride in Bismuth Telluride and Antimony Telluride, Solid Solubility of 6003
Infrared:
Microscopy, Localization of Dislocations in Silicon and Germanium by 6007
Optical Properties of Semiconductors, Theory of 6176
Quantum Converters 6237
Studies of Electron Irradiated Silicon 6050, 6051
Injection Electroluminescence, Irreversible Thermodynamics of 6185
Insulators,
Electromagnetic Properties of 6074
Theory of Current Flow in 6098
Interaction Between Arsenic and Aluminum in Germanium 6018
Interface Curvature and Rotation Rate, Relation Between 6025
Intermetallic:
Compound Solid Solutions, Optical Properties of 6030
Compounds,
Hydrothermal Preparation of Two-Component Solid Solutions of 6030
Theory of the Band Structure of 6058
Interstitial Impurities in Semiconductors, Theory of Solubility of 6020
Ion:
Adsorption on Relaxation Processes in Germanium, Effect of 6128
Bombardment Etching of Silicon and Germanium 6049
Counters, Surface Barrier 6301
Drift in NP Junctions, Investigation of Lithium-Boron Pairing in Silicon by 6019
Ionic Properties of Electroluminescent Zinc Sulfide 6080
Ionization Energy of Traps, Method of Determining 6190
Ions, Sputtering of Semiconductors by Low Energy Argon 6052
Ions in Silicon, Spin Resonance of Impurity 6164
Iron, Specific Heat of High Purity 6199
Iron Oxide Particle Size on Nickel Ferrite Formation, Effect of 6155
Isolators,
Prediction of High Power Performance of Ferrites in 6145
Single Crystal Ferrite 6240

Junction Temperatures in Power Transistors, Transient 6230
Junctions,
Avalanche Breakdown in Silicon 6221
Hot Electron Emission from Silicon 6222
Investigation of Lithium-Boron Pairing in Silicon 6019
Thermoelectric Behavior of P-N 6218

Lattice:
Defects, Low Temperature Thermal Resistivity of 6200
Defects, Scattering of Phonons by 6200
Defects on Lattice Thermal Conductivity, Influence of 6201
Sites, Distortions Produced by Ni^{2+} on Tetrahedral 6174
Thermal Conductivity 6201
Layer Structure in Dislocation Free Silicon Crystals, Observation of 6012
Layered Silicon Carbide, Crystal Structure of 174 6023
Lead,
Energy Gap in 6061
Solubility of Silicon in 6001
Lead:
Films, Penetration of Magnetic Field Through 6061
in Germanium, Solid Solubility of 6002
in Indium Arsenide, Determination of 6014
Lead Selenide, Optical Absorption in 6197
Lead Sulfide, Optical Absorption in 6197
Lead Sulfide Photocells, Operating Characteristics of 6234
Lead Telluride, Thermal Properties of 6238
Lead Zirconate Titanate Ceramics, Ferroelectric Characteristics of 6085
Lifetime:
of Carriers in Semiconductors, Determination of 6093
of Carriers in Silicon 6104
in Tellurium Single Crystals, Effect of Dislocations of 6096
Light Amplifiers, Improvements in 6236
Lighting Control Systems, Theater 6296
Line Width Narrowing in Gallium Substituted Yttrium Iron Garnet 6143
Liquidus Curves for Germanium and Silicon 6001
Lithium-Boron Pairing in Silicon 6019
Lithium Fluoride, Influence of F-Centers on Lattice Thermal Conductivity in 6201
Loss in High-Permittivity Ferroelectrics, Microwave 6076
Luminescence,
Electroenhancement and Electroquenching of X-Ray Excited 6191
Experimental Studies of 6197

Magnetic:
Amplifier-Transistor Power Supply for Missile Applications 6292
Amplifiers for Magnetic Memory Sensing, Miniature High Frequency 6244
Anisotropy of Iron, Explanation of the Low-Temperature Behavior of 6135
Cartridges, Transistor Stereo Preamplifier and Tone Control for 6275
Ceramics 6155
Coupling in Crystalline Compounds 6137
Diagrams, Use of a Hall Generator for Static Interrogation of 6298
Disc Random Access Memories 6287

Drum Storage for Computers 6285, 6286
Field Measurements, Use of a Hall Generator for 6298
Fields in Superconductors, Measurement of 6116
Film Files for Computer Storage 6284
Film Storage, Cylindrical 6288
Memory Sensing Amplifiers 6244
Films, Gas Absorption by Vacuum Evaporated 6149
Polarity Reversal of Manganese-Magnesium and Nickel-Zinc Ferrites 6142
Properties of:
Erbium Single Crystals 6151
a Garnet System 6159
Manganese Chromite-Aluminates 6157
Solids Using Configuration Interaction, Determination of 6134
Recorders, Increasing the Band Width of 6277
Recording Tapes, Particle Interaction in 6250
Remanence of Holmium Metal, Low-Temperature 6150
Structure of:
Manganous Carbonate 6154
$(Mn, Co)_4C$ 6153
Susceptibility of $CoBr_2 \cdot 6H_2O$ 6158
Tape Recording:
Input, Transistor Automatic Gain Adjustors for 6276
to Digital Computers, Applications of 6283
gnetic-Transistor Amplifiers, Self Regulation in 6262
agnetization Curves for TiFe 6152
agnetometer, Indium Antimonide Hall Effect 6297
agnetoplasma Reflection in Solids 6130
anganese:
Chromite-Aluminates, Magnetic Properties of 6157
Chromite-Aluminates, Preparation of 6157
Cobalt Carbide, Preparation of the Ternary Alloy 6153
anganese-Magnesium Ferrite, Magnetic Polarity Reversal of 6142
anganous Carbonate, Magnetic Structure of 6154
anometers, Piezoelectric Oscillator 6299
aser,
Duplexing a Ruby 6273
1420 MC 6247
aser Behavior, Effect of Temperature and Concentration on 6248
asers, Use of Ruby in Millimeter Wave 6169
ass Transport During Whisker Growth, Mechanism for 6034
easurement of:
Carrier Lifetime Using Transients in Junction Diodes 6223
Gas and Vapor Pressures, Piezoelectric Oscillator Manometers for 6299
Ion Beam Currents 6297
Magnetic Fields in Superconductors 6116
the Nernst Effect 6206
Transistor Parameters 6258
Tunnel Diode Characteristics 6312
emories, Magnetic Disc Random Access 6287
emory:
Elements, Barium Titanate Thin Film 6042
Sensing, Miniature High Frequency Magnetic Amplifiers for Magnetic 6244
rcury Selenide,
Dielectric Constant of 6130
Effective Mass of Electrons in 6130
Magnetoplasma Reflection in 6130
tal:
Films, Characteristic Energy Losses in 6177
Oxide Powder Compacts, Effect of Pressure on the Seebeck Coefficient of 6203
tals, Range of Electrons in 6053
tals:
at Low Temperatures, Ultrasonic Attenuation and Dispersion in 6211
by Low Energy Argon Ions, Sputtering of 6052
Microelectronics 6257
Microminiaturization of Transistor Modules 6257
Microphonism in Microwave Crystal Mixers 6215
Microplasma Current Pulses in Silicon Junctions 6221
Microscopic Observations on Electroluminescent Phosphors 6182
Microwave:
Crystal Mixers, Microphonism in 6215
Dielectric Dispersion and Loss in Ferroelectrics 6076
Diode Cartridge Impedance 6217
Heating of Carriers in Semiconductors 6090
Methods of Measuring Mobility in Semiconductors 6100
Paramagnetic Resonance Spectrum of Chromium Ions in Potassium Cobalticyanide 6163
Switch, Theory of the Germanium Diode 6216
Switching with Computer Diodes 6265
Video Detectors 6267
Microwaves, Hall Effect Device for the Generation of 6195
Millimeter Cyclotron Resonance in Silicon 6123
Minority Carrier Diffusion, Dipole Mode of 6214
Missile Applications, Magnetic Amplifier-Transistor Power Supply for 6292
Mixers, Microphonism in Microwave Crystal 6215
Mobility:
in Cadmium Tin Arsenide, Electron 6108
in Germanium, Calculation of Lattice 6109
in N-Type Gallium Arsenide, Calculation of 6107
in P-Type Silicon, Drift 6104
in Semiconductors, Microwave Methods of Measuring 6100
in Silicon and Germanium, Field-Dependence of Carrier 6101
in Silicon, Effects of Impurity on 6103
Killer in Gallium Arsenide, Indium Arsenide, and Indium Phosphide, Evidence for a 6105
of Holes in Silver Bromide, Hall 6106
Modes of a Ferrite Slab Loaded Waveguide 6249
Modulators, Diode 6223
Molecular Field:
Coefficients in Ferrimagnets, Determination of 6140
of Holmium Metal, Low-Temperature 6150
Mounting Washers, Transistors 6313
Multivibrator, Transistor Monostable 6268
Multivibrator Functional Unit, Binary 6309
Multivibrators with Linear Control of Output Pulse Duration 6268

Nernst Effect, Methods of Measuring the 6206
Neutral Transport in Cadmium Sulfide 6192
Neutron Diffraction Study of the Magnetic Structure of $(Mn, Co)_4C$ 6153
Nickel:
Ferrite-Aluminate, Ferromagnetic Resonance Absorption in 6145
Ferrite Formation, Effect of Iron Oxide Particle Size on 6155
Ferrite, Thermomagnetic Behavior of Pure 6156
-Zinc Ferrite, Magnetic Polarity Reversal of 6142
$NiCl_2 \cdot 6H_2O$ at Low Temperatures, Specific Heat of 6148
Noise:
in Junction Transistors, Shot 6232
in Semiconductors,
Generation-Recombination 6126
Theory of 6125
Measurements, Evidence for Neutral Energy Transport in Cadmium Sulfide Obtained from 6192
Performance of Tunnel Diode Amplifiers, Optimum 6261
Non-Reciprocal Single Crystal Ferrite Devices 6240
Nuclear:
Magnetic Resonance in Multidomain Ferromagnetic Cobalt Particles 6146
Spin-Lattice Relaxation Via Quadrupole Coupling 6175
Techniques for Measuring Magnetic Field in Superconductors 6116

Optical:
Absorption:
in Germanium 6180
in Tellurium 6178
Method of Determining Dislocation Densities in Silicon Crystals 6008
Studies of Impurities in Germanium 6196
Properties of:
Cadmium Indium Telluride 6198
Semiconductors in the Infrared Region, Theory of 6176
Solids, Research on 6197
some II-VI Compound Solid Solutions 6030
Tin Selenide 6132
Transmissivity and Characteristic Energy Losses, Relation of 6177
Oscillations in the Thermomagnetic Effect in Tin at Low Temperatures 6210
Oscillator-Generator, Multi-Frequency 6272
Oscillators, Transistor:
Blocking 6304
Design of High Power 6264
Oxide Coated Cathodes, Mobile Acceptor Model for 6252
Oxides, Properties of Solid 6057
Oxygen, Mechanical Damping of Germanium and Silicon Containing 6213
Oxygen Dissolved in Silicon 6050, 6051
Oxygen in Germanium, Electrical and Optical Effects of 6179

Paramagnetic:
Ni^{2+} Ions, Calculation of the 3d-Electronic State of 6174
Relaxation Times, Influence of Exchange Interaction on 6172
Resonance:
in Ferroelectric Materials 6166, 6167
in Solids 6161
Lines, Spin-Flip Narrowing of 6162
of Cr^{+++} in Guanidine Alum 6167
of Fe^{3+} in Rutile 6165
of X-Irradiated Rochelle Salt 6166
Spectrum of Chromium Ions in Potassium Cobalticyanide, Microwave 6163
Spin Coupling 6173
Parametric:
Amplification Using Surface Space Charge Varactors 6251
Amplifier Performance, Theoretical Limitations to Ferromagnetic 6245
Amplifiers, Periodically Distributed 6259
Amplifiers Using Gallium Arsenide Diodes 6226
Particle Interaction in Magnetic Recording Tapes 6250
Peritectic Compounds, Zone Refining and Crystal Growth of 6015
Permittivity in Perovskite-Type Ferroelectrics, Theory of the Electric Field Variation of Incremental 6077
Perovskite-Type Ferroelectrics, Theory of the Electric Field Variation of Incremental Permittivity in 6077
Piezoelectric:
Moduli of Crystals of Triglycine Sulfate 6043
Oscillator Manometers 6299
Properties of Barium Titanate 6307
Properties of a Mixed Titanate System 6088
Substances, Search for New 6089
Piezoresistance:
in N-Type Indium Phosphide 6111
of Gallium Antimonide, Effect of Pressure on 6068
Phonon-Phonon Interaction, Acoustic Absorption by 6212

Phonon-Spin Interaction in Yttrium Iron Garnet 6147
Phonons by Lattice Defects, Scattering of 6200
Phosphors,
Boron Nitride Electroluminescent 6235
Electroluminescence under Pulsed Square-Wave Excitation in 6184
Fatigue in Electroluminescent 6186
Microscopic Observations on Electroluminescent 6182
Preparation of Alkaline Earth Pyrophosphate 6189
Quantum Efficiency and Absorption of Powder 6188
Range of Electrons in 6053
Voltage Dependence and Particle Size Distribution of Electroluminescent 6183
X-Ray Photoconductivity of Sulfide 6191
Photoconductive:
Detectors, Operating Characteristics of Lead Sulfide 6234
Processes in Cadmium Sulfide 6192
Photoconductivity, Experimental Studies of 6197
Photoconductivity:
in Cadmium Sulfide at Low Temperatures 6112
in Rhombic Sulfur 6113
of Sulfide Phosphors, X-Ray 6191
Photoconductors, Thermally Stimulated Currents in 6190
Photodevices, Operating Characteristics of Lead Sulfide 6234
Photoelectric :
Emission from Tantalum, Field Dependence of 6193
Properties of Grain Boundary Layers 6072
Plasma Mechanism of Carrier Recombination in Homopolar Semiconductors 6092
Plastic Deformation on X-Ray Production of Color Centers in Potassium Chloride, Effects of 6005
Point Contact Rectification, Dipole Mode of Minority Carrier Diffusion with Reference to 6214
Polar Directions, Growth of Indium Antimonide Crystals in Particular 6026
Polarization:
of Microwaves, Rotation of the Plane of 6195
Reversal in Colemanite 6087
Polytype in Silicon Carbide Whiskers, Determination of 6022
Potassium Chloride Crystals, Thermo-activation Energies in 6209
Potassium Chloride,
Effects of Plastic Deformation on X-Ray Production of Color Centers in 6005
Growth of F-Centers in 6006
Potassium Cobalticyanide, Microwave Paramagnetic Resonance Spectrum of Chromium Ions in 6163
Powder Compacts, Effect of Pressure on the Seebeck Coefficient of 6203
Powder:
Effects in Ferrite Devices, High 6241
Generators, Transistor Ultrasonic-Frequency 6294
Measurement, Use of a Hall Generator for 6298
Performance of Ferrites in Isolators, Prediction of High 6145
Supply for Missile Applications, Magnetic Amplifier-Transistor 6292
Switches, Comparison of Three and Four Layer Devices as 6227
Transistors, Transient Junction Temperatures in 6230
Preferential Evaporation of Antimony during Heat Treatment of Indium Antimonide 6021
Preparation of:
Alkaline Earth Pyrophosphate Phosphors 6189
Cadmium Tin Arsenide by Directional Freezing 6108
Cesium Antimony Films 6070
Crystals of Triglycine Sulfate 6043
Ferroelectric Monocrystals by Zone Recrystallization 6041
Manganese Chromite-Aluminates 6157
Semiconducting Materials, Compensation Method for the 6029
Silicon Carbide by the Periodic Shock Wave Technique 6031
Solid Solutions from II-VI Compounds, Hydrothermal 6030
the Ternary Alloy Manganese Cobalt Carbide 6153
Tin Selenide 6132
Pressure on the:
Electrical Properties of Gallium Antimonide, Effects of 6068
Ferroelectric Properties of Triglycine Sulfate and Selenate, Effect of Hydrostatic 6083
Seebeck Coefficient of Powder Compacts, Effect of 6203
Purification of:
Silicon Tetrachloride by Adsorption Techniques 6017
Silicon Tetraiodide by Zone Melting, Continuous Multi-Stage 6016
Purity Silicon, Assessment of High 6013
Pyrophosphate Phosphors, Preparation of Alkaline Earth 6189

Quadrupole Coupling, Nuclear Spin-Lattice Relaxation Via 6175
Quantum:
Converters, Infrared 6237
Efficiency of Powder Phosphors 6188
Quartz:
Crucibles, Growth of Silicon Crystals from Fused 6028
Delay Lines 6282

Radar Systems, Use of a Maser in 6273
Radiation:
in Germanium, Influence of Degeneracy on Recombination 6181
Monitors, Transistor 6300
Range of Electrons in Solids 6053
Recombination, Theory of Plasma 6092
Recombination:
Centers in Germanium 6196
Radiation in Germanium, Influence of Degeneracy on 6181
Through Dislocations in Tellurium 6096
Recorders, Increasing the Band Width of Magnetic 6277
Rectifiers, Fabrication of Silicon Carbide 6037
Refraction in Wurtzite-Type Binary Compounds, Double 6194
Relaxation:
Processes in the Field Effect 6128
Times, Influence of Exchange Interaction on Paramagnetic 6172
Times:
in Cadmium Indium Telluride 6198
in Ruby, Spin-Lattice 6169
Resistivity, Growth of Single Crystals with Constant 6024
Resistivity of:
Copper Gold Alloys 6205
Erbium Single Crystals 6151
Rhodochrosite, Magnetic Structure of 6154
Ringing Generators, Transistor Multi-Frequency 6272
Rochelle Salt, Paramagnetic Resonance of X-Irradiated 6166
Ruby, Spin-Lattice Relaxation Times in 6169
Rutile,
Electron-Spin Resonance in 6170
Paramagnetic Resonance of Fe^{3+} in 6165

Satellite Telemetry, Data Conversion Circuits for Earth 6274
Scanners, Transistor Input 6315
Scattering of:
Hot Carriers in Germanium 6109
Phonons by Lattice Defects 6200
Seebeck Coefficient of Powder Compacts, Effect of Pressure on the 6203
Secondary Emission and Electron Energy Dissipation in Solids, Relation Between 6055
Seed Rotation on Growth of Silicon Crystals, Effects of 6025
Segregation Coefficients of Impurities in Indium Antimonide 6036
Semiconducting Materials, Compensation Method of Preparing 6029
Semiconductor Bicrystals, Anisotropy of Carrier Transport in 6071
Semiconductors,
Changing Space Charge and Added Carrier Concentrations in 6099
Decay of Excess Carriers in 6094
Determination of Minority Carrier Lifetime in 6093
Frequency Dependence of the Field Effect in 6127
Generation-Recombination Noise in 6126
Microwave:
Heating of Carriers in 6090
Methods of Measuring Mobility in 6100
Plasma Mechanism of Carrier Recombination in Homopolar 6092
Theory of Solubility of Interstitial Impurities in 6020
Zener Tunneling in 6131
Semiconductors:
by Low Energy Argon Ions, Sputtering of 6052
in the Infrared, Theory of Optical Properties of 6176
Shift Registers, Solid Circuit Binary Multivibrators for Use in 6309
Shot Noise in Junction Transistors 6232
Signal Converters, Pulse Height to Digital 6290
Signaling, Use of a Hall Generator for Contactless 6298
Silicon,
Assessment of High Purity 6013
Comparison of Drift Mobility, Carrier Lifetime and Hall Effect Measurement in 6104
Dielectric Constant Measurements in 6075
Effective Masses in 6065, 6123
Effects of Impurities on Mobility in 6103
Electron Capture by a Lattice Vacancy in 6097
Field Dependence of Carrier Mobility in 6101
Hot Electron Emission from 6222
Influence of Grain Boundaries on the Diffusion of Minority Carriers in 6073
Infrared Studies of Electron Irradiated 6050, 6051
Internal Impurity Levels in P-Type 6065
Ion Bombardment Etching of 6049
Lithium-Boron Pairing in 6019
Millimeter Cyclotron Resonance in 6123
Oxygen Dissolved in 6050, 6051
Plasma Mechanism of Carrier Recombination in 6092
Solid Solubilities of Impurity Elements in 6002
Spin-Lattice:
Interaction for Donor Electrons in 6168
Relaxation in Phosphorus-Doped 6171
Spin Resonance:
of Impurity Ions in 6164
of Transition Metals in 6164
Thermal:
Conductivity of 6202
Expansion of 6207
Silicon:
by Infrared Microscopy, Localization of Dislocations in 6007
by the Crucible, Contamination of 6027
by Zone Purification of Silicon Tetraiodide, Preparation of Transistor Grade 6039

Containing Impurity Oxygen, Mechanical Damping of 6213
Crystals,
Control of Dislocation Density of 6025
Determination of Dislocation Densities in 6008
Effects of Seed Rotation on the Growth of 6025
Observation of Layer Structure in Dislocation Free 6012
in Various Elements, Solubility of 6001
Junctions,
Avalanche Breakdown in 6221
Hot Electron Emission from 6222
Liquidus Curves 6001
Single Crystals,
Dislocations in 6010
Growth of 6013
Surfaces, Mass-Spectrometric Determination of Gases Adsorbed on 6046
icon Carbide, Crystal Structure of 174 Layered 6023
.con Carbide:
Crystals, Preparation of 6031, 6037
Rectifiers, Fabrication of 6037
Surfaces, Properties of 6048
Whiskers, Determination of Twist and Polytype in 6022
icon Tetrachloride by Adsorption Techniques, Purification of 6017
icon Tetraiodide:
by Zone Melting, Continuous Multi-Stage Purification of 6016
Preparation of Transistor Grade Silicon by Zone Purification of 6035
lver:
Bromide, Hall Mobility of Holes in 6106
Halides, Optical Absorption in 6197
icers, Crystal Wafer 6306
dium Chloride:
Crystals,
Influence of X-Rays on Electrification of 6078
Thermo-activation Energies in 6209
Whiskers, Dislocation Structure, Formation and Strength of 6009
lid:
Circuit Binary Multivibrators 6309
Oxides, Properties of 6057
Solubilities:
of Impurity Elements in Germanium and Silicon 6002
of Indium Telluride and Thallium Telluride in Bismuth Telluride and Antimony Telluride 6003
Solution in the System CIS-YIG 6159
Solutions, Optical Properties of Some II-VI Compounds 6030
Solutions:
in a Garnet System 6159
of II-VI Compounds, Hydrothermal Preparation of 6030
State Transducers 6311
lids,
Interpretation of Characteristic Energy Losses of Electrons in 6054
Magnetoplasma Reflection in 6130
Paramagnetic Resonance in 6161
Range of Electrons in 6053
Relation Between Electron Energy Dissipation and Secondary Emission in 6055
Research on Optical and Electrical Properties of 6197
lubilities of:
Germanium and Silicon in Various Elements 6001
Impurity Elements in Germanium and Silicon, Solid 6002
Indium Telluride and Thallium Telluride in Bismuth Telluride and Antimony Telluride, Solid 6003
Interstitial Impurities in Semiconductors, Theory of 6020
Solution in the System CIS-YIG, Solid 6159
Sonic Delay Lines 6282
Space Charge:
in Dielectric Layers Between Cylindrical Electrodes 6079
in Semiconductors, Transient 6099
Layer Varactors 6251
Specific Heat, Method of Determining 6199
Specific Heat of:
$CoBr_2 \cdot 6H_2O$ at Low Temperatures 6158
High Purity Iron 6199
$NiCl_2 \cdot 6H_2O$ and $CoCl_2 \cdot 2H_2O$ at Low Temperatures 6148
Some Magnetic Materials 6148
Spin Coupling in Crystals with Two Paramagnetic Species 6173
Spin-Flip Narrowing of Paramagnetic Resonance Lines 6162
Spin-Lattice:
Interaction for Donor Electrons in Germanium and Silicon 6168
Relaxation:
in Free Radicals 6172
in Phosphorus-Doped Silicon, Electron 6171
in Semiconducting Rutile 6170
Times in Ruby 6169
Via Quadrupole Coupling, Nuclear 6175
Spin-Phonon Interaction in Yttrium Iron Garnet 6147
Spin Resonance:
in Rutile 6165
of Conduction Electrons in Indium Antimonide 6124
of Impurity Ions in Silicon 6164
Spin-Wave Interactions in Ferro- and Antiferromagnetism, Theory of 6136
Sputtering of Semiconductors by Low Energy Argon Ions 6052
Stabilizer for an Electromagnet, Transistor Current 6293
Steady State, Fluctuation from the Nonequilibrium 6125
Steering Circuits for Controlling Reversible Counters 6281
Storage, Cylindrical Magnetic Film 6288
Storage:
Elements, Low Temperature 6289
Time in Junction Transistors,
Measurement of 6258
Prediction of 6253
Strength of Sodium Chloride Whiskers, Effect of Dislocations on the 6009
Structure of:
a System Having Ferroelectric and Ferromagnetic Properties 6082
Silicon Carbide Surfaces 6048
Suhl Instability in Ferrite Devices 6241
Sulfide Phosphors, X-Ray Photoconductivity of 6191
Sulfur, Photoconductivity in Rhombic 6113
Surface:
Barrier Counters 6301, 6302, 6303
States on Germanium 6129
Surfaces,
A-C and D-C Field Effect on Cleaned Germanium 6129
Properties of Silicon Carbide 6048
Surfaces during Heat Treatment, Beavhior of Indium Antimonide 6021
Superconducting:
Alloys, Thermodynamic Treatment of Dilute 6114
Crowe Cells 6289
Tin Film, Critical Fields of Thin 6118
Superconductivity:
and Ferromagnetism, Coexistence of 6138
of Dilute Indium-Mercury Alloys 6119
Superconductors,
Intermediate State in Cylindrical 6117
Measurement of Magnetic Fields in 6116
Transport Properties of 6115
Switches,
Theory of Germanium Diode Microwave 6216
Transistor-Diode Television Master 6271
Switching:
Characteristics of Junction Transistors 6229
Circuits, Application of Ferreeds to 6246
Mechanism in Ferroelectric Colemanite Crystals 6087
with Computer Diodes, Microwave 6265
Symmetry of the Low Temperature Phase of Barium Titanate, Crystal 6084
Synthesis of Aluminum Nitride Crystals 6038

Tantalum, Field Dependence of Photoelectric Emission from 6193
Telemetry,
Data Conversion Circuits for Earth Satellite 6274
Filters for Multiplexed 6269
Telephone Ringing Generators, Transistor 6272
Television:
Master Switchers, Transistor-Diode 6271
Tuners, Transistor Low Noise 6314
Tellurium,
Energy Band Structure of 6178
Optical Absorption in 6178
Recombination Through Dislocations in 6096
Thallium, Solubility of Germanium in 6001
Thallium Telluride in Bismuth Telluride and Antimony Telluride, Solid Solubility of 6003
Thallous Halides, Optical Absorption in 6197
Theater Lighting Control Systems 6296
Thermal:
Activation Energies:
from Glow Curves, Evaluation of 6208
in Sodium Chloride and Potassium Chloride Crystals 6209
Conductivity:
in Lithium Fluoride, Influence of F-Centers on Lattice 6201
of Germanium, Silicon and Indium Arsenide 6202
Detection Elements, Barium Titanate Thin Film 6042
Expansion of Silicon 6207
Properties of Lead Telluride 6238
Resistivity of Point Defects, Low Temperature 6200
Thermally Stimulated Currents in Photoconductors 6190
Thermionic Behavior of P-N Junctions 6218
Thermistor:
Choppers, D-C Amplifiers Using 6295
D-C-A-C Converters 6295
Thermoelectric:
Behavior of P-N Junctions 6218
Devices, Efficiency of 6239
Effects in Copper Gold Alloys 6205
Energy Convertors 6310
Power in Tin, Oscillations in the 6120
Properties of:
Cadmium Tin Arsenide 6108
P-N Junctions 6218
Thermo-emf of Cuprous Oxide at High Temperatures 6204
Thermoluminescence of Zinc Sulfide Single Crystals 6187
Thermomagnetic:
Behavior of Pure Nickel Ferrite 6156
Effect in Tin at Low Temperatures, Oscillations in the 6210
Thin Films of Germanium by the Disproportionation of Germanium Di-iodide, Formation of 6032
3d Metals, Theory of Magnetism in 6137
Time Delay, Transistor Linear 6268
Tin,
Domain Distribution in Superconducting 6117
Solubility of:
Germanium in 6001
Silicon in 6001

Tin:
at Low Temperatures, Oscillations in the Thermomagnetic Effect in 6210
Films, Critical Fields of Thin Superconducting 6118
Selenide,
Electrical and Optical Properties of 6132
Preparation of 6132
Titanate System, Piezoelectric Properties of a Mixed 6088
Titanium Dioxide,
Electron-Spin Resonance in 6170
Growth of Single Crystals of 6044
Paramagnetic Resonance of Fe^{3+} in 6165
Titanium Ion, Magnetization Curves for 6152
Transducers, Solid State 6311
Transient:
Behavior of Junction Diodes 6223, 6224
Junction Temperatures in Power Transistors 6230
Response of Junction Transistors 6253
Sweep-out on the Decay Rate of Excess Carriers, Effects of 6094
Transistor:
Behavior at High Frequencies 6255
Bias Method 6266
Cascode Configuration, Analysis of 6260
Current Stabilizer for an Electromagnet 6293
Driving Circuits for Counter Tubes 6304
Equivalent Circuits 6254
Input Scanners 6315
Linear Time Delay 6268
Logic Circuits, Direct Coupled 6279
-Magnetic Amplifier Power Supply for Missile Applications 6292
Matched Filter for Pulsed Sinusoids 6270
Matching Impedances 6256
Modules, Microminiaturization of 6257
Mounting Washers 6313
Parameters, Measurement of 6258
Pulse Height to Digital Signal Converters 6290
Radiation Monitors 6300
Stereo Preamplifier and Tone Control for Magnetic Cartridges 6275
Thermistor Filter for Subaudio Frequencies, Low Pass 6269
Ultrasonic Frequency Power Generators 6294
Transistors, Junction:
Base Connection for 6233
Drift 6102
Frequency Dependence of Current Amplification Factor in 6231
Frequency Dependence of Noise in 6231
Power 6230
Prediction of Storage Time in 6253
Saturation Condition 6229
Shot Noise in 6232
Storage Time in 6253
Theory of Drift 6102
Three and Four Layer Power Switches 6227
Transient Temperatures 6230
Transport Factors 6228
Transition Metals in Silicon, Spin Resonance of 6164
Transport:
Factors of Junction Transistors 6228
in Cadmium Sulfide, Neutral 6192
Properties of Superconductors 6115
Trapping, Current Noise in Cadmium Sulfide Due To Multiple Re- 6095
Traps, Method of Determining Ionization Energy of 6190
Traps in:
Cadmium Sulfide, Frequency Factor of Shallow 6095
Silicon, Electron Capture by 6097
Triglycine Sulfate,
Elastic Constants of 6043
Effect of Hydrostatic Pressure on the Ferroelectric Properties of 6083
Preparation and Properties of 6043
Tunnel Diode, Emission Spectrum of a 6181
Tunnel Diode:
Amplifiers, Optimum Noise Performance of 6261
Curve Tracer 6312
Tunnel Diodes, 6219
Pressure Dependence of the Characteristics of 6220
Tunneling in Semiconductors, Zener 6131
Twist in Silicon Carbide Whiskers, Determination of 6022

Ultrasonic:
Attenuation and Dispersion in Metals at Low Temperatures 6211
Frequency Power Generators Using Transistors 6294

Vacancy in Silicon, Electron Capture by a Lattice 6097
Varactor Diodes, Gallium Arsenide 6226, 6308
Varactors Using Space Charge Layers 6251
Video:
Amplifiers, Transistor 6258
Detectors, Microwave 6267

Wafer Slicer, Crystal 6306
Washers, Transistor Mounting 6313
Wave Functions for Bloch Electrons in an Electric Field 6091
Whisker Growth, Mechanism for Mass Transport During 6034
Whiskers,
Beryllium Oxide Flagpole 6045
Determination of Twist and Polytype in Silicon Carbide 6022
Effect of Dislocations on the Strength of Sodium Chloride 6009
Wurtzite-Type Binary Compounds, Double Refraction in 6194

X-Ray Photoconductivity of Sulfide Phosphors 6190

Yttrium Gadolinium Garnets, Ferromagnetic Resonance Absorption in 6145
Yttrium Iron Garnet,
Spin-Phonon Interaction in 6147
Line Width Narrowing In Gallium Substituted 6143
Yttrium Iron Garnet:
by the Flame Fusion Process, Growth of Single Crystals of 6040
Circulators 6243

Zener Tunneling in Semiconductors 6131
Zinc, Solubility of:
Germanium in 6001
Silicon in 6001
Zinc in Germanium, Solid Solubility of 6002
Zinc Sulfide, Ionic Properties of Electroluminescence 6080
Zinc Sulfide:
Crystals Grown from the Melt, Properties of 6039
Phosphors, Voltage Dependence and Particle Size Distribution of Electroluminescent 6183
Single Crystals, Thermoluminescence of 6184
Zinc Sulfide-Cadmium Sulfide, Preparation of Solid Solutions of 6030
Zinc Sulfide-Mercury Sulfide, Preparation of Solid Solutions of 6030
Zone:
Melting, Continuous Multi-Stage Purification of Silicon Tetraiodide by 6016
Purification of Silicon Tetraiodide, Preparation of Transistor Grade Silicon by 6030
Recrystallization, Preparation of Ferroelectric Monocrystals by 6041
Refiner, Electron Beam 6305
Refining Equipment, Growth of Peritectic Compounds Using 6015

AUTHOR INDEX

uham, R. P. 6255
ns, E. N. 6190
amiano, A. 6039
ovich, E. I. 6224
ngton, R. E. 6025
urg, H. 6184
sandrov, K. S. 6043
egaokar, V. 6074
ell, H. 6187
gast, C. L. 6210
Jr., W. B. 6166
ld, E. 6107
an, J. O. 6163
a, T. 6056
, M. 6039

nowski, A. E. 6225
n, K. S. 6120
er, P. K. 6174
w, H. M. 6100
rd, R. D. 6075
, L. F. 6156
N. W. 6295
ki, G. 6124
, W. 6254
Zvi, A. 6209
kin, A. B. 6275
ard, M. 6007
lone, N. P. 6034
, D. D. 6004
a, A. B. 6211
emore, J. S. 6046, 178
e, J. 6105
kenship, J. L. 6301, 6302
om, M. 6268
s, M. D. 6208
nberg, P. H. 6118
o, Z. 6093
le, A. G. 6256
ger, B. 6247
aks, B. I. 6069
mel, H. E. 6147, 212
en-Bruevich, V. L. 092
owski, C. J. 6302
er, C. S. 6088
rth, R. M. 6139
snaw, S. E. 6027
er, A. A. 6208, 209
non, P. 6234
ler, A. D. 6249
gs, G. R. 6244
k, E. G. 6167
ks, H. 6075
hy, J. J. 6095, 192
n, F. C. 6106
n, J. 6100
on, K. J. 6065

oos, F. P. 6153
onel, M. 6229
ona, M. 6075
son, R. D. 6281
Jr., W. J., 6135
uthers, P. 6200
on, D. N. 6274
er, D. 6165
npion, F. C. 6113
nplin, K. S. 6126
g, H. C. 6037
g, K.K.N. 6261
ers, M. L. 6084
ette, E. R. 6231
epanov, V. I. 6176
naya, N. S. 6128
er, P. F. 6170
nko, R. M. 6050
it, M. P. 6285
enger Jr., T. R. 6155
, P. L. 6278
; H. 6156

Cochran, J. F. 6116
Conwell, E. M. 6109
Cook, J. S. 6015
Corbett, J. W. 6050, 6051
Craven, J. H. 6267
Croft, W. J. 6141
Cutler, M. 6218
Czyzak, S. J. 6011

Dabbs, J. W. T. 6303
Damon, R. W. 6245
Daniels, J. M. 6162
Danielson, G. C. 6199
Davis Jr., L. 6243
Daw, A. N. 6228
Dean, P. J. 6113
DeBolt, H. E. 6300
Debye, P. P. 6064
Dejardin, G. 6191
De La Rue, R. E. 6044
DellaTorre, E. 6250
Detwiler, D. P. 6081
Deutschbein, O. 6007
Dhawan, S. K. 6174
Diamond, H. 6076, 6077
Diemer, G. 6236
Dillon Jr., J. A. 6048, 6049
Dransfeld, K. 6212, 6147
Dutton, D. 6197

Eckhart, G. 6008
Economos, G. 6155
Edwards, D. F. 6198
Edwards, P. L. 6045, 6157
Ekiss, J. A. 6263
Ensley, D. 6290
Eriksen, W. T. 6184
Erlbach, E. 6061
Eshbach, J. R. 6245

Fang, P. H. 6082
6086, 6160
Farach, H. A. 6162
Feher, G. 6062
Feiner, A. 6246
Feldman, G. 6042, 6053
Figielski, T. 6073
Filimonov, A. A. 6089
Fischler, A. S. 6121
Flock Jr., P. L. 6270
Folen, V. J. 6140
Forstat, H. 6158
Forster, J. H. 6225
Franklin, D. P. 6283
Frauenfelder, H. 6116
Friedberg, S. A. 6148
Fritts, R. W. 6238
Furuoya, T. 6010, 6012

Garber, M. 6158
Garrett, C. G. B. 6251
Garver, R. V. 6216, 6217
Garwin, R. L. 6061
Gashorov, G. 6030
Gatos, H. C. 6026
Geller, S. 6159
Gerson, R. 6085
Gilleo, M. A. 6159
Gilmartin, M. J. 6279
Githens, J. A. 6279
Gleason, F. R. 6149
Glover, A. C. 6287
Goldman, M. V. 6301
Goldsborough, J. P. 6172
Goodwin, F. E. 6273
Goorissen, J. 6024
Goss, A. J. 6025
Gossard, A. C. 6146
Gossick, B. 6214
Grannemann, W. W.
6230, 6290
Green, J. J. 6144
Green, M. 6099
Green, R. W. 6151
Greiner, J. H. 6149
Grenier, C. G. 6120
Griefer, A. P. 6141
Gubanov, A. I. 6058
Gumnick, J. L. 6193
Gutmann, P. F. 6304
Gutorov, Yu. A. 6069

Haering, R. R. 6190
Halbert, M. L. 6301
Halden, F. A. 6044
Hall, R. N. 6219, 6233
Halperin, A. 6187,
6208, 6209
Halsted, R. E. 6133
Hamasaki, J. 6259
Hamburger, T. 6291
Hamilton, D. R. 6022
Haneman, D. 6021
Hanson, R. C. 6106
Happel Jr., R. J. 6045
Hardies, C. E. 6262
Harman, C. G. 6057
Heasell, E. L. 6104
Heikes, R. R. 6239
Heller, G. S. 6123, 6242
Henisch, H. K. 6280
Henkels, H. W. 6227
Henry, W. E. 6150
Hensley, E. B. 6252
Hermann, F. 6067, 6122
Hersh, H N. 6005
Hilsum, C. 6297
Hoffman, G. R. 6288
Hormats, E. I. 6167
Hornig, A. 6171
Howald, B. W. 6272
Howard, N. R. 6013
Hrostowski, H. J. 6179
Hu, K. C. 6244

Irving, B. A. 6047
Ishii, Z. 6012
Ittner III, W. B. 6118

Jackson, G. E. 6278
James, J. R. 6260
Janin, J. 6191
Jennings, V. J. 6014
Johnson, L. F. 6196
Jona, F. 6083
Jones, R. D. 6290
Jones Jr., R. E. 6114
Jovanovic, D. T. 6304
Juenker, D. W. 6193

Kadanoff, L. P. 6115
Kaiser, W. 6179
Kane, E. O. 6131
Kanter, H. 6055
Karstensen, F. 6024
Kawaji, S. 6129
Kebler, R. W. 6040
Keffer, F. 6194
Keith, W. W. 6282
Kennedy, D. P. 6102
Kevane, C. J. 6221
Keyes, R. W. 6068
Kiel, A. 6173
Kilburn, T. 6288
Klasens, H. A. 6236
Klein, C. A. 6064
Kleinman, L. 6066
Knight, L. 6285
Ko, W. H. 6223
Kobelev, V. V. 6142
Kobuke, Y. 6188
Kohn, W. 6174
Kohra, K. 6012
Konstantinova, V. P. 6043
Kostelich, J. F. 6272
Kowalchik, M. 6001
Kozlovskaya, V. M. 6046
Kramarov, O. P. 6041
Kremheller, A. 6030, 6182
Kristianpoller, N. 6209
Kuhrt, F. 6298
Kurokawa, K. 6259
Laegreid, N. 6052
Lampert, M. A. 6098
Larach, S. 6235
Lavine, M. C. 6026
Lax, B. 6065, 6130
Lax, M. 6125
LeCraw, R. C. 6143
Lederhandler, S. 6008
Legvold, S. 6151
Lehmann, W. 6183
Levine, A. K. 6030
Lewis, H. R. 6116
Logan, R. A. 6103
Lommasson, T. 6290
Langerot, C. D. 6290
Lovell, C. A. 6246
Low, W. 6161
Lowen, J. 6226
Lowry, T. N. 6246
Ludwig, G. W. 6164
Lyashenko, V. I. 6128

Macklem, F. S. 6296
Maiman, T. H. 6248
Maissel, L. 6207
Mandel, M. 6172
Mapother, D. E. 6116
Markham, J. J. 6005
Marsden, B. 6271
Martin, P. C. 6115
Mason, D. R. 6015
Masuda, I. 6188
Matare, H. F. 6071, 6072
Matsumura, T. 6038
Matthias, B. T. 6138
McCaldin, J. O. 6018
McClure, D. S. 6067
McDonald, R. S. 6051
McKinney, J. E. 6088
Mendlowitz, H. 6177
Merz, K. M. 6139
Mieher, R. L. 6175
Milano, U. 6243
Miller, C. E. 6159
Miller, E. C. 6276
Miller, S. L. 6220
Mitchell, D. L. 6132
Mitchell, P. V. 6006
Miyake, K. 6070
Moates, G. H. 6016
Mochan, I. V. 6206
Mokrytzki, B. 6292
Moody, P. L. 6026
Mooney, R. W. 6189
Moore, R. A. 6211
Morita, A. 6097
Moulton, G. C. 16166
Moulton, W. G. 6166
Mudar, J. 6186
Murphy, J. C. 6163

Nadashkevich, I. I. 6142
Nanavati, R. P. 6253, 6268
Nash, F. 6165
Nathan, M. I. 6220
Nevitt, M. V. 6152
Newman, R. C. 6032
Nomura, K. C. 6096, 6178
Nran'yan A. A. 6058
Nudelman, S. 6186

Oguchi, T. 6136
Oka, M. 6056
O'Kane, D. 6198
Okaya, A. 6165
Okkerse, B. 6024
Oka, M. 6056
Okumura, K. 6265
Oman, R. M. 6048, 6049
Omura, K. 6056
Onstad, R. C. 6269

Pace, J. H. 6169
Pacey, D. J. 6299
Pake, G. E. 6172
Pan, P. M. 6160
Pankove, J. I. 6181
Paranjape, B. V. 6090
Paton, F. 6104
Paul, D. I. 6134
Paul, W. 6075
Peacock, R. N. 6116
Pell, E. M. 6019
Peters, A. J. 6103
Pfann, W. G. 6029, 6251
Phillips, J. C. 6066, 6180
Pickart, S. J. 6154
Piper, W. W. 6133
Pohl, R. O. 6201
Pollak, M. 6068
Pope, A. 6290
Portis, A. M. 6146
Pratt Jr., G. W. 6059
Prior, A. C. 6101
Prugh, T. A. 6257

Rado, G. T. 6140
Raney, W. P. 6212
Ransom, P. 6028
Ratner, M. 6080
Rauch, C. J. 6123
Rediker, R. H. 6226
Reeber, M. D. 6119
Reed, B. 6072
Reese, J. D. 6230
Reynolds, D. C. 6011
Reynolds, J. M. 6120
Rez, I. S. 6089
Rhoderick, E. H. 6289
Richards, J. C. S. 6293
Ridinger, P. G. 6246
Ridley, B. K. 6094
Roach, W. E. 6264
Robbins, P. B. 6203
Roberts, L. D. 6303
Robinson, B. J. 6247
Robinson, R. J. 6095, 6192
Robinson, W. A. 6237
Robinson, W. K. 6148
Rogh, R. S. 6086
Ropp, R. C. 6189
Rosado, J. A. 6216, 6217
Rose, F. W. G. 6104
Rosenberg, A. J. 6003, 6108
Roth, L. M. 6168
Roth, R. S. 6082, 6160
Royce, B.S.H. 6113
Rubin, B. 6035
Rudness, R. G. 6040
Rupprecht, G. 6064

Sagar, A. 6060, 6111, 6068
St. Johnson, A. 6284
Saito, H. 6056
Sampson, D. F. 6169
Sarachik, M. P. 6061
Sasaki, Y. 6010, 6012
Saunders, J. 6243, 6145
Saunders, W. K. 6215
Sawaguchi, E. 6084
Schlomann, E. 6145
Schofer, H. S. 6086
Schwartz, C. M. 6203
Swiden, P. E. 6241
Shaw, H. J. 6241
Shenker, H. 6112
Sherman, B. 6239
Shiffman, C. A. 6117
Shirane, G. 6083
Shrader, R. E. 6235
Sidhu, S. S. 6153
Sidles, P. H. 6199
Sil'vestrova, I. M. 6043
Sirvetz, M. H. 6145
Smirnova, T. V. 6206
Smith, A. C. 6220
Smith, A. D. 6290
Smith, J. F. 6210
Smith, P. H. 6221
Smoluchowski, R. 6006
Somlyody, A. 6266
Sonin, A. S. 6089
Sosnowski, L. 6073
Southgate, P. D. 6213
Spedding, F. H. 6151
Spence, R. D. 6158
Spencer, E. G. 6143
Spicer, W. E. 6222
Staniforth, A. 6267
Steele, D. R. 6277
Stein, F. S. 6227
Sternglass, E. J. 6054
Stickler, J. J. 6123
Strauss, A. J. 6003, 6108
Stuart, R. A. 6292
Stuckes, A. D. 6202
Stupp, E. 6171
Suhl, H. 6195, 6240
6138
Summers, T. 6290
Szaynok, A. 6078

Tallan, N. M. 6051
Tanabe, Y. 6038
Thaxter, J. B. 6242
Theuerer, H. C. 6017
Thompson, J. E. 6286
Thorp, J. S. 6169
Thurmond, C. D. 6001,
6179
Tomita, T. 6023
Trumbore, F. A. 6002
Tsepelevich, E. E. 6089
Turner, E. F. 6216
Turner, J. A. 6288
Turner, K. I. 6286

Ubbink, J. 6247
Uehara, Y. 6188
Unterleitner, F. C. 6167
Ure Jr., R. W. 6239

Van Allen, R. L. 6262
Van der Ziel, A. 6232

Wagner, R. S. 6033
Wakefield, J. 6032
Wallace, D. C. 6199
Walter, F. J. 6303
Wannier, G. H. 6091
Watkins, G. D. 6050,
6051
Webb, W. W. 6009,
Wehner, G. K. 6052
Wei, Y. M. 6294
Weinreich, G. 6063
Weinreich, O. 6072
Weisberg, L. R. 6105
Weiser, K. 6020
White, H. G. 6063
Whitlock, W. S. 6297
Wieder, H. H. 6087

Whitlock, W. S. 6297
Wieder, H. H. 6087
Wiegand, D. A. 6006
Williams, F. E. 6185
Williams, R. C. 6122
Wilson, D. K. 6062
Wilson, W. B. 6203
Wollan, E. O. 6137
Woodbury, H. H. 6164
Woodward, J. G. 6250
Wright, G. B. 6130

Yetter, L. R. 6149
Young, A. P. 6203
Yunovich, A. E. 6127

Zallen, R. 6184
Zauberis, D. D. 6153
Zeiger, H. J. 6123
Zigenlaub, R. 6110
Zimmer, C. R. 6258
Zuev, K. P. 6204
Zwerdling, S. 6065

List of Periodicals scanned for SOLID STATE ABSTRACTS (Journal and Cards)

Acta Crystallographica (Acta Cryst.)
Acta Metallurgica (Acta Met.)
Acta Physica (Acta Phys.)
Acta Physica Hungaricae (Acta Phys. Hungar.)
Acta Physica Polonica (Acta Phys. Polon.)
Acta Polytechnica Scandanavica (Acta Polyt. Scand.)
Advances in Physics (Advances Phys.)
A.E.G. Progress (AEG Prog.)
Alta Frequenza (Alta Frequenza)
American Ceramic Society Bulletin (Am. Ceram. Soc. Bull.)
American Journal of Physics (Am. J. Phys.)
American Mineralogist (Am. Mineral.)
Analyst (Analyst)
Analytical Chemistry (Analyt. Chem.)
Annalen der Physik (Ann. Physik)
Annales de Chimie et Physique (Ann. Chim. et Phys.)
Annales de Physique (Ann. Phys., Paris)
Annales de Radioelectricite (Ann. Radioelect.)
Annales des Telecommunications (Ann. Telecommun.)
Annals of Physics (Ann. Phys.)
Applications and Industry (Applic. and Industr.)
Applied Scientific Research (Appl. Sci. Res.)
Archiv der Elektrischen Ubertragung (Arch. Elekt. Uber-tragung)
Archiv für Elektrotechnik (Arch. Elektrotech.)
Archiv für Technisches Messen (Arch. Tech. Messen)
Arkiv för Fysik (Arkiv Fysik)
Asea Journal (Asea J.)
A. T. E. Journal (ATE J.)
Audio (Audio)
Australian Journal of Physics (Aust. J. Phys.)
Australian Journal of Scientific Research (Aust. J. Sci. Res.)
Automatic Control (Auto. Control)
Automation and Remote Control (Russian Translation) (Automa. Remote Control)

Battelle Technical Review (Battelle Tech. Rev.)
Beama Journal (Beama J.)
Bell Laboratories Record (Bell Labs. Rec.)
Bell System Technical Journal (Bell Sys. Tech. J.)
British Communications and Electronics (Brit. Commun. Electronics)
British Journal of Applied Physics (Brit. J. Appl. Phys.)
Bulletin de L'Academie Pol. des Sciences (Bull. L'Acad. Pol. Sci.)
Bulletin of the Academy of Sciences of the USSR - Physical Series (Russian Translation) (Bull. Acad. Sci. USSR-Phys. Ser.)
Bulletin of the American Physical Society (Bull. Am. Phys. Soc.)
Bulletin of the Research Council of Israel (Bull. Res. Counc. of Israel)

Cables and Transmission (Cables and Transm.)
Canadian Journal of Chemistry (Can. J. Chem.)
Canadian Journal of Physics (Can. J. Phys.)
Ceramics Industry (Ceram. Ind.)
Ceskoslovensky casopis pro fysiku (Cs. cas. fys.)
Chemical Reviews (Chem. Revs.)
Chemical and Engineering News (Chem. Engrg. News)
Cobalt (Cobalt)
Communication and Electronics (Commun. and Electronics)
Communications of the Association for Computing Machinery (Commun. Assoc. Computing Mach.)
Comptes Rendus Hebdomadaires des Seances de l'Academie des Sciences (Comptes Rendus)
Control Engineering (Control Engrg.)
Croatia Chemica Acta (Croat. Chem. Acta)
Czechoslovak Journal of Physics (Czech. J. Phys.)

Direct Current (Direct Curr.)
Dissertation Abstracts (Diss. Abstr.)

Electrical Communication (Elect. Commun.)
Electrical Engineering (Elect. Engrg.)
Electrical Manufacturing (Elect. Mfg.)
Electrical World (Elect. World)
Electronic Applications (Electronic Applic.)
Electronic Design (Electronic Des.)
Electronic Engineering (Electronic Engrg.)
Electronic Equipment Engineering (Electronic Equipm. Engrg.)
Electronic Industries (Electronic Ind.)
Electronic Technology (Electronic Tech.) formerly Electronic and Radio Engineer
Electronics (Electronics)
Electronics and Communications (Electronics and Commun.)
Electrotechnical Journal of Japan (Electrotech. J. Japan)
Elektronische Rundschau (Elektron. Rundschau)
Elektrotechnicky Obzor (Elektrotech. Obzor)
Elektrotechnische Zeitschrift (Elektrotech. Z.)
Energia Nucleare (Energia Nucleare)
Engineering and Mining Journal (Engrg. Mining J.)
Ericsson Technics (Ericsson Technics)

Faraday Society Discussions (Faraday Soc. Disc.)
Fernmeldetechnische Zeitschrift (Fernmeldetech. Z.)
Fortschritte der Physik (Fortschritte Phys.)
Frequenz (Frequenz)

General Electric Review (GE Rev.)
General Telephone Technical Journal (Genl. Tel. Tech. J.)

Helvetica Physica Acta (Helv. Phys. Acta)
Hochfrequenztechnik und Elektroakustik (Hochfrequenztech. u. Elektroakust.)

I. B. M. Journal of Research and Development (IBM J. Res. and Dev.)
Indian Journal of Physics (Indian J. Phys.)
Industrial Laboratories (Indus. Labs.)
Instruments and Automation (Instr. and Automa.)
IRE National Convention Record (IRE Natl. Conv. Rec.)
IRE Transactions:
- on Aeronautical and Navigational Electronics (IRE Trans., Vol. ANE)
- on Audio (IRE Trans., Vol. AU)
- on Automatic Control (IRE Trans., Vol. AC)
- on Broadcast and Television Receivers (IRE Trans., Vol. BTR)
- on Broadcast Transmission Systems (IRE Trans., Vol. BTS)
- on Circuit Theory (IRE Trans., Vol. CT)
- on Communication Systems (IRE Trans., Vol. CS)
- on Component Parts (IRE Trans., Vol. CP)
- on Electron Devices (IRE Trans., Vol. ED)
- on Electronic Computers (IRE Trans., Vol. EC)
- on Industrial Electronics (IRE Trans., Vol. IE)
- on Information Theory (IRE Trans., Vol. IT)
- on Instrumentation (IRE Trans., Vol. I)
- on Medical Electronics (IRE Trans., Vol. ME)
- on Microwave Theory and Techniques (IRE Trans., Vol. MTT)
- on Military Electronics (IRE Trans., Vol. MIL)
- on Nuclear Science (IRE Trans., Vol. NS)
- on Production Techniques (IRE Trans., Vol. PT)
- on Reliability and Quality Control (IRE Trans., Vol. RQC)
- on Space Electronics and Telemetry (IRE Trans., Vol. SET)
- on Vehicular Communications (IRE Trans., Vol. VC)

Journal of the Acoustical Society of America (J. Acoust. Soc. Am.)
Journal of the American Ceramic Society (J. Am. Ceram. Soc.)
Journal of the American Chemical Society (J. Am. Chem. Soc.)
Journal of Applied Physics (J. Appl. Phys.)
Journal of the Audio Engineering Society (J. Audio Engrg. Soc.)
Journal of the British IRE (J. Brit. IRE)
Journal of Chemical Physics (J. Chem. Phys.)
Journal de Chimie Physique (J. Chim. Phys.)
Journal of the Electrochemical Society (J. Electrochem. Soc.)
Journal of Electronics and Control (J. Electronics Control)
Journal of the Franklin Institute (J. Franklin Inst.)
Journal of the Institution of Electrical Engineers (London) (J. IEE)
Journal of the Institute of Metals (J. Inst. Metals)
Journal of Metals (J. Metals)
Journal of Molecular Spectroscopy (J. Mol. Spectrosc.)
Journal of the Optical Society of America (J. Opt. Soc. Am.)
Journal of Physical Chemistry (J. Phys. Chem.)
Journal of the Physics and Chemistry of Solids (J. Phys. Chem. Solids)
Journal de Physique et le Radium (J. Phys. Radium)
Journal of the Physical Society of Japan (J. Phys. Soc. Japan)
Journal of Research of the National Bureau of Standards (J. Res. Natl. Bur. Stand.)
Journal of Scientific Instruments (J. Sci. Instr.)
Journal of the Society of Motion Picture and Television Engineers (J. Soc. Mot. Pict. TV Engrs.)
Journal of the Television Society (J. TV Soc.)

Marconi Review (Marconi Rev.)
Materials in Design Engineering (Matls. Des. Engrg.)
Metallurgical Reviews (Metal. Revs.)
Military Electronics (Mil. Electronics)
Missiles and Rockets (Missiles and Rockets)
Molecular Physics (Mol. Phys.)
Mullard Technical Communications (Mullard Tech. Commun.)

Nachrichtentechnik (Nachrichtentech.)
Nachrichtentechnische Zeitschrift (Nachrichtentech. Z.)
Nature (London) (Nature)
Naturwissenschaften (Naturwissenschaften)
NBS Technical News Bulletin (NBS Tech. News Bull.)
Nuclear Instruments and Methods (Nuc. Instr. Methods)
Nuclear Power (Nuc. Power)
Nuclear Science Abstracts (Nuc. Sci. Abstr.)
Nucleonics (Nucleonics)
Nuovo Cimento (Nuovo Cim.)

Onde Electrique (Onde Elect.)
Optics and Spectroscopy (Russian Translation) (Optics and Spectrosc.)
Optik (Optik)

Philips Research Reports (Philips Res. Rep.)
Philips Technical Review (Philips Tech. Rev.)
Philips Telecommunication Review (Philips Telecommun. Rev.
Philosophical Magazine (Phil. Mag.)
Physica (Physica)
Physical Review (Phys. Rev.)
Physical Review Letters (Phys. Rev. Lett.)
Physics of Metals and Metallography (Russian Translation) (Phys. Metals Metallog.)
Physics Today (Phys. Today)
Physik (Physik)
Post Office Electrical Engineers Journal (P. O. Elect. Engrs. J.)
Power Apparatus and Systems (Power Appar. Sys.)
Proceedings of the Institution of Electrical Engineers (Proc. IEE)
Proceedings of the Institute of Radio Engineers (Proc. IRE)
Proceedings of the IRE, Australia (Proc. IRE, Aust.)
Proceedings of the National Academy of Sciences (U.S.A.) - (Proc. Natl. Acad. Sciences)
Proceedings of the Physical Society (Proc. Phys. Soc.)
Proceedings of the Royal Society (Proc. Roy. Soc.)
Proceedings of the Royal Netherlands Academy of Science (Proc. Roy. Neth. Acad. Sci.)
Process Control and Automation (Proc. Control Automation)
Product Engineering (Prod. Engrg.)
Progress in Metal Physics (Prog. Metal Phys.)
Progress of Theoretical Physics (Prog. Theoret. Phys.)

Radiation Research (Rad. Res.)
RCA Review (RCA Rev.)
Radio Engineering (Russian Translation) (Radio Engrg.)
Radio Engineering and Electronics (Russian Translation) (Radio Engrg. Electronics)
Refrigeration Engineering (Refrig. Engrg.)
Research (Research)
Research Reviews (Res. Revs.)
Reviews of Modern Physics (Revs. Mod. Phys.)
Review of Scientific Instruments (Rev. Sci. Instr.)
Revista Electrotechnica (Rev. Electrotech.)
Ricerca Scientifica (Ricerca Sci.)
Rozprawy Elektrotechniczne (Rozpr. Elektrot.)
RRE Journal (RRE J.)
Russian Journal of Inorganic Chemistry (Russian Translation) (Russ. J. Inorg. Chem.)

Science (Science)
Scientia Sinica (Sci. Sinica)
Scientific American (Sci. Amer.)
Semiconductor Products (Semicon. Prod.)
Siemens Edison Swan Journal (Siemens Ed. Swan J.)
Siemens Review (Siemens Rev.)
Siemens Zeitschrift (Siemens Z.)
Signal (Signal)
Solar Energy (Solar Energy)
Solid State Journal (Solid State J.)
Solid State Electronics (Solid State Electronics)
Note: The six items below are Russian Translations
Soviet Physics - Crystallography (Soviet Phys.-Cryst.)
Soviet Physics - Doklady (Soviet Phys.-Doklady)
Soviet Physics - JETP (Soviet Phys.-JETP)
Soviet Physics - Solid State (Soviet Phys.-Solid State)
Soviet Physics - Technical Physics (Soviet Phys.-Tech. Phys.
Soviet Physics - Uspekhi (Soviet Phys.-Uspekhi)
Sperry Engineering Review (Sperry Engrg. Rev.)
Sylvania Technologist (Sylvania Technologist)
Telecommunications (Russian Translation) (Telecommun.)
Telefunken Rohre (Telefunken Rohre)
Telefunken Zeitung (Telefunken Z.)
Transactions of the Faraday Society (Trans. Faraday Soc.)
Transactions of the Metallurgical Society of AIME (AIME Trans.)
Transactions of the New York Academy of Sciences (Trans. N. Y. Acad. Sci.)

U. S. Government Research Reports (U. S. Gov. Res. Rep.)

Vacuum (Vacuum)
Vestnik Akademii Nauk SSR (Vestnik Akad. Nauk SSR)

Welding Engineer (Welding Engr.)
WESCON Convention Record (WESCON Conv. Rec.)
Western Electric Engineer (Western Elec. Engr.)
Westinghouse Engineer (Westinghouse Engr.)
Wireless World (Wireless World)

Zeitschrift für Angewandte Chemie (Z. Angew. Chem.)
Zeitschrift für Angewandte Physik. (Z. Angew. Phys.)
Zeitschrift für Elektrochemie (Z. Elektrochem.)
Zeitschrift für Instrumentenkunde (Z. Instrumentenk.)
Zeitschrift für Kristallographie (Z. Krist.)
Zeitschrift für Metallkunde (Z. Metallkde.)
Zeitschrift für Naturforschung (Z. Naturforsch.)
Zeitschrift für Physik (Z. Physik)
Zeitschrift für Physikalische Chemie (Z. Physik. Chem.)
Zhurnal Eksperimental'noi i Teoreticheskoi Fiziki (Zhur. Eksp. i Teoret. Fiz.)
Zhurnal Fizicheskoi Khimii (Zhur. Fiz. Khim.)
Zhurnal Neorganicheskoy Khimii (Zhur. Neog. Khim.)

Abridged Table of Contents for SOLID STATE ABSTRACTS ON CARDS

Category M: Solid State Metallurgy

Alloys (Phase Diagrams, Solubility, Segregation)

Crystal Structure (Lattices, Imperfections, Impurities)

Crystal Growth (Methods, Crystal Forms)

Crystal Surfaces (Surface Chemistry, Crystal Processing, Connections)

Environmental Effects (Heat Treatment, Radiation)

Category P: Solid State Physics

Crystal Physics (Binding and Lattice Properties, Energy Bands and Levels)

Electrical Properties (Dielectric, Carrier, Conductive, Breakdown, Magnetoelectric, Noise, Surface)

Magnetic Properties (Ferro-, Ferri-, Para-, and Diamagnetic)

Optical Properties (Absorptive, Radiative, Luminescent, Photoconductive, Photovoltaic)

Thermal Properties (Thermoelectric)

Mechanical Properties (Deformation)

Category D: Solid State Devices

(Theory, Fabrication, Properties, Measurements)

Conductive Devices (Diodes and Rectifiers, Varistors, Transistors, Functional Units)

Magnetoelectric Devices (Hall Effect, Magnetoresistive)

Photodevices (Photoconductive, Photodiode and Phototransistor, Photovoltaic, Luminescent)

Thermal Devices (Thermistor, Thermoelectric)

Ferrite Devices (Isolators, Circulators, Memory Elements, etc.)

Paramagnetic Devices (Masers)

Dielectric Devices (Transducers, Memory Cells, Amplifiers)

Superconductive Devices (Cryotrons)

Category B: Solid State Device Circuits

Amplifiers

Oscillators

Switching Circuits

Signal Converters (Modulators, Detectors, Mixers, Frequency Multipliers and Dividers)

Wave Generators

Pulse Circuits

Category A: Solid State Device Applications

Communications (Radio, Television, Telephony)

Radar

Telemetry

Computers

Power

Control

Instrumentation

ORDER FORM

CAMBRIDGE COMMUNICATIONS CORPORATION
238 Main St., Cambridge 42, Mass.

Gentlemen:

Please enter my order for the publications which I have checked below:

☐ **SOLID STATE ABSTRACTS** (Journal) — Vol. 1 (1960 abstracts) $25.00

SOLID STATE ABSTRACTS ON CARDS — Vol. 1 (1960 abstracts) [A subscription to **Solid State Abstracts** (Journal) — Vol. 1 is included with any order for one or more card categories without additional charge.]

☐ All Categories (Complete) $250.00

☐ Semiconductor Abstracts 175.00
(selected from all categories)

☐ Magnetic, Dielectric, etc. Abstracts 100.00
(selected from all categories)

☐ Category M (Metallurgy) 50.00

☐ Category P (Physics) . . . . . $ 75.00

☐ Category D (Devices) 50.00

☐ Category B (Circuits) 50.00

☐ Category A (Applications) 50.00

Name.....

Address.....

.....

.....

☐ Payment Enclosed.

☐ Bill me.

Sample Page from the Classification System for the PHYSICS section of SOLID STATE ABSTRACTS ON CARDS

P2 ELECTRICAL PROPERTIES (see also P4.4, P5.3, a, b)

P2.0 General
- P2.0.1 Theory of the Electrical Properties of Solids
  - P2.0.1.0 General
- P2.0.2 Measurement of the Electrical Properties of Solids (see also under specific properties)
- P2.0.3 Effect of:
  - P2.0.3.1 Temperature (see also P5)
  - P2.0.3.2 Pressure
  - P2.0.3.3 Deformation
  - P2.0.3.4 Radiation (see also P4)
  - P2.0.3.5 Dislocations (see also M3.2.1.2.5.2)
  - P2.0.3.6 Impurities
  - P2.0.3.7 Melting
  - P2.0.3.8 High Fields
  - P2.0.3.9 Crystalline Order
    - P2.0.3.9.1 Long Range
    - P2.0.3.9.2 Short Range
  - P2.0.3.10 Heat Treatment
- P2.0.4 Electrical Properties of Special Structures
  - P2.0.4.1 Single Crystals
  - P2.0.4.2 Thin Films
    - P2.0.4.2.1 Theory
  - P2.0.4.3 Grain Boundaries

P2.1 Dielectric Properties
- P2.1.0 General
  - P2.1.0.3 Effect of:
    - P2.1.0.3.6 Electromagnetic Radiation
  - P2.1.0.5 Dielectric Constant (Permittivity)
    - P2.1.0.5.3 Effect of (Variation with):
      - P2.1.0.5.3.1 Temperature
      - P2.1.0.5.3.2 Pressure
      - P2.1.0.5.3.3 Frequency
    - P2.1.0.5.9 Dielectric Constant of Specific Materials
  - P2.1.0.6 Charge on (or in) Dielectrics
    - P2.1.0.6.3 Effect of:
      - P2.1.0.6.3.4 Electric Field
      - P2.1.0.6.3.5 Geometry
      - P2.1.0.6.3.6 Radiation
        - P2.1.0.6.3.6.1 X-Rays
        - P2.1.0.6.3.6.2 Beta-Rays
  - P2.1.0.7 Current Flow in Dielectrics (see also P2.2.6)
    - P2.1.0.7.4 Carriers
  - P2.1.0.8 Dielectric Loss
    - P2.1.0.8.9 Dielectric Loss in Specific Materials
- P2.1.1 Ferroelectricity
  - P2.1.1.3 Effect of:
    - P2.1.1.3.2 Pressure
  - P2.1.1.9 Ferroelectric Properties of Specific Materials
- P2.1.2 Piezoelectricity
  - P2.1.2.2 Measurement of Piezoelectric Properties
  - P2.1.2.3 Effect of:
    - P2.1.2.3.1 Temperature
    - P2.1.2.3.2 Pressure
  - P2.1.2.9 Piezoelectric Properties of Specific Materials
- P2.1.9 Dielectric Properties of Specific Materials

P2.2 Carrier Properties
- P2.2.0 General
  - P2.2.0.1 Theory of Carrier Properties
  - P2.2.0.3 Effect of:
    - P2.2.0.3.1 Temperature
    - P2.2.0.3.2 Pressure
    - P2.2.0.3.3 Radiation
  - P2.2.0.4 Types of Carriers
    - P2.2.0.4.1 Electrons
      - P2.2.0.4.1.3 Effect of:
        - P2.2.0.4.1.3.4 High Electric Field
          1. Hot Electrons
             3. Effect of:
                2. Pressure
                3. Magnetic Field
                4. Impurities
                5. Microwave Heating
                6. Scattering of Hot Electrons
    - P2.2.0.4.2 Holes
    - P2.2.0.4.3 Excitons
      - P2.2.0.4.3.1 Theory of Excitons
        - P2.2.0.4.3.1.5 Relation of Excitons to Plasmons
        - P2.2.0.4.3.1.6 Fine Structure of Excitons
      - P2.2.0.4.3.3 Effect of:

P2.2 Carrier Properties (Cont.)
- P2.2.0.4.3.3.3 Magnetic Field (Zeeman Effect)
  1. Theory
  6. Fine Structure
- P2.2.0.4.3.3.4 Electric Field
- P2.2.0.4.3.4 Types of Excitons
  1. Direct
  2. Indirect
- P2.2.0.4.3.5 Creation of Excitons
  - P2.2.0.4.3.5.2 Methods
    1. Injection
    2. Absorption
- P2.2.0.4.3.6 Disintegration of Excitons
  - P2.2.0.4.3.6.2 Methods
    1. Phonons
- P2.2.0.4.3.7 Exciton Binding Energy
- P2.2.0.4.3.8 Other Properties of Excitons
  - P2.2.0.4.3.8.1 Excitonic Ions
  - P2.2.0.4.3.8.2 Interaction with:
    1. Electrons
- P2.2.0.4.3.9 Excitons in Specific Materials
- P2.2.0.5 Sources of Carriers
  - P2.2.0.5.1 Donors
  - P2.2.0.5.2 Acceptors
- P2.2.0.6 Carrier Wave Functions
  - P2.2.0.6.4 Types of Wave Functions
    - P2.2.0.6.4.1 Bloch
      - P2.2.0.6.4.1.5 Modified Bloch
    - P2.2.0.6.4.2 Wannier
    - P2.2.0.6.4.3 Luttinger-Kohn
    - P2.2.0.6.4.4 Haering
- P2.2.0.7 Interactions of Carriers
  - P2.2.0.7.4 Types of Interactions
    - P2.2.0.7.4.1 With Impurity Ions
      - P2.2.0.7.4.1.5 Ionization Energies
    - P2.2.0.7.4.2 With Other Carriers
- P2.2.1 Carrier Concentrations
- P2.2.2 Generation of Carriers
- P2.2.3 Recombination of Carriers (Carrier Lifetime)
  - P2.2.3.1 Theory of Carrier Recombination
    - P2.2.3.1.4 Recombination Mechanisms
      - P2.2.3.1.4.4 Plasma
  - P2.2.3.2 Measurement of Carrier Lifetime
    - P2.2.3.2.2 Methods
      - P2.2.3.2.2.1 Photoconductive Decay
        - P2.2.3.2.2.1.5 Special Techniques
          1. Use of Filters
      - P2.2.3.2.2.2 Photoelectromagnetic Effect
      - P2.2.3.2.2.3 PC - PEM Ratio
      - P2.2.3.2.2.4 Photodiffusion
      - P2.2.3.2.2.5 Infrared Absorption
      - P2.2.3.2.2.6 Microwave Absorption
      - P2.2.3.2.2.7 Radiation-Produced Pulses
      - P2.2.3.2.2.8 Junction Diodes
      - P2.2.3.2.2.9 Carrier Injection Electroluminescence
  - P2.2.3.3 Effect of:
    - P2.2.3.3.1 Temperature
    - P2.2.3.3.2 Pressure
    - P2.2.3.3.3 Radiation
    - P2.2.3.3.4 Heat Treatment
    - P2.2.3.3.5 Impurity (Carrier) Concentration
    - P2.2.3.3.8 Transient Sweep-Out
  - P2.2.3.5 Recombination Centers
    - P2.2.3.5.2 Properties of Recombination Centers
      - P2.2.3.5.2.1 Energy Distribution
      - P2.2.3.5.2.2 Frequency Factor
      - P2.2.3.5.2.3 Ionization Energy
    - P2.2.3.5.3 Effect of:
      - P2.2.3.5.3.4 Etching
    - P2.2.3.5.4 Types of Recombination Centers
      - P2.2.3.5.4.1 Classification by Crystal Imperfection
        - P2.2.3.5.4.1.1 Impurities
        - P2.2.3.5.4.1.2 Dislocations
        - P2.2.3.5.4.1.3 Lattice-Vacancies
      - P2.2.3.5.4.2 Classification by Process of Recombination
        - P2.2.3.5.4.2.1 Traps
        - P2.2.3.5.4.2.2 Deathnium
    - P2.2.3.5.5 Introduction of Recombination Centers (see also M3.2.2.4)
    - P2.2.3.5.6 Capture Cross Sections of Recombination Centers

← ORDER FORM FOR SOLID STATE ABSTRACTS ON CARDS

mple Page from the Classification System for the CIRCUITS section of SOLID STATE ABSTRACTS ON CARDS

B1 AMPLIFIERS

- .0 General
  - B1.0.3 Gain Control
    - B1.0.3.4 Types
      - B1.0.3.4.1 Automatic
  - B1.0.4 Multistage Amplifiers
    - B1.0.4.4 Interstage Coupling
      - B1.0.4.4.4 Types
        - B1.0.4.4.4.1 Direct Coupled
        - B1.0.4.4.4.2 RC Coupled
        - B1.0.4.4.4.3 Transformer Coupled
        - B1.0.4.4.4.4 Twin-T Network Coupled
    - B1.0.4.5 Alignment of Multistage Amplifiers
  - B1.0.5 Noise in Amplifiers
  - B1.0.6 Power Dissipation in Amplifiers
    - B1.0.6.5 Limitation of Dissipation
  - B1.0.7 Distortion in Amplifiers
  - B1.0.8 Feedback in Amplifiers
    - B1.0.8.4 Neutralization of Feedback
  - B1.0.9 Capacity in Amplifiers
    - B1.0.9.4 Neutralization of Capacity

- 1 Theory and Design of Amplifiers
  - B1.1.5 Determination of Parameters

- .3 Stabilization of Amplifiers
  - B1.3.4 Stabilization against:
    - B1.3.4.1 Temperature Variations
    - B1.3.4.2 Parameter Variations

- .4 Types of Amplifiers
  - B1.4.1 Classification by Frequency
    - B1.4.1.1 Direct Current (see also B1.4.2.2 and B1.4.2.4)
      - B1.4.1.1.3 Stabilization
        - B1.4.1.1.3.5 Drift-Gain Ratio
        - B1.4.1.1.3.6 Drift Correctors
      - B1.4.1.1.4 Types
        - B1.4.1.1.4.1 Direct Coupled
        - B1.4.1.1.4.2 Chopper
    - B1.4.1.2 Audio Frequency
    - B1.4.1.3 Radio Frequency
      - B1.4.1.3.1 Very Low Frequency (<30kc)
      - B1.4.1.3.2 Low Frequency (30kc - 300kc)
      - B1.4.1.3.3 Medium Frequency (300kc - 3mc)
      - B1.4.1.3.4 High Frequency (3mc - 30mc)
      - B1.4.1.3.5 Very High Frequency (30mc - 300mc)
      - B1.4.1.3.6 Ultra High Frequency (300mc - 3kmc)
    - B1.4.1.4 Microwave Frequency (~1 - 30kmc)
      - B1.4.1.4.1 L Band (0.39 - 1.55kmc)
      - B1.4.1.4.2 S Band (1.55 - 5.20kmc)
      - B1.4.1.4.3 X Band (5.20 - 10.90kmc)
      - B1.4.1.4.4 K Band (10.90kmc - 36kmc)
    - B1.4.1.5 Broadband Amplifiers
      - 2. Video
  - B1.4.2 Classification by Function
    - B1.4.2.1 Intermediate Frequency Amplifiers
      - B1.4.2.1.4 Application
        - B1.4.2.1.4.1 Radio
        - B1.4.2.1.4.2 Television
    - B1.4.2.2 Operational Amplifiers (see A2.2.1.1)
    - B1.4.2.3 Linear Amplifiers
    - B1.4.2.4 Differential Amplifiers
      - B1.4.2.4.3 Stabilization
    - B1.4.2.5 Pulse Amplifiers
      - B1.4.2.5.3 Active Element
        - B1.4.2.5.3.3 Breakdown Devices
      - B1.4.2.5.4 Special Types
        - B1.4.2.5.4.1 Pulse-Regenerative Amplifiers
        - B1.4.2.5.4.2 Pulse-Width Control Amplifiers
    - B1.4.2.6 Wideband Amplifiers
    - B1.4.2.7 Low Noise Amplifiers
    - B1.4.2.8 Rectangular Wave Amplifiers
    - B1.4.2.9 Decade Amplifiers
    - B1.4.2.10 Unilateral Amplifiers
    - B1.4.2.11 Phase Inverter Amplifiers
    - B1.4.2.12 Low Distortion Amplifiers
  - B1.4.3 Classification by Mode of Operation
    - B1.4.3.1 Single-Ended Amplifiers
    - B1.4.3.2 Push-Pull Amplifiers
    - B1.4.3.3 Feedback Amplifiers
    - B1.4.3.4 Switched Mode Amplifiers
    - B1.4.3.5 Tuned Amplifiers
    - B1.4.3.6 Bridge Amplifiers
    - B1.4.3.7 Chopper Amplifiers
    - B1.4.3.8 Carrier Storage Amplifiers
    - B1.4.3.9 Parametric (Reactance) Amplifiers
      - B1.4.3.9.1 Theory and Design
      - B1.4.3.9.3 Active Elements
        - B1.4.3.9.3.a Diodes
        - B1.4.3.9.3.f Photoelectronic Devices
        - B1.4.3.9.3.p Ferromagnetic Devices
        - B1.4.3.9.3.t Dielectric Devices
      - B1.4.3.9.4 Types of Parametric Amplifiers
        - B1.4.3.9.4.1 Variable Capacitance Amplifiers
          - B1.4.3.9.4.1.1 Theory and Design
          - B1.4.3.9.4.1.3 Parameters
            - 1. Gain-Bandwidth Product
            - 2. Noise Figure
          - B1.4.3.9.4.1.4 Types
            - 1. Cavity
              - 1. Three-Terminal
              - 2. Four-Terminal
            - 2. Travelling Wave
              - 1. Forward
              - 2. Backward
            - 3. Reactatrons
            - 4. Directional Bridge
            - 5. Transmission Line
            - 6. Very Low Frequency
            - 7. Modulation-Demodulation
          - B1.4.3.9.4.1.5 Frequency Range
            - 8. S-Band
      - B1.4.3.9.5 Special Techniques
        - B1.4.3.9.5.3 Variable Coupling (to reduce noise)
        - B1.4.3.9.5.4 Subharmonic Pumping
      - B1.4.3.9.7 Special Modes of Operation
        - B1.4.3.9.7.1 Superregenerative
      - B1.4.3.9.9 Other Aspects of Parametric Amplifiers
        - B1.4.3.9.9.1 Relaxation Oscillations
      - B1.4.3.10 Maser Amplifiers (see q1.1.1.4.1)
      - B1.4.3.11 Negative Mass Amplifiers
      - B1.4.3.12 Cascode Amplifiers
  - B1.4.4 Classification by Active Element
    - B1.4.4.a Diodes
    - B1.4.4.b Transistors
      - B1.4.4.b.1 Theory and Design of Transistor Amplifiers
      - B1.4.4.b.2 Analysis of Transistor Amplifiers
      - B1.4.4.b.3 Stabilization of Transistor Amplifiers
      - B1.4.4.b.4 Basic Transistor Amplifier Circuits
        - B1.4.4.b.4.1 Common Base
        - B1.4.4.b.4.2 Common Emitter
        - B1.4.4.b.4.3 Common Collector
      - B1.4.4.b.5 Types of Transistors
      - B1.4.4.b.7 Frequency Compensation
    - B1.4.4.p Magnetic Amplifiers
  - B1.4.5 Classification by Power Level
    - B1.4.5.1 Low Power Amplifiers (Preamplifiers)
    - B1.4.5.2 Intermediate Power Amplifiers
    - B1.4.5.3 High Power Amplifiers
  - B1.4.6 Classification by Impedance Level
    - B1.4.6.1 Low Impedance Amplifiers
      - B1.4.6.1.1 Input
      - B1.4.6.1.2 Output
    - B1.4.6.2 Intermediate Impedance Amplifiers
    - B1.4.6.3 High Impedance Amplifiers
      - B1.4.6.3.1 Input
      - B1.4.6.3.2 Output
    - B1.4.6.4 Constant Impedance Amplifiers
      - B1.4.6.4.1 Input
      - B1.4.6.4.2 Output
  - B1.4.7 Classification by Voltage Level
  - B1.4.8 Classification by Current Level
  - B1.4.9 Classification by Class of Operation
    - B1.4.9.1 Class A
    - B1.4.9.2 Class AB
    - B1.4.9.3 Class B
    - B1.4.9.4 Class C

- B1.5 Specific Applications
  - B1.5.1 Communications
    - B1.5.1.1 Radio
    - B1.5.1.2 Television
    - B1.5.1.3 Telephone
  - B1.5.2 Computers
  - B1.5.4 Control

B2 OSCILLATORS

- B2.0 General
  - B2.0.1 Frequency of Oscillation
    - B2.0.1.5 Frequency Control
  - B2.0.2 Conditions of Oscillation
  - B2.0.3 Oscillation Waveforms

may cost your company many times the price of

SOLID STATE ABSTRACTS ON CARDS

These cards enable anyone — scientist, engineer, librarian, file clerk — to maintain a cumulative reference file of up-to-date information in the solid state field. Classification numbers on each card make it easy to file this information in a logical sequence and hundreds of guide cards make it possible to locate required references immediately.

This service, which amounts to a continuous literature search on more than 4000 topics, covers conference papers, U.S. patents, and commercial new product releases in addition to some 250 technical journals published throughout the world.

Take full advantage of the billions of dollars of research results that are reported each year. This annotated and classified bibliography of current research in the solid state field is inexpensive insurance that your scientific efforts are not duplicating the work of others.

See the inside back cover and the last three pages of this issue for a list of journals abstracted, a list of subjects covered, sample pages of our detailed classification system, and an order form.

CAMBRIDGE COMMUNICATIONS CORPORATION

238 Main Street • Cambridge 42, Massachusetts

N O T I C E

THIS VOLUME IS INCOMPLETE

THE FOLLOWING ISSUES ARE NOT AVAILABLE:

VOL. 1 NO. 2 NOVEMBER 1960

BINDING UNIT

NOTICE

THIS VOLUME IS INCOMPLETE

THE FOLLOWING ISSUES ARE NOT
AVAILABLE:

BINDING UNIT